



Cite this: *Nanoscale Horiz.*, 2024, 9, 1630

## Oxidative stress modulating nanomaterials and their biochemical roles in nanomedicine

Kapil D. Patel, \*<sup>abcdef</sup> Zalike Keskin-Erdogan, <sup>fgh</sup> Prasad Sawadkar, <sup>in</sup> Nik Syahirah Aliaa Nik Sharifulden, <sup>g</sup> Mark Robert Shannon, <sup>abc</sup> Madhumita Patel, <sup>j</sup> Lady Barrios Silva, <sup>g</sup> Rajkumar Patel, <sup>k</sup> David Y. S. Chau, <sup>g</sup> Jonathan C. Knowles, <sup>efg</sup> Adam W. Perriman\*<sup>abc</sup> and Hae-Won Kim\*<sup>deflm</sup>

Many pathological conditions are predominantly associated with oxidative stress, arising from reactive oxygen species (ROS); therefore, the modulation of redox activities has been a key strategy to restore normal tissue functions. Current approaches involve establishing a favorable cellular redox environment through the administration of therapeutic drugs and redox-active nanomaterials (RANs). In particular, RANs not only provide a stable and reliable means of therapeutic delivery but also possess the capacity to finely tune various interconnected components, including radicals, enzymes, proteins, transcription factors, and metabolites. Here, we discuss the roles that engineered RANs play in a spectrum of pathological conditions, such as cancer, neurodegenerative diseases, infections, and inflammation. We visualize the dual functions of RANs as both generator and scavenger of ROS, emphasizing their profound impact on diverse cellular functions. The focus of this review is solely on inorganic redox-active nanomaterials (inorganic RANs). Additionally, we deliberate on the challenges associated with current RANs-based approaches and propose potential research directions for their future clinical translation.

Received 22nd April 2024,  
Accepted 8th July 2024

DOI: 10.1039/d4nh00171k

rsc.li/nanoscale-horizons

<sup>a</sup>John Curtin School of Medical Research, Australian National University, Canberra, ACT 2601, Australia. E-mail: kapildpatel20@gmail.com, chawp@bristol.ac.uk

<sup>b</sup>Research School of Chemistry, Australian National University, Canberra, ACT 2601, Australia

<sup>c</sup>School of Cellular and Molecular Medicine, University of Bristol, BS8 1TD, UK

<sup>d</sup>Institute of Tissue Regeneration Engineering (ITREN), Dankook University, Cheonan, 31116, Republic of Korea. E-mail: kimhw@dku.edu

<sup>e</sup>Department of Nanobiomedical Science & BK21 PLUS NBM Global Research Center for Regenerative Medicine Research Center, Dankook University, Cheonan, 31116, Republic of Korea

<sup>f</sup>UCL Eastman-Korea Dental Medicine Innovation Centre, Dankook University, Cheonan, 31116, Republic of Korea

<sup>g</sup>Division of Biomaterials and Tissue Engineering, UCL Eastman Dental Institute, University College London, Royal Free Hospital, Rowland Hill Street, NW3 2PF, London, UK

<sup>h</sup>Department of Chemical Engineering, Imperial College London, Exhibition Rd, South Kensington, SW7 2BX, London, UK

<sup>i</sup>Division of Surgery and Interventional Science, UCL, London, UK

<sup>j</sup>Department of Chemistry and Nanoscience, Ewha Women University, 52 Ewhayeodae-gil, Seodaemun-gu, Seoul 03760, Republic of Korea

<sup>k</sup>Energy & Environment Sciences and Engineering (EESE), Integrated Sciences and Engineering Division (ISED), Underwood International College, Yonsei University, 85 Songdongwhak-ro, Yeonsungu, Incheon 21938, Republic of Korea

<sup>l</sup>Department of Biomaterials Science, School of Dentistry, Dankook University, Cheonan 31116, Republic of Korea

<sup>m</sup>Cell & Matter Institute, Dankook University, Cheonan 31116, Republic of Korea

<sup>n</sup>The Griffin Institute, Northwick Park Institute for Medical Research, Northwick Park and St Mark's Hospitals, London, HA1 3UJ, UK

## 1. Introduction

In the past few decades, nanomaterials with redox-activities (oxidant and antioxidant) have gained massive attention for their therapeutic purposes in deadly diseases such as cancer, strokes, osteoarthritis, and other neurodegenerative disorders such as Alzheimer's, Huntington's, and Parkinson's disease. The ability of nanomaterials to generate reactive oxygen species (ROS) is oxidant-activity, and scavenging of ROS is antioxidant-activity. Moreover, ROS are generated in normal biological processes and can decrease or increase pathological conditions.<sup>1-3</sup> Therefore, the dual actions of redox-active foreign particles/nanoparticles as ROS generators and scavengers, can act like a double-edged sword to control the ROS in various pathological conditions as presented in schematic Fig. 1. The generation and scavenging of ROS are two important properties of redox-active nanoparticles which have tremendous potential for application in biomedicine as ROS scavengers to aid ischemia-reperfusion injury, stroke, skeletal conditions, myocardial infarction, neurodegeneration, and diabetes.<sup>4-7</sup> However, controlling the properties of redox-active nanomaterials (RANs) *in vivo* and under pathological conditions is challenging.

Reactive oxygen species (ROS) include free oxygen radicals and other molecules with at least one oxygen atom and one or

more unpaired electrons that can exist independently.<sup>8</sup> The presence of an unpaired electron in these species makes them extremely unstable and reactive. Radicals can act as oxidants or reductants, depending on whether they give or take an electron.



**Kapil D. Patel**

*to Research Professor at Dankook University and worked at University College London (UCL), UK as visiting Research Fellow (2019–2020). He moved to the Korea University, South Korea (2020–2021) as a Research Professor, and then to the University of Bristol, UK as a Senior Research Associate (2021–2023). Currently, he is Research Fellow (Level B) at the Australian National University, Australia. His research interests include the development of functional nano-biomaterials for tissue repair and regeneration, 3D bioprinting, redox-active nanomaterials, and cancer theranostics.*

*Kapil D. Patel received his MSc in Physics from the Indian Institute of Technology (IIT) Guwahati, India, in 2010, and PhD in Nanobiomedical Science with a major in Tissue Regeneration Engineering from Dankook University, South Korea, in 2015. He continued his research as a Postdoctoral Research Fellow at the Institute of Tissue Regeneration Engineering (ITREN), Dankook University (2016–2019). He was promoted*

Several common biological functions, such as aerobic metabolism and pathogenic defense mechanism, produce radicals. Furthermore, external exposures including radiation, pollution, dust particles, and smoke from cigarettes can also cause free



**Zalike Keskin-Erdogan**

*Tissue Engineering. Currently, she is a postdoctoral research fellow at Imperial College London (ICL), UK in the Department of Chemical Engineering. Her research expertise spans multiple disciplines, including materials science, biomaterials, cell biology, and tissue engineering, and utilization of biomaterials and hydrogels for 3D cell cultures and cell encapsulation, and microfluidics.*

*Zalike Keskin Erdogan completed her BEng (2013) and MSc (2015) degree in Bioengineering, specialized in Biomaterials, at Ege University, Izmir, Turkiye. She was awarded a prestigious fully funded scholarship by the National Ministry of Education to pursue her studies abroad, leading her to complete her PhD (2022) at University College London (UCL), UK in the Medical Sciences Faculty, focusing on Biomaterials and*



**Adam W. Perriman**

*novel synthetic biomolecular systems, and his research interests span the field of biomaterials, biophysics, and synthetic biology.*

*Adam Perriman is a Professor of Bioengineering at the Australian National University and holds a joint appointments with the School of Cellular and Molecular Medicine, University of Bristol, UK. His position at the ANU is held across the Research School of Chemistry (RSC), and the John Curtin School of Medical Research (JCSMR). He is internationally distinguished for his pioneering research on the construction of*



**Hae-Won Kim**

*Center (2009), Global Research Lab (GRL, 2015), UCL Eastman-Korea Joint Center (2017), and Medical Research Center (MRC, 2021). The fundings gained are in total of ~50 M USD. Currently, he is Editor-in-Chief of Journal of Tissue Engineering (IF 8.2), Associate Editor of Med-X and Frontiers in Bioeng. and Biotech., and editorial board member of many other journals (Biomaterials, Bioactive Materials, etc.). Prof. Kim's research includes therapeutic biomaterials for tissue regeneration and mechanobiological studies on cell-matrix interactions.*

*Hae-Won Kim is Director and Professor of Institute of Tissue Regeneration Engineering at Dankook University. He received his degrees from Seoul National University (BS in 1997, PhD in 2002). Prof. Kim has authored 510 peer-reviewed papers, with 39 000 citations and h-index of 102. He's also written 12 books and holds 165 patents. He has led various prestigious national and international research programs, including Priority Research*

radical production. Antioxidants are compounds that inhibit oxidation and work in two different ways to combat radicals.<sup>9</sup> Enzymatic antioxidants function by oxidizing damaging ROS to produce H<sub>2</sub>O<sub>2</sub>, which is then converted to water. Superoxide dismutase (SOD) catalyzes the formation of oxygen and H<sub>2</sub>O<sub>2</sub> from two superoxide anions. Furthermore, vitamin E, vitamin C, and glutathione are examples of non-enzymatic antioxidants that function by directly interacting with radical. For instance, glutathione has a free sulphydryl group, which makes it a desirable target for radical attacks. The enzyme glutathione reductase then squelches the free radical and recycles the oxidized glutathione.

Redox-active nanomaterials are mainly classified as inorganic, organic, or composite based on their chemical composition. Inorganic redox-responsive nanosystems offer unique physicochemical properties such as robustness, cost-effectiveness, stability, and ease of synthesis and modification.<sup>10</sup> These systems can achieve controlled drug release by incorporating reduction- or oxidation-responsive bonds and are generally easier to prepare and modify compared to organic ones.<sup>11</sup> Organic redox nanomaterials, on the other hand, are typically more biodegradable and biocompatible.<sup>12</sup> Composite redox-responsive nanomaterials, which integrate both inorganic and organic components, combine the strengths of each type, enhancing their physicochemical properties and often exhibiting synergistic effects.<sup>13</sup> In this study, our focus will mainly be on inorganic redox-active nanomaterials.

Various types of nanoparticles with a ROS generating or scavenging propensity have recently been synthesized and are currently at different stages of manufacturing. These are also being scrutinized for potential clinical translational application in nanomedicine. These nanomaterials are defined as RANs that include metallic/metallic oxide nanoparticles, carbon-based nanomaterials (CBNs) and some other sources of nanomaterials. Metallic nanoparticles of silver, gold, iron, zinc, palladium, platinum, and ruthenium, as well as nonmetal selenium nanoparticles are known to have intrinsic antioxidant properties, thus, these nanoparticles do not require any functional modification for additional antioxidant function. To enhance the antioxidant activities of these metallic nanoparticles, strategies such as oxygen moiety grafting,<sup>14–16</sup> peptide coating,<sup>17,18</sup> ligand-exchange,<sup>19–21</sup> and chemical conjugation of functional groups have been applied.<sup>14,22</sup> Metallic nanoparticles such as magnesium oxide (MgO), titanium dioxide (TiO<sub>2</sub>), vanadium oxide (V<sub>2</sub>O<sub>5</sub>), manganese oxide (MnO<sub>2</sub>), iron oxide (Fe<sub>3</sub>O<sub>4</sub>), copper oxide (CuO), zinc oxide (ZnO), gadolinium oxide (Gd<sub>2</sub>O<sub>3</sub>), and cerium oxide (CeO<sub>2</sub>) have been tested for better antioxidant and catalytic activities. CBNs including fullerenes, carbon nanotubes (CNTs), carbon nanodots and metal-doped carbon nanodots, graphene oxide (GO), reduced graphene oxide (rGO), graphene quantum dots (GQDs) and few layer graphene (FLG), and metal nanoparticles conjugated GO have also been investigated for their antioxidant and redox-activities.<sup>23–26</sup> Lately, up-conversion nanoparticles (UCNPs) have also gained significant attention for antioxidant and redox-active applications in nanomedicine.

This review paper highlights oxidative stress in physiological and pathological conditions, and the roles of RANs-associated ROS linked to cellular and molecular mechanisms. The redox-active mechanism of RANs and their roles in oxidase, peroxidase, SOD, radical, and peroxynitrite activities have thoroughly been explored and summarized. Finally, the roles of ROS generated by RANs in various diseases such as cancer, neurodegeneration, infection, and other conditions, along with their role in tissue engineering, have also been discussed in detail.

In recent years, the therapeutic applications of RANs to target ROS have been intensively studied. Current research has emphasized the roles of ROS in some pathological conditions and suggested ROS-based nanomedicine.<sup>27–30</sup> However, the review papers mainly focused on ROS's roles in certain diseases' pathological condition. In this review, we discuss the broad range of nanomaterials and their ROS generating or scavenging properties and underlying mechanisms of ROS *in vitro* and *in vivo* disease models. We have also listed nanomaterials with their application in various diseases and regenerative medicine. The family of RANs, various redox-activities and their roles in diseases and regenerative medicine are depicted in Fig. 1.

## 2. Oxidative stress in biology and medicine

The impact of oxidative stress has been intensively studied in the field of biomedicine over the last few decades.<sup>27,31,32</sup> An imbalance between ROS and antioxidants is known as oxidative stress, this can be caused by any form of free radical, oxygen-containing molecules such as superoxide ion/radical, hydrogen peroxide and peroxynitrate. These radicals contain an uneven number of electrons that easily react with proteins/lipids disrupting redox reaction/signalling and eventually causing molecular damage in the body.<sup>33</sup> Oxidative stress plays a vital role in normal physiology and the pathophysiology of many life-threatening diseases. Essentially all complex organisms are affected by oxidative stress and free radicals. Although oxidative stress in biology and medicine has been studied for decades, its functional and mechanistic diversity in varying microenvironments has attracted huge attention in the last few years.<sup>34–37</sup> Oxidative stress in biology and medicine is part of research of human and animal biology at both the cellular and molecular level.<sup>36</sup> Redox homeostasis-based strategy to control the ROS in production has gained great attention due to controllable scale. Lin *et al.* have developed a radiotherapy-mediated redox homeostasis-controllable nanomedicine for amplifying ferroptosis sensitivity in tumor therapy.<sup>38</sup> This strategy can achieve high efficacy of ROS production and modulate the tumor cell microenvironment antioxidant to amplify ferroptosis. Moreover, many of the biological consequences of vitamin and selenium deficiency or excess radiation exposure are thought to be the result of oxidative damages.<sup>39</sup> Several reports have also highlighted the role of oxidative damage in human diseases such as cancer, osteoarthritis, chronic inflammatory

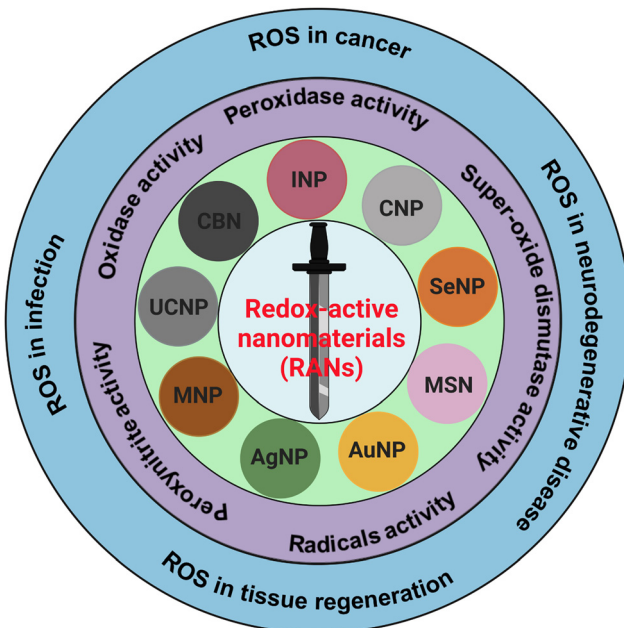


Fig. 1 RANs and their diverse redox-activities and applications in diseases and regenerative medicine. Various nanoparticles including silver nanoparticles (AgNPs) gold nanoparticles (AuNPs), magnetic nanoparticles (MNP), mesoporous silica-based nanoparticles (MSNs), selenium nanoparticles (SeNPs), cerium oxide nanoparticles (CNP), iron oxide nanoparticles (INPs), carbon-based nanoparticles (CBNs), up-conversion nanoparticles (UCNPs), and several other nanoparticles are summarized for its redox-activities in biomedicine.

diseases, neurodegenerative diseases, and retinopathy of prematurity.

## 2.1. The oxygen paradox

A variety of biological processes, including cell viability/death, cell signalling, differentiation, and the creation of inflammation-related factors, are naturally triggered by ROS during aerobic respiration in the cell. Radicals and non-radicals are two subcategories of biologically significant ROS. A list of free radicals in human biology, its origin, roles, and applications are summarized in Table 1. In a living organism, ROS are created as a result of regular cellular metabolism and external influences including metal toxicity, cigarette smoke, air pollutant, salinity and drought.<sup>40</sup>

ROS are highly reactive, thus excessively produced ROS can rapidly bind to cell membrane proteins or lipids, nucleic acids, and carbohydrates leading to irreversible structural alteration. Thus, controlling the reducing and oxidizing (redox) states of ROS is critical for cellular activation, viability, proliferation and, ultimately, organ function. Endogenous antioxidant systems exist, in that, enzymatic and non-enzymatic mechanisms normally operate to chelate ROS in healthy normal organisms. Nevertheless, overproduction of ROS in the pathological conditions mentioned above often leads to an imbalance of oxidant and antioxidant levels, resulting in an oxidative stress condition. Highly reactive oxygen radicals can also affect gene expression by up-regulation of redox-sensitive transcription

factors and chromatic remodeling through modulation of histone acetylation and deacetylation.<sup>69,70</sup>

In healthy physiology, the simultaneous oxidation and reduction of  $O_2^-$ , and  $\cdot OH$  form  $H_2O_2$  which is then broken down by the enzyme glutathione peroxidase in the presence of metals in the reduced state. For instance, mitochondria produce about one-third of the liver's total glutathione peroxidase activity.<sup>71</sup>  $O_2^-$ , the mediator in an oxidative chain reaction and the product of the one electron reduction of oxygen (from  $^1O_2$ ) molecules, is the precursor to the majority of ROS. Additionally, superoxide, which can be reduced to  $H_2O$  or  $\cdot OH$ , catalyzes the dismutation of  $O_2$  to produce  $H_2O_2$ .<sup>72</sup> Among normal biological processes, most ROS are produced as by-products of the interaction of oxygen with the leaking electrons from the electron transport chain (ETC), in particular protein complexes CI and CIII of the mitochondrial respiratory chain.<sup>73</sup> Additionally, metal-catalyzed oxidation reactions generate ROS as intermediates. In the outer shell of the oxygen atom, there are two unpaired electrons. The sequential reduction of oxygen by adding electrons results in the formation of excessive ROS summarized in Fig. 2(a). The breadth of ROS generated by oxygen reduction is demonstrated by the application of photo-sensitive gold nanoparticles in photodynamic cancer therapy. Fig. 2(b) highlights that the stepwise oxidation and reduction processes triggered by photocatalyst absorption can produce ROS from  $H_2O_2$  or  $O_2$ , respectively.

Ranking ROS in terms of their toxicity in mammalian systems involves considering their reactivity, stability, and potential to cause cellular damage. Table 2 is the general ranking of ROS based on their toxicity from most to least harmful:

In summary, superoxide and peroxynitrite both are harmful to mammalian cells. Peroxynitrite is generally considered as more toxic due to its reactivity and potential to cause significant damage to the cell membrane. The impact of upregulated ROS levels should be evaluated in the context of the overall redox balance and the cell's ability to neutralize the ROS with antioxidants.

## 2.2. Molecular switches in oxidative stress

Eukaryotic cells have evolved to harness energy in the form of adenosine triphosphate (ATP). Enzymatic reduction of ATP (catabolic) enables the generation of macromolecular precursor nucleotides, and amino acids (anabolic). ROS are generated within the electron transport chain (ETC) in mitochondria which facilitates this energy utilization, with about 0.1–0.2% of the total  $O_2$  consumed through ETC type I and III complexes generating ROS.<sup>86,87</sup> Additionally, in the process of energy metabolism, the signalling molecule known as the mammalian target of rapamycin complex 1 (mTORC1) receives signals from both amino acids and glucose.<sup>88</sup> Eukaryotic cells frequently include mTORC1 downstream signalling, serving as an important signalling node that connects nutrition sensing and metabolic control. Since cellular metabolism and cell survival are tightly related, signalling pathways for metabolic activity and autophagy may interact despite being functionally

Table 1 Summary of free radicals involved in biological processes

Name of free radicals	Chemical formula	Origin and role	ROS concentration level and disease	Ref.
Superoxide radical	$O_2^{\bullet-}$	<ul style="list-style-type: none"> <li>Superoxide radical generated as by product of cellular respiration (mitochondrial respiratory chain) and can lead to the formation of other types of ROS.</li> <li>It plays a dual role, at physiological balance level, by product of <math>O_2</math> reduction for the cellular signalling.</li> <li>At pathological level, induces cellular apoptosis, necrosis, ferroptosis, pyroptosis, and cell death.</li> </ul>	<ul style="list-style-type: none"> <li>Diffusion-limited rate <math>2 \times 10^9 \text{ M}^{-1} \text{ s}^{-1}</math>.</li> <li>Superoxide radical-based ROS level in normal cell is in nanomolar (nM) range, while in cancer cell range is in micromolar (<math>\mu\text{M}</math>)</li> </ul>	41 and 42
Hydroxyl radical	$\bullet\text{OH}$	<ul style="list-style-type: none"> <li>Hydroxyl radical is formed from water during various biochemical reactions.</li> <li>In presence of hydrogen peroxide and iron ions produced hydroxyl radical <i>via</i> Haber–Weiss reaction.</li> <li>It is highly reactive, and can damage the DNA, proteins, and lipids.</li> </ul>	<ul style="list-style-type: none"> <li>Diffusion limit rate for hydroxyl radical is <math>1.9 \times 10^{10} \text{ M}^{-1} \text{ s}^{-1}</math>.</li> <li>Hydroxyl radical concentration range in normal cell is very low nanomolar.</li> <li>However, in cancer, inflammation, and neurodegenerative diseases it is in mid high nanomolar to micromolar range.</li> <li>In infection, high nanomolar to low micromolar range.</li> </ul>	43–45
Peroxyl radical	$\text{ROO}^{\bullet}$	<ul style="list-style-type: none"> <li>Hydroxyl radical induces polymerization of human fibrinogen.</li> <li>Peroxyl radical commonly formed during oxidation of lipids.</li> <li>They form as a natural byproduct during the various cellular events including metabolism of lipids, and chain reaction of lipid peroxidation.</li> <li>It plays main role in lipid peroxidation, cellular damage, oxidative stress, antioxidant defense, and cell signalling.</li> </ul>	<ul style="list-style-type: none"> <li>Diffusion limit rate for hydroxyl radical is <math>1.9 \times 10^{10} \text{ M}^{-1} \text{ s}^{-1}</math>.</li> <li>Peroxyl radical concentration range in normal cell is very low nanomolar.</li> <li>However, in cancer, inflammation, and neurodegenerative diseases it is in mid high nanomolar to micromolar range.</li> <li>In infection, high nanomolar to low micromolar range.</li> </ul>	46–49
Hydroperoxyl radical	$\text{HO}_2^{\bullet}$	<ul style="list-style-type: none"> <li>Hydroperoxyl radical generate in biological systems during the dismutation of superoxide.</li> <li>Excessive level of hydroperoxyl radicals can leads to oxidative damage to biomolecules including lipids in cell membranes.</li> <li>Hydroperoxyl radical is associated with various pathological conditions and contribute to the aging process.</li> <li>Hydroperoxyl radicals are also associated with the immune's system defense against pathogens.</li> </ul>	<ul style="list-style-type: none"> <li>Diffusion limit rate for hydroperoxyl radical is <math>2.3 \times 10^8 \text{ M}^{-1} \text{ s}^{-1}</math>.</li> <li>Hydroperoxyl radical concentration for normal cell is low nanomolar range.</li> <li>However for cancer cell, inflammation, are mid to high nanomolar to low micromolar.</li> <li>Neurodegenerative diseases mid to high nanomolar to micromolar range.</li> </ul>	45 and 50–52
Alkoxy radical	$\text{RO}^{\bullet}$	<ul style="list-style-type: none"> <li>Alkoxy radicals are generated during the breakdown of peroxides.</li> <li>Alkoxy radicals are reactive and participate in redox reactions.</li> <li>They involved in the lipid peroxidation process, free radicals damage lipids in cell membranes.</li> </ul>	<ul style="list-style-type: none"> <li>Diffusion limit rate for hydroperoxyl radical is <math>1 \times 10^9 \text{ M}^{-1} \text{ s}^{-1}</math>.</li> <li>Alkoxy radical concentration range for normal cell is low nanomolar.</li> <li>However, for cancer and inflammation range is mid to high nanomolar to low micromolar.</li> <li>For infection, high nanomolar to low micromolar.</li> <li>Neurodegenerative diseases, mid to high nanomolar to micromolar range.</li> </ul>	53–55
Carbonate radical	$\text{CO}_3^{\bullet-}$	<ul style="list-style-type: none"> <li>The carbonate radicals can be formed through different pathways including reaction involving peroxides and other ROS.</li> <li>It can generate in presence of hydrogen peroxide and bicarbonate ions.</li> <li>Carbonate radicals are highly reactive and can oxidized organic and inorganic molecules and leads to the modification of biomolecular and cellular structure.</li> <li>Potentially contribute the oxidative stress in the biological system,</li> </ul>	<ul style="list-style-type: none"> <li>Diffusion limit rate for carbonate radical is <math>5.27 \times 7.89 \times 10^5 \text{ M}^{-1} \text{ s}^{-1}</math>.</li> <li>Carbonate radical concentration for normal cell is low picomolar range.</li> <li>For cancer, it is low to mid nanomolar.</li> <li>For inflammation, it is mid to high nanomolar range.</li> <li>Infection, it is high nanomolar range.</li> <li>Neurodegenerative diseases, it is mid to high nanomolar to low micromolar range.</li> </ul>	56–60
Nitric oxide radical	$\text{NO}^{\bullet}$	<ul style="list-style-type: none"> <li>Nitric oxide radicals are synthesized endogenously by various cell types, primarily through the action of enzyme called nitric oxide synthases (NOS).</li> <li>Nitric oxide radicals act as a cell signalling molecules in various physiological process.</li> <li>It is involved in blood vessel dilation in cardiovascular system, and relaxation in smooth muscle cells.</li> <li>Act as neurotransmission in nervous system, body defense system against pathogens, anti-inflammatory.</li> </ul>	<ul style="list-style-type: none"> <li>Diffusion limit rate for nitric oxide radical is <math>6.7 \times 10^9 \text{ M}^{-1} \text{ s}^{-1}</math>.</li> <li>Nitric oxide radical for normal cells is 1 to 100 nanomolar range.</li> <li>For cancer, it is from 20 to 500 nanomolar range.</li> <li>For inflammation, it is 100 nanomolar to 1 micromolar range.</li> <li>Infection, it is 100 nanomolar to 1 micromolar range.</li> <li>Neurodegenerative diseases, it is 50 nanomolar to 1 micromolar range.</li> </ul>	61–64

Table 1 (continued)

Name of free radicals	Chemical formula	Origin and role	ROS concentration level and disease	Ref.
Thiyl radical	$\text{RS}^{\bullet-}$	<ul style="list-style-type: none"> <li>• Thiyl radicals are formed through the homolytic cleavage of sulphur-hydrogen bond.</li> <li>• In biological system, thiyl radicals are generated during the oxidative stress, and redox reactions involving thiol-containing biomolecules.</li> <li>• Thiyl radicals serve as intermediates in the transfer of electrons during various cellular processes including antioxidant defense, cellular signalling, and redox balance in cellular process.</li> <li>• Dysregulation of thiyl radicals and thiol redox balance are associated with various diseases including neurodegenerative disorder, and cardiovascular diseases.</li> </ul>	<ul style="list-style-type: none"> <li>• Diffusion limit rate for thiyl radical is <math>1 \times 10^8 \text{ M}^{-1} \text{ s}^{-1}</math>.</li> <li>• Thiyl radical concentration range for normal cells is picomolar to low nanomolar range.</li> <li>• Cancer cell, low to mid nanomolar range.</li> <li>• Inflammation condition, mid to high nanomolar.</li> <li>• Infection, it is high nanomolar to low micromolar range.</li> <li>• Neurodegenerative diseases, it is mid to high nanomolar to micromolar range.</li> </ul>	65–68

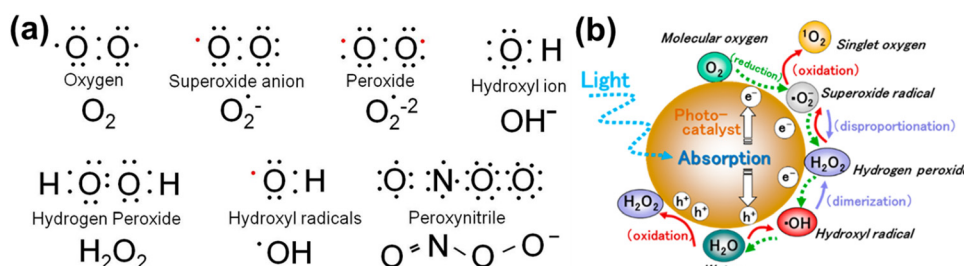


Fig. 2 (a) Electronic structure of some common ROS. The structure of chemical formula and corresponding name are provided, and unpaired electron are designated as a red dot (●). (b) Reactive oxygen species generated in the photocatalytic redox-reactions, and steps into  $\text{O}_2$  and  $\text{H}_2\text{O}_2$ . ROS in free-radical form such as superoxide radicals, hydrogen peroxide, and hydroxyl radicals may be produced sequentially from molecular oxygen ( $\text{O}_2$ ) via a stepwise reduction mechanism, and reversibly from hydroxyl radicals, hydrogen peroxide, superoxide radicals, and singlet oxygen as well from water ( $\text{H}_2\text{O}$ ) via a stepwise oxidation mechanism. Reproduced with permission from Nosaka *et al.*<sup>29</sup> [Copyright 2019, American Chemical Society].

independent.<sup>89</sup> According to a study by Dibble *et al.*, mTORC1 may serve as a link between the anabolic process and the circumstances that promote cellular development.<sup>90</sup> Moreover, mTORC1 signals are integrated with systemic signals, including secreted growth factors, as well as intracellular signals, such as amino acids, glucose, oxygen, and ATP.

Autophagy, a catabolic process responsible for clearing out damaged organelles and unnecessary dysfunctional components in cells, occurs in normal and stressed conditions including viral infection, nutrient deprivation, and genotoxic effects. Recent studies have reported that the oxidative stress created by ROS and reactive nitrogen species (RNS) might converge to trigger sustained autophagy.<sup>91</sup> Furthermore, autophagy is closely linked to redox homeostasis and metabolic networks, which involve both nitrosative and oxidative stress.

Thiol-containing proteins can undergo reversible post-translational changes, which are known to be damaging to both biological biomolecules and signal mediators.<sup>92</sup> Protein activity is regulated by these thiol-based redox switches, which are also essential for cellular ROS response and adaptation to local and global changes. First responder proteins control redox levels *via* ROS-specific transcription factors, chaperones,

or metabolic enzymes to protect cells from increasing amounts of oxidants, repair the damage, and restore redox homeostasis. In addition, phosphatases and kinases are regulated by redox-regulation, resulting in ROS generation that is considered to be a crucial second messenger in growth, development and differentiation.<sup>93</sup> ROS are essential for cell growth and differentiation, and excessive ROS production in the cell causes apoptosis.<sup>94</sup> Several studies have reported the roles of ROS during the differentiation of embryonic stem cells (ESC).<sup>95</sup> For example, ROS are transiently elevated during the G2/M period of the cell cycle, differing from other differentiated mature cells. It is of interest to highlight that ESCs produce little ATP due to their immature mitochondria, leading ESCs to be presumably resistant to the oxidative stress condition.<sup>5</sup> To meet energy demand, ESCs mainly utilize glycolysis instead of mitochondrial oxidative phosphorylation to avoid ROS production. Thus, the produced nicotinamide adenine dinucleotide phosphate (NADPH) from glycolysis can maintain thioredoxin and glutathione to support scavenging ROS.<sup>96,97</sup> ROS also plays a crucial role in the differentiation of embryonic hematopoietic stem cells and cardiomyocytes.<sup>95,98</sup> Adult stem cells (ASC) have the capability to regenerate in injured tissues throughout their

Table 2 Summary of free radicals with ranking of ROS level toxicity in mammalian cells

ROS species	Toxicity level	Description	Ref.
Hydroxyl radical ( $\cdot\text{OH}$ )	Extremely high	<ul style="list-style-type: none"> <li>It is one of most reactive ROS, can cause significant damage to DNA, proteins, and lipid due to high reactivity and lack of selectivity.</li> <li>Even at very low concentration, can induce severe oxidative damage.</li> </ul>	74 and 75
Peroxynitrite ( $\text{ONOO}^-$ )	Very high	<ul style="list-style-type: none"> <li>Peroxynitrite is a potent oxidant formed from the reaction of nitric oxide (<math>\text{NO}^\bullet</math>) with superoxide (<math>\text{O}_2\cdot^-</math>).</li> <li>It can nitrate tyrosine residues in proteins, leading to functional alteration and damage.</li> <li>Highly damaging to the cells and tissue.</li> </ul>	76 and 77
Superoxide anion ( $\text{O}_2\cdot^-$ )	High	<ul style="list-style-type: none"> <li>Superoxide is a primarily ROS that can lead to the formation of other, or more reactive species like hydrogen peroxide, hydroxyl radicals.</li> <li>It is less reactive than hydroxyl radicals with significant toxicity.</li> <li>It can disrupt the cellular functions and contribute to the formation of other toxic ROS.</li> </ul>	78 and 79
Alkoxy radical ( $\text{RO}^\bullet$ )	Moderate	<ul style="list-style-type: none"> <li>Alkoxy radicals are intermediate in reactivity.</li> <li>It is generated from decomposition of organic peroxides and can propagate lipid peroxidation.</li> </ul>	80 and 81
Hydroperoxyl radical ( $\text{HO}_2\cdot^\bullet$ )	Moderate	<ul style="list-style-type: none"> <li>Hydroperoxyl radicals are in equilibrium with superoxide and involved in lipid peroxidation.</li> <li>It is less reactive than hydroxyl radicals but still contribute to oxidative stress.</li> </ul>	50 and 82
Carbonate radical ( $\text{CO}_3\cdot^-$ )	Moderate	<ul style="list-style-type: none"> <li>Carbonate radicals can oxidize biomolecules but are generally less reactive than hydroxyl and peroxynitrite radicals.</li> <li>It is formed during the reactions involved peroxynitrite and bicarbonate.</li> </ul>	83 and 84
Nitric oxide radical ( $\text{NO}^\bullet$ )	Low to moderate	<ul style="list-style-type: none"> <li>Nitric oxide radical is less reactive than many other ROS.</li> <li>It has physiological importance such as vasodilation, and cell signalling.</li> <li>However, in high concentration or in combination with superoxide, it forms peroxynitrite, which is highly toxic.</li> </ul>	61 and 85

whole life span, retaining a propensity to differentiate into specific lineages. ASC such as neural and mesenchymal stem cells also maintain low levels of ROS by utilizing glycolysis with suppression of mitochondrial oxidative phosphorylation.<sup>99–101</sup> The mechanism of ROS scavenging changes under hypoxic conditions; hypoxia-inducible factor-1 $\alpha$  (HIF-1 $\alpha$ ) is produced through oxidative phosphorylation in the presence of elevated ROS. In ASC, Meis Homeobox 1 (MEIS1) regulates HIF-1 $\alpha$ ; Kocabas *et al.* have demonstrated that MEIS1 knockout in mice is entirely mediated through ROS and treatment of MEIS1 with the scavenger N-acetylcysteine maintains ASC function.<sup>102</sup> However, HIF-1 $\alpha$  enhances glycolytic metabolism from oxidative phosphorylation to glycolysis by upregulating gene expression with pyruvate dehydrogenase kinase (PDK1), glucose transporter 1 (GLUT1) and acetate dehydrogenase A (LDHA).<sup>103,104</sup> These all factors suggest that the glycolytic metabolism and hypoxia signalling are crucial for ROS regulation.

### 2.3. Cellular mechanisms of oxidative stress in human health

Oxidative stress plays a significant part in a wide range of diseases, including cancer, inflammation, wound healing, and neurological disorders. An imbalance in the generation and clearance of ROS can lead to oxidative stress, thus directly affecting cellular functions. If the imbalance is severe enough and not controlled by redox homeostasis, then it can lead to serious injuries in the cell and possibly cell death, either by apoptosis or necrosis.<sup>105,106</sup> This condition may involve the initiation and progression of certain disease pathologies. In response to tissue injury, cells develop various responses induced by ROS and activate repair mechanisms *via* modulation of downstream signalling molecules. In this section, we will discuss the mechanisms of oxidative stress within cancer

pathology, inflammation, wound healing, and neurodegenerative disease.

Oxidative stress is more prevalent in cancer cells than normal cells.<sup>107,108</sup> As mechanisms for normal cell repair and division fail during tumorigenic progression, the cycle of cancer cells speeds up resulting in higher energy demands for fast growth, uncontrolled cell division and cellular migration. The high cellular metabolism and oxygen consumption required to keep these energetic demands result in a higher accumulation of ROS leading to oxidative stress being more prevalent in cancer cells compared to normal cells.<sup>109</sup> The radicals and ROS produced in cancer cells induce several effects in the body, such that low concentrations of ROS mediate cell proliferation and tumor progression to the metastatic stage resulting in aggregation of tumor cells. On the other hand, high level of ROS induce a more contradictory outcome, activating cell death pathways in cancers as well as mediating cancer recurrence.<sup>110</sup> In the case of cell death initiation, the antioxidant system in cancer cells fail to control excessive ROS generation during oxidative stress resulting in cell death within the tumor. Thus, deciding how to implement ROS to affect tumors is challenging. Their use as part of combination therapies has been suggested, for example, using ROS modulating antioxidants together with chemotherapy could be more effective to deal with the different stages of tumor progression.<sup>111</sup>

In cancer cells, oxidative stress can be induced by oncogenic signalling, mitochondrial activation, metabolic activity, and increased enzyme activity.<sup>112,113</sup> Additionally, cytokines and growth factors such as insulin, platelet-derived growth factor (PDGF), transforming growth factor (TGF), tumor necrosis factor (TNF), and epidermal growth factor (EGF) can drive cancer cells to create intracellular ROS.<sup>114–116</sup> Under the hypoxic conditions observed during the intermediate stage of

tumor development due to inadequate vascularization, ROS-induced transcription of HIF-1 $\alpha$ , a fundamental member of hypoxia-inducing factors, stabilizes the encoded protein, which should be hydroxylated within five minutes by iron-dependent prolyl 4-hydroxylase (PDH), a HIF-1 $\alpha$  degrading enzyme.<sup>117</sup> As a consequence of HIF-1 $\alpha$  activation, several essential genes in cancer progression, such as vascular endothelial growth factor (VEGF) and VEGF-receptors, are induced.<sup>118</sup> It has been shown that epidermal growth factor receptors (EGF-receptors) and PDGF-receptors, along with activating mutations in K-ras, can initiate Akt signalling mediated by oxidative stress. In addition, hydrogen peroxide activates Akt either directly or *via* ROS-induced activation of phosphoinositide-dependent kinase 1 (PDK1), its upstream kinase.<sup>119</sup> Additionally, mutations of downstream growth factor receptors, like Kars-RAS 77, 78, can also result in an increase in superoxide generation.<sup>120,121</sup> Another downstream effector of numerous growth factor receptors, including EGF receptors and c-Mets, is the tiny Rho GTPase Rac-1.<sup>122</sup> Chavda *et al.* have recently summarized the role of ROS and the molecular mechanism of oxidative stress in cancer and brain stroke.<sup>123</sup> It has been well established that oxidative stress plays an important role in tumorigenesis *via* inflammation, immune evasion, autophagy and apoptosis control through signalling pathway regulation, angiogenesis, and drug resistance. The mitochondrial ROS cause of cell apoptosis and the oxidative-stress-mediated molecular mechanism of cancer progression are presented in Fig. 3.

The primary function of inflammation is to protect the body from infectious pathogens. It is usually not a disease condition itself but is commonly observed in various pathological conditions such as hepatitis B & C, malaria, dengue, and tuberculosis (TB) infections, autoimmune diseases, radiation, or toxic chemical damage, and even in obesity. Inflammation also occurs in non-pathological processes, including tissue rearrangement, elimination of cellular waste, and tissue regeneration. Recent investigations have shown that the progression of many chronic diseases is closely related to the situation of oxidative stress, where the resulting protein oxidation accelerates inflammatory responses.<sup>124,125</sup> Protein-oxidation induces the release of inflammatory signalling molecules including peroxiredoxins 2 (PRDX2).<sup>126</sup> During this response, proinflammatory mediators like tumor necrosis factor- $\alpha$  (TNF- $\alpha$ ) are released through activation of disintegrin, metalloproteinase-17 (ADAM-17), and PRDX2, a ubiquitous redox-active intracellular enzyme which also acts as a redox-dependent inflammatory mediator to activate macrophages after the release of TNF- $\alpha$ . It is of note that chronic inflammatory responses are commonly observed in insulin resistance, type 2 diabetes mellitus (T2DM), and cardiovascular diseases.

Wound healing is another redox-regulated biological process involving continuous and extending phases of homeostasis, inflammatory related events, cell proliferation, and new tissue formation.<sup>127</sup> Immediately after blood vessel injury, platelet aggregation and activation are initiated, forming blood clots that temporarily seal the wound site. The subsequent inflammatory response involves different immune cells such as

neutrophils and monocytes that are recruited into the wound. These immune cells secrete proteolytic enzymes and proinflammatory cytokines together with excessive ROS, which are essential to kill invading bacteria and other microorganisms. During normal aging or oxidative-stress-related pathological conditions such as diabetes, alcohol abuse, smoking, or infectious disease, the normal inflammatory response can be delayed or impaired.<sup>128</sup> Some interesting studies have suggested that ROS might be crucial regulators involved in all stages of wound healing process. Although ROS function as important regulators during wound healing, over production of ROS could cause molecular damage, disrupting the wound healing process resulting in the formation of chronic wounds. In fact, many studies have suggested that antioxidant strategies are effective and beneficial during the wound healing inflammatory response. Antioxidant strategies such as mitochondrial-targeted peptides like elamipretide, can protect against mitochondrial dysfunction and inflammation by activating NOD-like family receptors, including the pyrin domain 3 (NLRP3) inflammasome and inhibiting the nuclear factor-kappa B (NF- $\kappa$ B) signalling pathway, and the nuclear factor (erythroid derived 2)-like 2 (Nrf2).<sup>129</sup> Furthermore, sustained oxidative stress accelerates the inflammatory response in the chronic period of wound healing *via* ROS-stimulated chemotaxis and migration of neutrophil and macrophage cells to the wound area by expressing adhesion molecules in blood vessels. ROS can directly affect cell migration, proliferation, and extracellular matrix (ECM) production in fibroblast and keratinocytes.<sup>130</sup>

In neurodegenerative disorders including AD, PD, HD, and ALS, the ROS-induced oxidative stress is extremely high with comparatively low levels of antioxidants. Particularly in AD among other neurodegenerative disorders mentioned above, ROS-induced oxidative stress plays a critical role in the accumulation and deposition of  $\beta$ -amyloid peptide (A $\beta$  peptide). The aggregation of A $\beta$  peptides can lead to mitochondrial dysfunction and energy failure prior to plaque formation in the brain *via* impairing the electron transport system complex I and IV.<sup>131,132</sup> Similarly,  $\alpha$ -synuclein, a presynaptic protein in PD that forms Lewy bodies (LBs), is misfolded and aggregated causing a decrease of mitochondrial functions.<sup>133,134</sup> Importantly, the PD-related genes such as PINK1, DJ-1, LRRK2, and PARK2 (Parkin), are all involved in homeostasis of mitochondrial ROS.<sup>135,136</sup> Moreover, the induction of mitochondrial recruitment of Parkin by mitochondrial ROS plays an important role in the PINK1/Parkin-related mitophagy, as well as mutations or deficiency of PINK1.<sup>137</sup> HD is caused by a mutation in the Huntingtin (HTT) gene located on chromosome 4 (4p63).<sup>138</sup> This mutation leads to the expansion of CAG trinucleotide repeats, causing the aggregation of Huntingtin proteins and eventually neuronal death in the brain at the early stages of HD. Oxidative damage is suggested as one of the major pathological mechanisms due to the higher lipid concentrations and high energy requirement in the HD brain.<sup>139</sup> Mutant HTT proteins serve as of the initiator of ROS, due to oxidized proteins in partially purified mHTT aggregates.<sup>140</sup> Thus, oxidative damage

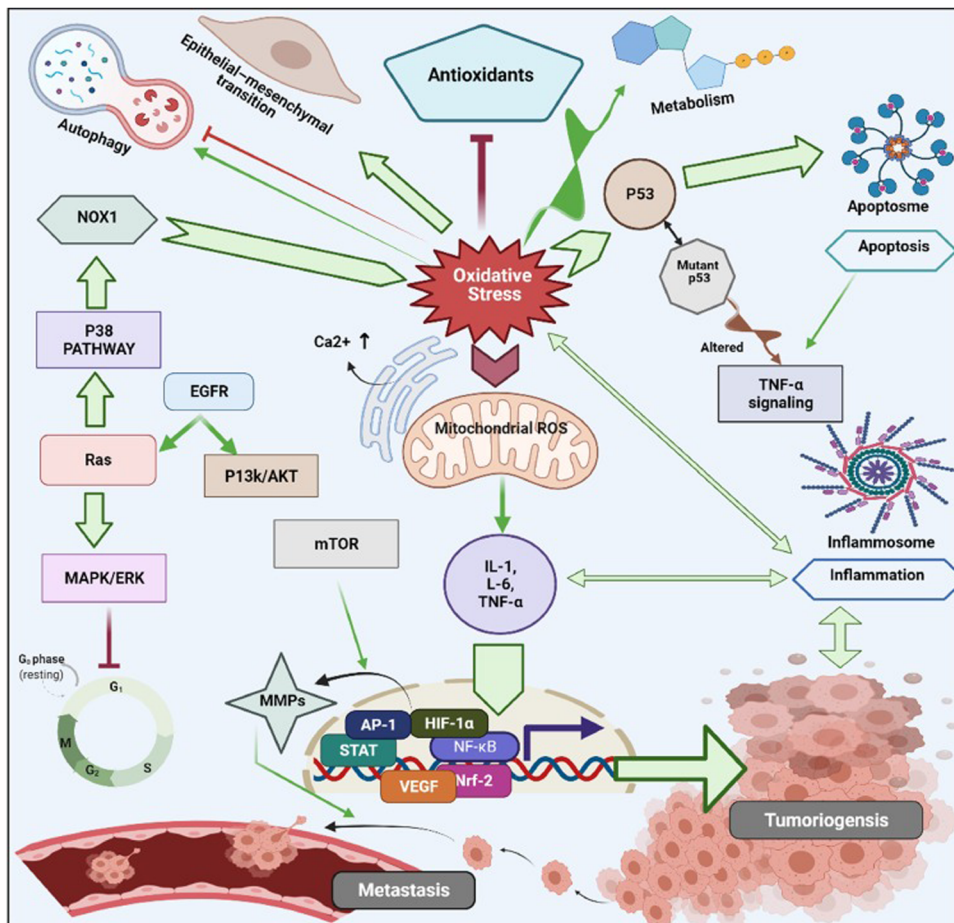


Fig. 3 Schematic illustration of various cell signalling pathways associated to oxidative stress mediated progression of tumorigenesis and metastasis. Under oxidative stress, intracellular ROS activates cancer cell surviving signalling cascades such as MAPK/ERK1/2, p38, JNK, PI3K/Akt, which leads to activation of transcription factors such as NF- $\kappa$ B, MMPs, AP-1, HIF-1 $\alpha$ , STAT, Nrf2, VEGF. These transcriptional factors cause imperative pathophysiolgies aggravating carcinogenesis, and cancer metastasis. Reproduced with permission from Chavda *et al.*<sup>123</sup> [Copyright 2022, Elsevier].

has been suggested as one of the major pathological mechanisms in the early stages of HD progression.<sup>141</sup> The roles of oxidative stress in neurodegenerative diseases such as AD, PD, and HD and corresponding cellular and molecular details are summarized in Fig. 4.

Reactive oxygen species play a crucial role in the ageing process as pathogenic components. These extremely reactive chemicals, such as superoxide (a free radical) and hydrogen peroxide (a non-radical molecule), are naturally produced during cellular metabolism, especially in the mitochondria. Under normal physiological conditions cells have a homeostatic equilibrium in between ROS and presence of antioxidant mechanisms. As we age this equilibrium shifts towards higher levels of ROS as a result of a decrease in mitochondrial activity and antioxidant capability.

Elevated levels of ROS are detrimental and can result in significant harm to cellular and organelle membranes, DNA, and proteins.<sup>142</sup> Gradual oxidation over a period of time and decline in ATP production cause damage to cells and tissues which is one of the causes of aging. ROS are involved in the development of other age-related illnesses, including

neurological conditions like Alzheimer's and Parkinson's diseases, cardiovascular diseases, and malignancies.<sup>143,144</sup> These molecules have the ability to initiate and alter various cellular signalling pathways that result in apoptosis, inflammation and cellular senescence, hence affecting the process of ageing and the progression of diseases.<sup>145</sup>

ROS have a crucial impact on the ageing process and the emergence of age-related ailments through the initiation of oxidative harm and the disturbance of cellular equilibrium. Gaining a comprehensive understanding of the processes involved in the generation and reduction of ROS is essential for the development of effective treatment approaches to address the effects of ageing and its related diseases.

### 3. Nanomaterials possessing antioxidant and redox-activities

Antioxidants are molecules/compounds/materials that can react with radicals by donating an electron,<sup>8</sup> radical addition,<sup>46</sup> H-atom donation,<sup>146</sup> as well as regeneration by

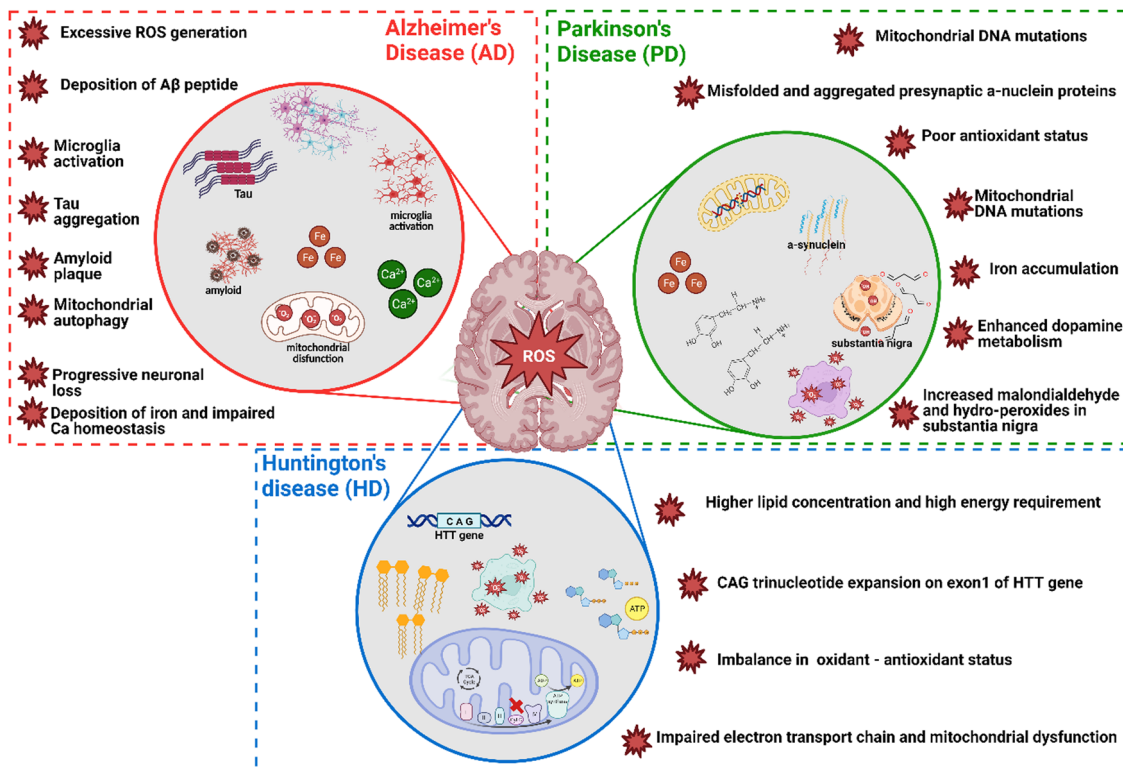


Fig. 4 The role of oxidative stress in neurodegenerative disease namely AD, PD and HD; three circles in the figure represent three main neurodegenerative diseases, red star ROS symbols provide the detailed role of oxidative stress and associated cellular and molecular effects. Figure created by authors using BioRender.com.

other reducing agents,<sup>147</sup> preventing unfavorable biochemical chain reactions by converting them to nontoxic metabolites. In other words, antioxidants can bind to oxidizable molecules, protecting cells by delaying or inhibiting their autoxidation.<sup>148</sup> Antioxidants can therefore reduce oxidative stress, playing a key role in the mediation and control of ROS induced deadly diseases. They can be categorized as preventive antioxidants and chain breaking antioxidants. Preventative antioxidants are a heterogeneous class of molecules/compounds including metal chelators,<sup>149</sup> hydroperoxide-decomposing agents,<sup>150</sup> and glutathione peroxidase;<sup>151</sup> their main role is to interrupt the initiation rate of ROS generation.<sup>152</sup> On the other hand, the main role of chain-breaking antioxidants is to slow down (or inhibit) the autoxidation. The antioxidants that break chains are also known as radical-trapping antioxidants. For example, phenols are the best-known chain-breaking antioxidant as they can rapidly trap 2-preoxyl radicals per molecule. Tocopherols (vitamin E), ascorbate (Vitamin C) flavonoids, and stilbenes are some other examples of chain-breaking antioxidants.<sup>153</sup>

Some best practices to measure oxidative-stress induced by nanoparticles, it is important to have strong and sensitive assays to detect reactive oxygen species and related oxidative damage.<sup>8,145</sup> There are several potential assays that can be used, including the dichloro-dihydro-fluorescein diacetate (DCFH-DA) assay, the thiobarbituric acid reactive substances (TBARS) assay, and the glutathione (GSH/GSSG) assay. The DCFH-DA assay is commonly used to measure oxidative stress

and assess ROS generation.<sup>154–156</sup> The TBARS assay measures malondialdehyde (MDA), a byproduct of lipid peroxidation caused by nanoparticles.<sup>157,158</sup> Additionally, the GSH/GSSG assay measures reduced (GSH) and oxidized (GSSG) glutathione levels, which can give insight into the cellular redox state.<sup>159,160</sup> According to the previous report, it is important to include both positive (e.g.,  $H_2O_2$  treatment) and negative controls (untreated cells) when conducting these assays.<sup>155</sup>

In the last several decades, numerous nanomaterials have been developed and evaluated for their antioxidant properties to see if they can provide defense against oxidative damage.<sup>153</sup> Nanomaterials such as metals/nonmetals (Cu, Ag, Au, Pt, and Se), metal oxides ( $TiO_2$ ,  $ZnO$ ,  $Fe_3O_4$ ,  $CeO_2$ ), carbon-based nanomaterials (fullerenes, CNTs, GO, GQDs, nanodiamonds), nanomaterials developed as delivery tools ( $Ce@SiO_2$ ,  $Ce@GO$ ), and UCNPs have shown intrinsic redox-activities like superoxide dismutase (SOD) or catalase-like activities often associated in radicals trapping. Grafting or modifying nanomaterials with low molecular weight antioxidants can sometimes make them antioxidants. In this section, we have categorized the above nanomaterials and discussed their antioxidant/redox-activities and mechanism of action in different physiological conditions.

### 3.1. Metallic nanomaterials

Metallic nanoparticles (silver, gold, palladium, platinum, and ruthenium) and nonmetal (selenium) mostly possess intrinsic antioxidant properties and these nanoparticles do not require

any functional modification for having antioxidant properties. These nanoparticles do not need to be functionally modified in order to exhibit antioxidant activities and they exhibit oxidase-like activity under acidic conditions and in the presence of oxidizing agents like 2,2-azinobis(3-ethylbenzothiazoline-6-sulfonic acid) and 3,3',5,5'-tetramethylbenzidine (TMB).<sup>161–165</sup> Unlike antioxidant activity, which only occurs at neutral or basic pH levels, this redox-activity occurs at acidic pH levels, similar to that of peroxidase enzymes. A Fenton-like reaction on the surface releases OH radicals, resulting in the peroxidase activity.<sup>29</sup>

**3.1.1. Silver nanoparticles.** Silver nanoparticles (AgNPs) are well known antibacterial and antioxidant materials used for biomedicine. Keshari *et al.* have demonstrated the antioxidant property of AgNPs by employing 2,2-diphenyl-1-picrylhydrazyl, hydrogen peroxide, hydroxyl radical and superoxide radical scavenging methods.<sup>166</sup> They suggest that the antioxidant activity of AgNPs is caused by the presence of bioactive-compound (molecules/functional) groups on their surface. The mechanism underlying the antioxidant activity of AgNPs is complicated and seems to vary depending on synthesis protocols, physical parameters, and particle surface chemistry. In a study by Prasad *et al.*, a complex antioxidant enzyme network was proposed as a possible mechanism of biosynthesis for AgNPs.<sup>167</sup> Moreover, internalization of AgNPs into cells by endocytosis is followed by release of the compounds from the surface of particles, particle aggregation, and surface oxidation, resulting in the release of silver ions.<sup>168</sup> The interaction of AgNPs with membrane proteins activates signalling pathways and inhibits the cell proliferation in cancer cells.<sup>169,170</sup> AgNPs and surface oxidized silver oxide exhibit great affinity for sulfur containing functional groups and are thus able to bind with proteins, enabling direct modulation of antioxidant enzymes. Moreover, AgNPs themselves and other nanoparticles doped with AgNPs have been proven as effective antibacterial agents, acting as an antineoplastic drug with anti-apoptotic activity. ROS production depends on the size of AgNPs, with the smaller size of nanoparticles exhibiting higher ROS production. In line with this finding, Onodera *et al.* have recently found that AgNPs-induced ROS production occurs in a size dependent manner.<sup>171</sup> They found that the ROS were rapidly generated right after treatment with 1 nm and 70 nm AgNPs for 5 and 60 min; but there was no ROS production by AgNO<sub>3</sub>. They also detected ROS from whole cell lysate and mitochondria at 5 and 60 min after AgNPs exposure; this was the first study reporting the local production of ROS induced by AgNPs. Similarly, Carlson *et al.* also reported a significantly higher ROS production together with a decrease to undetectable levels of the reduced state of glutathione (GSH), an important antioxidant, in macrophages exposed to smaller (15 nm) AgNPs as opposed to their larger counterparts.<sup>172</sup> This interaction of AgNPs with cellular proteins *via* thiol groups has been suggested to interfering with thiol based redox switches that regulate ROS production, such as ROS-specific transcriptional regulators, and GSH antioxidant defense mechanisms by interacting with GSH reductase.<sup>173</sup> The higher surface area of smaller AgNPs

relative to their volume have been suggested as one of the characteristics making these particles more reactive for interactions with thiol groups. A significant reduction of both protein and non-protein sulphydryl (thiol) groups has also been reported *in vivo* studies upon exposure to AgNPs.<sup>174</sup> Moreover, smaller size AgNP were reported to cause larger loss of the mitochondrial membrane potential exacerbating the already known inactivation of the enzymatic complexes in the ETC and resulting in higher ROS production.<sup>175</sup>

Several studies have further reported AgNPs-induced ROS generation in mouse fibroblasts and human hepatocytes, showing reduced membrane potential of mitochondria with subsequent release of cytochrome *C* into the cytosol followed by JNK activation and Bax translocation.<sup>176,177</sup> Contrary to this result antiapoptotic protein Bcl2 is highly expressed in HCT116 cells (human colon cancer cells) that are resistant to AgNPs.<sup>176</sup> Ag<sup>+</sup> from AgNPs directly mediates the synthesis of ROS, such as superoxide, hydroxyl radicals and hydrogen peroxide, in free-cell environments.<sup>178,179</sup> This report has been further supported by Mendis *et al.* showing ROS generated from AgNPs can lead to cell membrane disruption, mitochondrial dysfunction, and DNA damage.<sup>180</sup> Another study by Chang *et al.* has suggested the antibacterial properties of AgNPs result from the formation of multiple forms of ROS, observing a reduction in antibacterial activity on addition of the ROS scavenging enzymes super oxide dismutase and catalase.<sup>181</sup> Inoue *et al.* have found that the bacterial activity induced by the introduction of Ag<sup>+</sup> into zeolite is mediated by four forms of ROS under aerated conditions, the activity of which can again specifically be decreased by scavenger addition.<sup>182</sup>

Despite evidence for ROS generation from AgNPs and its antibacterial effect, the potential toxicity of Ag<sup>+</sup>, the structure of AgNPs, and their combinatorial effect with other factors confounds a clear understanding of AgNPs functional mechanisms. Jones *et al.* have investigated the possible reactions involved in ROS generation by AgNPs and the potential interaction between Ag<sup>+</sup> and ROS once they have been generated.<sup>183</sup> Henglein group has reported a possible reformation of AgNPs by O<sub>2</sub><sup>•-</sup> as a result of O<sub>2</sub><sup>•-</sup> mediated charging of AgNPs.<sup>184,185</sup> A schematic illustration of AgNPs acting as an electron pool during ROS generation is shown in Fig. 5(a), proposing potential interactions among AgNPs, Ag<sup>+</sup>, H<sub>2</sub>O<sub>2</sub> and O<sub>2</sub><sup>•-</sup>. A second source of ROS is the leakage of O<sub>2</sub><sup>•-</sup> through cell membranes, which can be neutralized by natural antioxidants as shown in Fig. 5(b). Since AgNPs and Ag<sup>+</sup> have a strong affinity for thiol groups (-SH) in cysteine residues, it is conceivable for AgNPs to be internalized and disrupt mitochondrial function through altered membrane permeability, disruption of the electron transfer chain, and disruption of mitochondrial membrane proteins.

Gold nanoparticles (AuNPs) have been employed extensively in nanomedicine applications, for example biosensing,<sup>187</sup> drug delivery,<sup>188</sup> theranostics,<sup>189</sup> biolabeling,<sup>190</sup> wound healing,<sup>191,192</sup> and medicine.<sup>193</sup> The development of plant extract and bio-object derived green synthesized AuNPs with high redox-ability has started to gain interest among

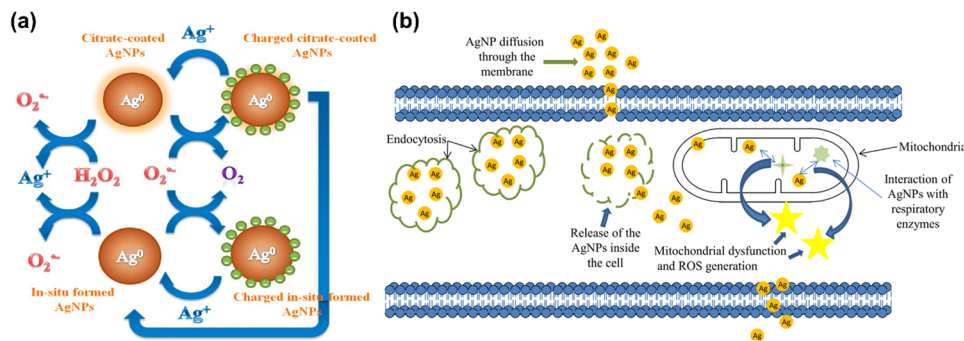


Fig. 5 (a) Schematic illustration of the action of silver nanoparticles in generation of ROS in the form of radical. Reproduced with permission from He *et al.*<sup>179</sup> [Copyright 2012, American Chemical Society]. (b) Interactions of AgNPs with cellular membranes and mitochondria and generation of ROS, causing cellular apoptosis. Reproduced with permission from Flores-López *et al.*<sup>186</sup> [Copyright 2018, Wiley].

researchers. Green synthesized AuNPs are mainly derived from bacteria, virus, yeast, fungi, algae, and plants.<sup>194,195</sup> Plant extract-based nanoparticles (also known as phytosynthesized NPs) are more effective compared to microorganism sources, and their preparation method requires fewer additional reagents.<sup>196–198</sup> Stozhko *et al.* have recently introduced a photosynthetic method to create AuNPs using leaf extract (phyto-AuNPs) and demonstrated their antioxidant activity together with details of the phytosynthesis kinetics, particle size, and dispersibility of the created nanoparticles.<sup>199</sup> They found that smaller phyto-AuNPs produced a higher antioxidant activity with an increase of the absolute value of zeta-potential. Nie *et al.* has developed antioxidant-functionalized AuNPs using self-assembly of thiol ligands derived from Trolox (Vitamin E analogue).<sup>19</sup> Surprisingly, the Vitamin E (tocopherol) analogue-functionalized AuNPs has shown strong reactivity towards 2,2-diphenyl-1-picrylhydrazyl radicals (DPPH $^\bullet$ ), about eight times higher than AuNPs alone. Hamelian *et al.* have developed Thyme-derived green AuNPs as a reducing agent, exhibiting antibacterial and antioxidant activity specifically for DPPH $^\bullet$ .<sup>200</sup> Quercetin capped AuNPs have also been synthesized using a green route by Milanezi *et al.* for antioxidant, antibacterial application. The antioxidant activity of quercetin both free and on AuNPs has been proven by free radical scavenging methods using ABTS, DPPH, and nitric oxide. In addition, quercetin-capped AuNPs ( $IC_{50}$  0.37  $\mu$ g mL $^{-1}$ ) demonstrated higher anti-oxidant activity than free quercetin ( $IC_{50}$  0.57  $\mu$ g mL $^{-1}$ ) in nitric oxide free radical scavenging method.<sup>201</sup> In a recent study by Nieves *et al.* have reviewed silver chalcogenide-based hybrid nanoparticles for its synthesis methodologies, and thorough biomedical applications including bio-imaging, theranostic agents, and biosensors.<sup>202</sup> For example, Mantri *et al.* synthesized iodine-doped silver shell/gold core metal nanorod for measuring the oxidative stress *in vivo* via photoacoustic imaging.<sup>203</sup>

**3.1.2. Gold nanoparticles.** Gold nanoparticles (AuNPs) are attractive and promising nanocarriers in nanomedicine due to their unique size/shape-dependent optical properties, high stability, low cytotoxicity, and easy surface modification.<sup>204,205</sup> In addition, AuNPs are very useful in drug delivery for targeting and controlling of drug release and serve as a sensitive imaging

tool for early detection of diseases or injury.<sup>188,206,207</sup> Of note, AuNPs themselves have no redox-activities, however, they can induce a redox-response by interacting with other molecules *via* their unique surface properties.<sup>27,30</sup> According to recent reports, endocytosis of AuNPs causes intracellular ROS production, which in turn sets off oxidative stress in cells.<sup>208,209</sup> AuNPs are suggested as an ideal platform for electrochemical biosensing due to their redox-catalytic properties, which improve electron transport across a wide range of electroactive biological species, primarily redox-proteins, without using mediators.<sup>210–212</sup> In fact, Lee *et al.* have used AuNPs to image intracellular ROS after modifying the surface of AuNPs with fluorescent dye-labeled hyaluronic acid.<sup>213</sup> Monodispersed polystyrene (PS) particles of varying sizes and chemical functional groups on their surfaces can be assessed for cellular toxicity by ultrasensitive detection of intracellular ROS. PEGylation of PSNP surfaces was also tested for its detection of intracellular ROS production. Further, PSNPs intracellular ROS levels were well correlated with their cytotoxicity, apoptosis-inducing activity, and cellular uptake. It was found that linear and branched polyethylenimine (PEI) can generate ROS intracellularly and can cause cellular damage. Higashi *et al.* have developed enzyme-free electrochemiluminescence (ECL) immunosensing detection using approximately 5 nm size AuNPs to generate ROS in an aqueous solution of trishydroxymethylaminomethane (Tris).<sup>214</sup> They demonstrated the catalytic pathways of new ECL detection and ROS generation can be varied and chemically regulated with parameters such as shape, size, concentration, and dispersant types of AuNPs. AuNPs were employed to an ECL-based enzyme-free sandwich immunoassay using magnetic beads (MBs), and disposable screen-printed electrode (SPE) chips as shown in Fig. 6(a). It is easy to modify AuNPs with biomolecules such as antibodies, thus they can be used for various biosensing applications through functional immobilization of biomolecules/antibodies.<sup>215,216</sup>

In addition to the ROS generating effect of AuNPs, many research groups have reported a ROS independent effect of AuNPs. AuNPs have been shown to be capable modulating cell interaction, and to have an apoptotic effect on *Escherichia coli* *via* a redox imbalance followed by decreased GSH without ROS generation.<sup>35,217</sup> By transcriptomic and proteomic approaches,

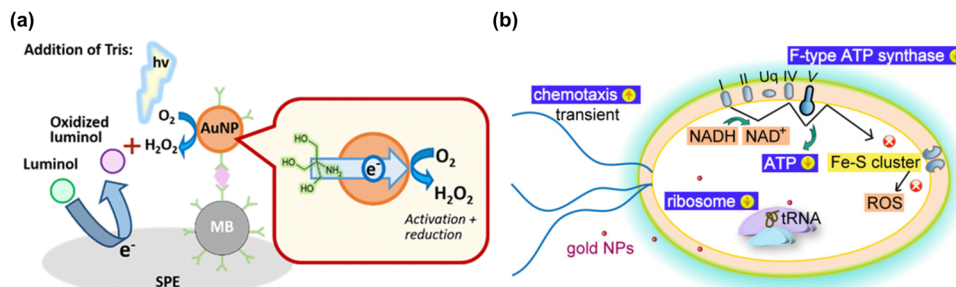


**Fig. 6** (a) A schematic illustration of gold nanoparticle-generated ROS controlled on a disposable screen-printed electrode using an enzyme-free electrochemiluminescence-based immunoassay. Reproduced with permission from Higashi *et al.*<sup>214</sup> [Copyright 2018, American Chemical Society]. (b) Schematic diagram illustrating the cellular mechanism of bactericidal gold nanoparticles on *E. coli*, and subsequent gold nanoparticles inducing the reduction of oxidative phosphorylation pathway (F-type ATP synthase and ATP level) and ribosome pathways, and the transient up-regulation of chemotaxis. During the process, the gold nanoparticles do not induce any change in ROS-related processes. Reproduced with permission from Cui *et al.*<sup>217</sup> [Copyright 2012, Elsevier].

the Cui group has investigated the molecular mechanism by which AuNPs exert their antibacterial activity against multidrug-resistant Gram-negative bacteria.<sup>218</sup> The antibacterial actions by AuNPs could occur through two routes; first, by changing membrane potential and inhibiting ATP synthase causing a subsequent metabolic decline through decreased ATP; second, by inhibiting ribosome binding to tRNA, causing a collapse of biological processes as demonstrated in Fig. 6(b). The antibacterial activity by AuNPs seems to be a bactericidal antibiotic effect that is independent from ROS.<sup>219</sup> Mateo *et al.* have investigated the cytotoxic role of oxidative stress in human tumor cells, which is suggested to involve an AuNP-induced decrease of superoxide dismutase activity.<sup>220</sup> Overall, AgNPs and AuNPs have potential for some important biological applications including for antibiotic effect, drug delivery, biosensing, and cancer theranostics, however they are not very effective catalytically due to low coordination numbers and so frequently require complex surface modifications with biologically active molecules.

**3.1.3. Platinum and palladium nanoparticles.** Platinum and palladium nanoparticles (PtNPs and PdNPs, respectively) have antioxidant properties due to their strong catalytic activity which can quench radical.<sup>221,222</sup> In fact, PAPLAL, a mixture of PdNPs and PtNPs, has been used to treat chronic diseases for several decades. Shibuya *et al.* used a diseased condition in mice related to aging to study the anti-aging effects of PAPLAL.<sup>114</sup> For *Sod1*<sup>-/-</sup>-deficient (*Sod1*<sup>-/-</sup>) mice with thin skin brought on by enhanced lipid peroxidation, PAPLAL transdermal therapy is beneficial. *Col1a1*, *MMP2*, *IL-6*, *TNF- $\alpha$* , and *p53* gene expression, which is abnormal in the skin of *Sod1*<sup>-/-</sup> mice, was restored by PAPLAL. This group has also shown PtNPs with high SOD and catalase activities, while PdNPs were demonstrated to have weak SOD and catalase activity. Compared to the SOD and catalase activity of PtNPs, which decreased right after being oxidized in the air, the mixture of PAPLAL exhibited stronger SOD and catalase activity even after oxidation, suggesting PdNPs possibly inhibit the degradation of PtNPs by oxidation.<sup>223</sup> Elhusseiny *et al.* have demonstrated the antitumor and antimicrobial activity of a complex of PtNPs and

PdNPs against human cell lines such as breast carcinoma (MCF7), liver carcinoma (HEPG2), and colon carcinoma (HCT 116) cells.<sup>224</sup> In their study, palladium complexes of polyamides containing sulfones were found to be the most potent for antibacterial and antifungal effects, whereas platinum complexes with flexible sulfone and ether flexible linkages and chloro (chloride) groups demonstrated high antitumor and antimicrobial agents. Further, Kora *et al.* have synthesized environmentally friendly PdNPs using gum ghatti (*Anogeissus latifolia*), for better application as an antioxidant and catalyst.<sup>225</sup> These green synthesized PdNPs showed relatively high antioxidant activity even with a lower dose of nanoparticles, and homogenous catalytic activity was also confirmed using reduction of dyes such as, methylene blue, Coomassie brilliant blue G-250, methyl orange, and 4-nitrophenol with sodium borohydride. The presence of large surfaces and the large proportion of metal atoms on the surfaces of most metallic nanoparticles results in strong catalytic activity in hydrogenation, hydration, and oxidation reactions.<sup>226,227</sup> These nanoparticles that possess SOD and catalase activity may be useful for biomedical research and clinical practice, as well as in material science and engineering.<sup>228,229</sup>

**3.1.4. Ruthenium nanoparticles.** Ruthenium nanoparticles (RuNPs) and ruthenium-containing nanomaterials (Ru-cNMs) combined with platinum and palladium or with nonmetal phosphorous and oxygen have been tested for antioxidant, anticancer, antimicrobial activities, and a wide range of catalytic applications.<sup>230,231</sup> Srivastava *et al.* have reported multiple metal nanoparticles synthesized by bacterial-extract (*Pseudomonas aeruginosa*) SM1.<sup>232</sup> Green bioextract-derived RuNPs possesses antioxidant and catalytic activity. RuNPs synthesized from *Nephrolepis biserrata* showed significant antifungal activity *via* DPPH, ABTS, SORS, and HAS assays. Cao *et al.* have reported the ROS scavenging activities of RuNPs.<sup>233</sup> They found that RuNPs can break down H<sub>2</sub>O<sub>2</sub>, scavenge hydroxyl radical, superoxide, singlet oxygen, 2,2'-azino-bis(3-ethylbenzothiazoline-6-sulfonic acid) derived radical (ABTS<sup>•+</sup>) and 1,1-diphenyl-2-picrylhydrazyl radicals (•DPPH), as well as exert cytoprotective effects against H<sub>2</sub>O<sub>2</sub>-induced oxidative

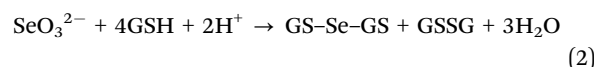
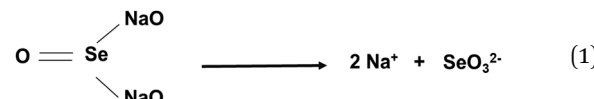
stress *in vitro*. In addition, the oxidation of *o*-phenylenediamine (OPD), and dopamine hydrochloride (DA) by  $\text{H}_2\text{O}_2$  to produce the colorimetric products in the aqueous solution can also be catalyzed by RuNPs, which also have inherent HRP-like, oxidase-like mimetic capabilities.

**3.1.5. Selenium nanoparticles.** Selenium nanoparticles (SeNPs) are one of the more promising and intensively studied materials in recent years. From the Greek word 'Selene', which means moon, selenium was discovered as a byproduct of sulphuric acid synthesis by Jöns Jacob Berzelius in 1817.<sup>234</sup> Selenium is a non-metal which is categorized as non-metal, physical appeared as a red/brown colored powder.<sup>235</sup> The atomic number of selenium is 34 and its electronic distribution is  ${}^{34}\text{Se} = 1s^2, 2s^2 2p^6, 3s^2 3p^6 3d^{10}, 4s^2 4p^4$ . It has various oxidation states like  $2^-$ ,  $0$ ,  $2^+$ ,  $4^+$ ,  $6^+$ . Because of its varying oxidation states, selenium is very useful for biomedical applications. The dietary form of selenium known as sodium selenite is a common dietary source of selenium for animals and humans, in which it is a trace element.<sup>236</sup> Selenium-based compounds such as seleno-amino acids and various synthetic organo-selenium compounds are known to be effective tumorigenesis inhibitors in many animal and cell models.<sup>237–239</sup> When selenium is injected to live animals in *in vivo* conditions, it is primarily found as selenoproteins that play critical roles in cellular redox-reaction, detoxification, and immune-system protection.<sup>240</sup> There are 25 selenoproteins discovered in humans and 24 kinds in rodents.<sup>241</sup> It is highly expressed in the human brain, functioning as an antioxidant and neuroprotectant for preventing the onset and progression of Alzheimer's disease.<sup>242</sup>

Selenium is known to be involved in various biological processes including the immune response. Some pathological conditions associated with the immune system have also been affected by selenium content level, and its different salt forms. In the past, concerns have been raised about the metabolism of selenium compounds into metabolites and potential hereditary factors influencing their utilization. Due to low levels of selenium in soils and food, selenium deficiency is uncommon in the United States and Canada,<sup>243</sup> while it is also common in some regions of China, New Zealand, and portions of Europe and Russia.<sup>244</sup> Recent studies have observed selenium deficiency in immune-related diseases and suggested selenium supplementation to solve the health issues associated with selenium deficiency, although the cellular and molecular mechanisms underlying the effects of selenium in immune-related diseases are not fully understood.<sup>245</sup> One possible mechanism by selenium is to activate leukocytes in an immune response including adherence, migration, phagocytosis, and cytokine secretion at an optimal dose. The redox-activities of selenoproteins seem very important in modulating cell signalling in these immune responses. Thus, the redox-activities of selenium-based materials could be a promising therapy for immunity-related pathologies including chronic inflammation, by generating reduced forms of thioredoxin to balance the reduced and oxidized molecules within the cell.<sup>245–247</sup>

The range of oxidation states accessible to selenium ( $2^-$ ,  $0$ ,  $2^+$ ,  $4^+$ ,  $6^+$ ) and its electronegativity are the two properties which are important in redox biology. Because selenium possesses different oxidation states, it has interesting redox activities and therefore a capability to generate ROS. In proteins, selenium can be incorporated in the place of sulfur in cysteine residues forming selenocysteine (Se-Cysteine), the electronegativity of which is lower than cysteine ( $-0.23$  V Cysteine,  $-0.38$  V Se-Cysteine). This incorporation occurs by the action of diverse antioxidant enzymes like thioredoxin reductase, glutathione peroxidase, and selenoprotein.<sup>248</sup> Selenium acts as a redox center for all of these enzymes which are essential for biochemical activities. Compared to disulfide, diselenide has a much lower binding energy ( $\text{H}-\text{Se}-\text{Se}-\text{H}$ ,  $172$  kJ mol $^{-1}$ ) than disulfide ( $\text{H}-\text{S}-\text{S}-\text{H}$ ,  $240$  kJ mol $^{-1}$ ).<sup>249</sup> The lower binding energy of diselenide bond allows having redox-activity accompanying with visible light radiation in an effective manner.<sup>250–252</sup> Diselenide can produce seleninic acid or selenol under redox conditions by the cleavage of the diselenide bond, and selenium radicals under stress conditions such as under irradiation or heating could be generated. Selenium can be reduced by thiol compounds or oxidized by oxygen leading to ROS production in both reactions and subsequently to apoptotic cell death. However, studies have reported that selenium has a narrow therapeutic window for clinical application.<sup>253–255</sup>

SeNPs made from sodium selenite ( $\text{Na}_2\text{SeO}_3$ ) can be an alternative form to modulate oxidative stress, presenting an advantage for therapeutic purposes. The ionization of sodium selenite to sodium ions and selenite ( $\text{SeO}_3^{2-}$ ) is the most common fabrication method (eqn (1)). Selenite has a high affinity with glutathione (GSH), producing selenodiglutathione (GS-Se-GS) as reported previously (eqn (2)).<sup>256</sup>



In the presence of excessive GSH, selenodiglutathione is further reduced by glutathione into glutathioselenol (GS-SeH/GH-Se $^-$ ) as shown in eqn (3). Subsequently, glutathioselenol is dismantled to selenium and glutathione as shown in eqn (4). Selenite also reacts with thiols, generating ROS such as  $\text{O}_2^{\cdot-}$ ,  $\cdot\text{OH}$  and  $\text{H}_2\text{O}_2$ .<sup>256</sup> Therefore, it is crucial to understand the detailed reaction mechanism of selenite/selenium nanoparticle ROS generation and its byproducts, as well as to identify intermediates in these reactions to understand their role in biochemical processes.

Selenium has been tested in several disease models including ischemic cerebral stroke, an acute brain degeneration with

a high mortality rate and no appropriate treatment so far.<sup>257,258</sup> Amani *et al.* have developed biodegradable SeNPs to target ischemic brain stroke, demonstrating a dramatic effect. They found that SeNPs reduced brain edema, protected axons and promoted axonal growth, and enhanced remyelination in the hippocampal area.<sup>257</sup> The group has also suggested an effective delivery of SeNPs to target a specific area with minimal side effects. SeNPs possibly modulate cellular signalling pathways in inflammatory and metabolic responses including the ubiquitin-proteasome system (ERK5), Tsc1/Tsc2 complex, ubiquitin-proteasome system (ERK5), FoxO1, and wnt/β-catenine. The activation of JAK2/STAT3 and Adamts1 are important in inflammatory responses. Studies suggest that SeNPs are promising therapeutics for cerebral stroke *via* its antioxidant and anti-inflammatory properties.

Redox homeostasis is critical in living organisms and excessive ROS damage cellular biomolecules during oxidative stress. GSH is a tripeptide of L-glutamate, glycine, and L-cysteine, which plays a critical role in many biological functions in mammals. GSH is a major nonprotein thiol in organisms that is required for intracellular redox homeostasis. Importantly, GSH and •OH are natural counterparts functioning as reducing and oxidizing agents, respectively. Yang *et al.* have developed selenium-conjugated graphene quantum dots (Se-GQDs) based on an ultrasensitive reversible redox-fluorescent switch for detecting •OH and reductive GSH in aqueous solution and living cells.<sup>259</sup> They found that the fluorescence of Se-GQDs is statically quenched by •OH, causing a condition known as fluorescence OFF condition that is brought on by Se–Se groups right after reduction of Se–Se groups to C–Se groups upon GSH addition, and fluorescence can be turned ON in the reverse process. This fluorescence-based switch can be useful for detecting redox-activity in cells.

Although the cytotoxic effects of selenium against many cancer cells are thought to be due to its ROS producing activities,<sup>260–262</sup> the biochemical mechanism involved in tumor suppression by selenium remains to be studied. Wang *et al.* have developed biodegradable and pH-responsive selenium-doped hydroxyapatite (SeHA) nanoparticles for osteosarcoma treatment, using *in vitro* and *in vivo* osteosarcoma models.<sup>263</sup> The molecular mechanism involved in suppression of osteosarcoma is presented in Fig. 7(a) and (b). In another study, Li *et al.* have demonstrated selenium-containing amphiphiles reduced and stabilized AuNPs suggesting that the selenium in the particles possibly induces high levels of ROS, leading to cancer cell death.<sup>264</sup> Zheng *et al.* have further investigated the therapeutic use of SeNPs in a co-delivery system of selenium and small interfering RNAs (siRNAs).<sup>265</sup> This approach aims to overcome drug resistance in breast cancer therapy mostly caused by P-glycoprotein (P-gp) and class III β-tubulin. For co-delivery of selenium and siRNAs (anti-P-gp and anti-β-tubulin III), they have designed layered double hydroxide (LDH) nanoparticles and found a more efficient gene-silencing effect than siRNA alone by a significant downregulation of P-gp and β-tubulin III expression. In addition, apoptotic cells undergo morphological change with an increase of intracellular ROS

and altered signalling pathways such as Bcl-2/Bax, caspase-3, PI3K/AKT/mTOR and MAPK/ERK pathways. A similar trial was also performed for dual delivery of siRNAs and cisplatin (DDP) to A549/DDP cells, a breast cancer cell line exhibiting multidrug resistance (MRD). The co-delivery of gene and drug (siRNA and DDP) in A549/DDP cells showed a synergistic effect in anti-cancer therapy, leading to a decreased expression of P-gp and MRP.<sup>266</sup> Although selenium conjugated nanomaterials have been intensively explored in many disease conditions, the diagnostic or therapeutic applications of these NPs require more investigation. Furthermore, the exact mechanisms of SeNPs in certain pathological conditions remain unclear. Redox-activity and biocompatibility are considered as the main properties of selenium-based NPs that are applicable for clinical applications. The current challenges of SeNP-based therapies in clinical applications are limiting due to a lack of information on dosing accuracy, potential cytotoxicity, and metabolism in the body.

Sun *et al.* have created an innovative drug delivery system that targets Bor and utilizes Fc-β-CD loaded with Res to treat AD through multiple channels.<sup>267</sup> The researchers have shown that using MNSe-Res/Fc-β-CD/Bor can effectively prevent the aggregation of Aβ proteins, reduce oxidative stress, and suppress tau hyperphosphorylation. Moreover, this treatment successfully protected neurons and restored impaired memory in APP/PS1 mice. It is interesting to note that the MSe/Fc-CD/Bor loaded with rivastigmine (Riv) displayed a higher pharmacokinetic index than Riv alone. A schematic illustration of synthesized MNSe-Res/Fc-β-CD/Bor for gradual release of drug is presented in Fig. 7(c). The *in vivo* therapeutic approach is illustrated in Fig. 7(c), where the compound MNSe-Res/Fc-β-CD/Bor was administered *via* the tail vein of mice with the APP/PS1 model. The Bor present on the nano-system's surface contains an ester bond, which can be broken down by esterases in the bloodstream. This drug delivery system utilizing nanomaterials has been demonstrated to cross the blood–brain barrier and accumulate consistently in the brain. Treatment with MNSe-Res/Fc-β-CD/Bor effectively restored the diminished cognitive function in APP/PS1 mice, accompanied by a decrease in the total levels of Aβ, hyperphosphorylated tau, and the loss of neurons in the brain.

### 3.2. Metal oxide nanomaterials

Metal oxide nanoparticles such as magnesium oxide (MgO), titanium dioxide (TiO<sub>2</sub>), vanadium oxide (V<sub>2</sub>O<sub>5</sub>), manganese oxide (MnO<sub>2</sub>), iron oxide (Fe<sub>3</sub>O<sub>4</sub>), copper oxide (CuO), zinc oxide (ZnO), gadolinium oxide (Gd<sub>2</sub>O<sub>3</sub>), and cerium oxide (CeO<sub>2</sub>) have antioxidant and catalytic properties. By developing pH-responsive oxide nanomaterials, we can modulate oxidative stress inside the cells through redox-chemistry.<sup>268</sup> It is important to note that the reaction mechanisms for these types are not well understood.<sup>29,269</sup> The reaction of these metal oxide NPs can be modulated by a given condition, which can be a major factor to favour either antioxidant or redox reaction. Understanding the detailed conditions will provide important information for the use of metal oxide NPs as redox-regulators,

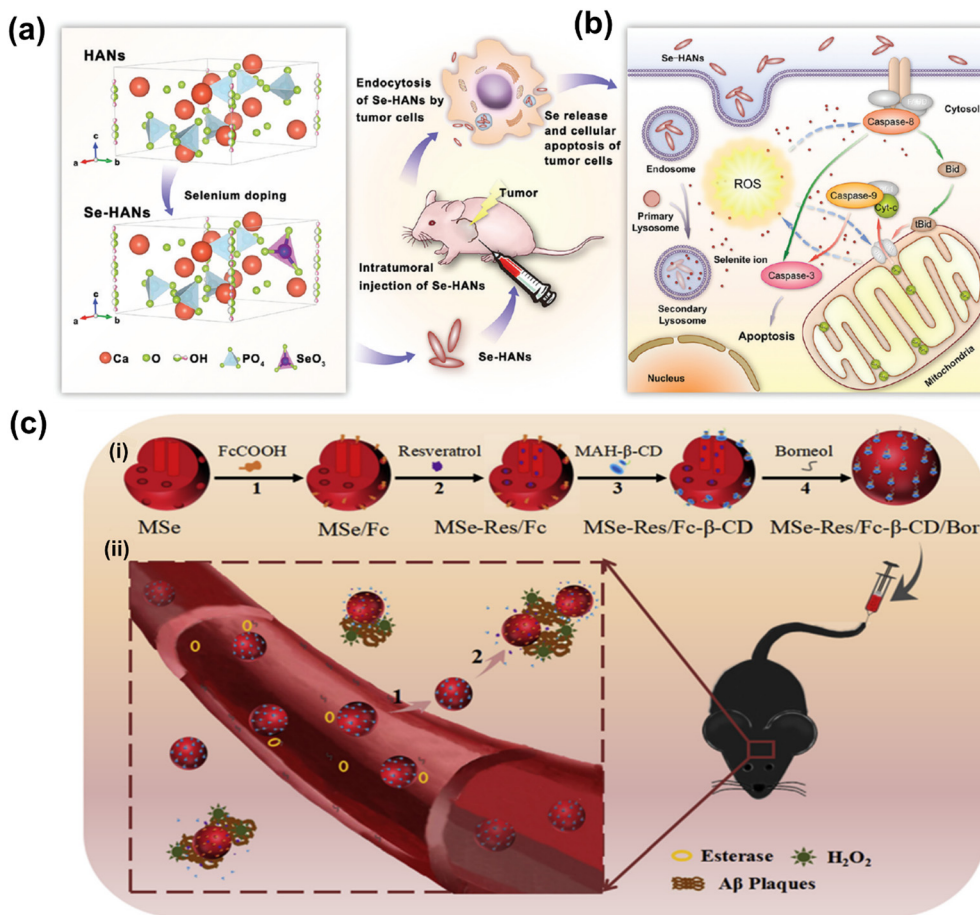


**Fig. 7** (a) Schematic chemical structural diagram represents the synthesis and acting mechanism of antitumor nanoparticles (Se-HANs) using selenite to replace phosphate groups in hydroxyapatite nanoparticles (HANs). Next, intratumorally injection of Se-HANs into xenograft osteosarcoma mice model. (b) Further, cellular schematic diagram illustrates the non-specific endocytosis of Se-HANs into tumor and subsequent rapid degradation in lysosome (acidic pH) to release selenite. Finally, selenium-induced, caspase-dependent apoptosis pathway activates the cellular apoptosis together orchestrated with the intracellular ROS generation. Reproduced with permission from Wang *et al.*<sup>263</sup> [Copyright 2016, American Chemical Society]. (c) (i) Step-by-step schematic illustration of synthesis and various surface functionalization of MNSe-Res/Fc-β-CD/Bor; including (1) Ferrocene loading into mesoporous nanoselenium (MNSe/Fc), (2) Further loading with resveratrol to MNSe/Fc. (3) Then surface functionalized with MAH modifiedβ-CD on to the surface of MNSe-Res/Fc. (4) Finally, grafting of borneol onto the NPs surface via ester bond to create drug delivery carrier for AD with capability to penetrate the blood–brain–barrier. (ii) Schematic illustration of *in vivo* circulation of MNSe-Res/Fc-β-CD/Bor in mice: (1) the release of borneol of from the nanocarrier (MNSe-Res/Fc-β-CD/Bor) and passing the blood–brain barrier (BBB). (2) Targeting the amyloid plaques and controlled release of resveratrol by hydrogen peroxide from MNSe-Res/Fc-β-CD/Bor. Reproduced with permission from Sun *et al.*<sup>267</sup> [Copyright 2019, Elsevier].

however the exact reaction mechanisms of metal oxide NPs need to be thoroughly investigated.<sup>29,268,269</sup> In this section, we will discuss and detail the mechanisms of their antioxidant and redox activities on the physiology and pathology of living organisms.

**3.2.1. Magnesium oxide nanoparticles.** Magnesium oxide nanoparticles (MgONPs) are promising solid-base catalysts that have gained significant attention due to their superior catalytic reaction. The catalytic property of MgONPs is highly dependent on their size, shape, morphology, crystallinity, and surface area. Sutradhar *et al.* have developed several different forms of MgONPs such as flower shaped nanoflakes, house of card structures, spheres, cubes, and hexagonal plates *via* calcination of magnesium carbonate hydrates as an intermediate.<sup>270</sup> The same group have reported that the amount and distribution of carbonate ions in the crystal is the key factor in the formation

of different morphologies of MgONPs using hydrothermal fabrication. Considering that the newly synthesized MgONPs contain many edges and corners, step edges and step corners, as well as many base sites, the surface hydroxyl group is highly coordinated with O<sup>2-</sup> sites, which are considered to be active basic sites in heterogeneous catalysts. Dobrucka *et al.* have prepared MgONPs using *Artemisia abrottonum* herb extract and examined their antioxidant and photocatalytic and antioxidant activities.<sup>271</sup> The antioxidant activity of these herb based MgONPs was tested using DPPH radicals by reducing 2,2-diphenyl-1-picrylhydrazyl (DPPH) into stable nitrogen radicals. Any oxygen atom donor can result in reduction of DPPH, which result in the loss of the violet color of the solution. Antioxidant effectiveness in scavenging radical is indicated by the degree of color change in the DPPH solution immediately following the reaction with antioxidants. Similarly, Sushma *et al.* have

investigated the antioxidant activity of MgONPs synthesized from *Clitoria ternatea*.<sup>272</sup> Kiranmai *et al.* have demonstrated that the exposure of rats to MgONPs decreases the rats' antioxidant capacity including SOD and catalytic activity in blood samples of the animals in a dose-dependent manner compared to a PBS (with 1% Tween 80) exposed control group.<sup>273</sup> The reduction in the antioxidant capacity in MgONPs-exposed rats indicated the antioxidant defense mechanism is triggered by the nanoparticles, suggesting a possibly hazardous effect of nanoparticles in case of chronic exposure. Recently, Kuo *et al.* have produced surface defect-rich MgONPs to enhance surface oxygen vacancies which exhibited greater antibacterials activity against *Escherichia coli*, and *Staphylococcus aureus* after incorporation in cellulose acetate thin film.<sup>274</sup> Thus, by increasing the oxygen vacancies on MgONPs surface and thereby releasing a greater number of superoxide anions may increase the antibacterial activity.

**3.2.2. Titanium oxide nanoparticles.** Titanium oxide nanoparticles ( $\text{TiO}_2$ NPs) with varied size, shape, and morphology have been widely studied for practical applications including cosmetics (including as skin protectors from ultraviolet (UV) light), food components, inks, toothpastes, pharmaceuticals, and antibacterial agents.<sup>275,276</sup> Titanium and its related materials are also widely used in biomedical devices and products due to their high Young's modulus and excellent biocompatibility, for example, as replacement materials for hard tissues or replacement for cardiac and cardiovascular tissues.<sup>277–280</sup>  $\text{TiO}_2$ NPs have been often used as metal implants for dental and orthopedic implants. However, the biocompatibility of  $\text{TiO}_2$ NPs and their effect on osteoblast cells have not been fully understood.<sup>281</sup> Titanium oxide-based nanomaterials have been suggested as a potential photosensitizer, with potential use for photodynamic cancer therapy due to their hydrophobic nature and electron–hole-pair generating propensity under UV radiation. The electron–hole pair being generated from  $\text{TiO}_2$ NP inside or in proximity to tissue or cells under UV exposure reacts with ROS lessening the intracellular oxidative stress.<sup>282</sup> The best application of this mechanism is the use of  $\text{TiO}_2$  nanomaterials to protect skin from sunlight. Moreover,  $\text{TiO}_2$  nanoparticles can also be used for pollution remediation, using light induced radical generation to remove dyes and phenols from water.<sup>283,284</sup> Successful application of ROS generated from  $\text{TiO}_2$ NPs as a cytotoxic reagent has been reported in human cervical adenocarcinoma, leukemia, breast, and lung cancer, and hepatocarcinoma cell lines.<sup>285–288</sup> Some other studies have implicated the antioxidant potential of  $\text{TiO}_2$ NPs by generation of ROS.<sup>289,290</sup>  $\text{TiO}_2$ NPs may also be suitable for antibacterial application; ROS generated by photocatalysis at the particle surface can cause an imbalance between antioxidant and oxidant, and the ROS themselves can damage proteins, lipids, and DNA in bacterial cells.<sup>291</sup> Li *et al.* have studied the mechanism of  $\text{TiO}_2$ NP-generated ROS toxicity together with a mechanical characterization of the particles using electron spin resonance (ESR).<sup>292</sup> Photobleaching of  $\text{TiO}_2$ NPs results in ROS generation on the surface of photoexcited  $\text{TiO}_2$ NPs. In detail,  $\text{TiO}_2$ NPs absorbs light in the ultraviolet A (UVA) (320–400 nm)

and ultraviolet B (290–320 nm) ranges of the electromagnetic spectrum. When  $\text{TiO}_2$ NPs absorb photons with energy equal to or higher than their energy band gap (3.0 and 3.2 eV for rutile and anatase phase, respectively), electrons become excited and jump from the valence band to the conduction band resulting in the formation of an electron–hole pair.<sup>293</sup> When the holes in the valence band are created, they become highly oxidizing and can produce hydroxyl radicals when in contact with water or hydroxide ions. While, the conduction band electrons can further convert oxygen molecules to form superoxide radical anions.<sup>294</sup> This redox-activity of  $\text{TiO}_2$ NPs has a significant impact in various biological systems. Recently, Cai *et al.* have reported that repeated oral administration of inorganic nanoparticles such as  $\text{TiO}_2$ NPs, Au, and  $\text{NaYF}_4$  at low concentration can promote lipid degradation and alleviate steatosis in the liver of male mice.<sup>295</sup> The low dose of these nanoparticles evokes an unusual antioxidant response in hepatocytes *via* up-regulation of *Ces2h* expression and resulted rapid ester hydrolysis. The authors claim that the low dose administration of these nanoparticles may serve as a potential candidate for metabolic regulation treatment.

**3.2.3. Vanadium oxide nanoparticles.** The outstanding structural versatility of vanadium oxide nanoparticles ( $\text{V}_2\text{O}_5$ NPs) has led to significant progress in their use as a catalyst in electrochemical devices developments.  $\text{V}_2\text{O}_5$ NPs, also known as vanadium pentoxide, are regarded as a promising candidate to serve as cathode materials for lithium-ion batteries. Various types of  $\text{V}_2\text{O}_5$  have been developed including one dimensional structures (nanorods,<sup>296</sup> nanowires,<sup>297</sup> nanotubes,<sup>298</sup> nanofibers,<sup>299,300</sup> nanobelts<sup>301,302</sup>), two dimensional nanosheets,<sup>303</sup> and three dimensional hollow and porous nanostructures.<sup>304–306</sup> Recently, these  $\text{V}_2\text{O}_5$ NPs structures have been tested for biomedical applications. For example, Natalio *et al.* have investigated vanadium halo-peroxidase mimicking  $\text{V}_2\text{O}_5$ NPs to inhibit the formation of bacterial biofilms.<sup>307</sup> They found that  $\text{V}_2\text{O}_5$  nanowires with vanadium haloperoxidase-like activity are capable of simultaneously producing hypobromous acid (HBrO) and  ${}^1\text{O}_2$ , with potent antibacterial properties. Furthermore, HBrO may react with other  $\text{H}_2\text{O}_2$  molecules being able to produce  ${}^1\text{O}_2$  in the absence of an organic acceptor, which has a stronger antibacterial activity adequate for prevention of biofilm formation. Vernekar *et al.* has also shown that  $\text{V}_2\text{O}_5$  nanowires (vanadia nanowires) act like glutathione peroxidase, an antioxidant enzyme that consumes cellular glutathione, suggesting  $\text{V}_2\text{O}_5$ NPs could be used as potential therapeutics in many oxidative stress associated diseases including aging, cardiovascular disorder, and other neurological disorders such as AD and PD.<sup>308</sup> They have also shown that vanadium nanowires are readily internalized into mammalian cells of various organs, exhibiting a robust enzyme like activity through ROS scavenging under intrinsic and extrinsic oxidative stress conditions. Vanadia nanowire nanozymes maintain redox balance without perturbing cellular antioxidant defense, thus protecting cells against harmful oxidative stress. In general,  $\text{V}_2\text{O}_5$ NPs exhibit vanadium haloperoxidase mimetic activity in response to  $\text{H}_2\text{O}_2$  in the presence of

vanadium haloperoxidase substrates (*i.e.*, tyrosine/iodide or dopamine/iodide) producing vanadium peroxydo species on the surface of vanadia nanowires.<sup>307,308</sup> Recently, Das *et al.* have prepared the V<sub>2</sub>O<sub>5</sub>NPs using the microwave assisted polyol method and investigated for cytotoxicity against various cancer cell lines, and endothelial cells.<sup>309</sup> They found that the developed nanoparticle was anti-angiogenic in both *in vitro* and *in vivo* assays, and showed significant inhibition of melanoma B16F10 cells proliferation, and subcutaneous tumor growth in C57BL6/J mice. Through various biological assays they found that the generation of superoxide radicals from nanoparticles causes the up-regulation of p53 protein and down-regulation of surviving protein might be the underlying mechanism for anti-cancer activity of V<sub>2</sub>O<sub>5</sub>NPs.

**3.2.4. Manganese oxide nanoparticles.** Manganese oxide nanoparticles (MnO<sub>2</sub>NPs/Mn<sub>3</sub>O<sub>4</sub>NPs) have gained significant interest for a broad-range of applications because of their unique properties including magnetism,<sup>310,311</sup> catalytic activity,<sup>312,313</sup> and high energy density.<sup>314</sup> Nanosized MnO<sub>2</sub>NPs have long been applied for drug delivery,<sup>315</sup> as imaging tools,<sup>316</sup> for chelation of heavy metal ions,<sup>317</sup> and as optical sensors.<sup>318</sup> Recently, manganese-based nanomaterials have been utilized as nanomedicines in regenerative medicine due to their ability to scavenge intracellular ROS to minimize oxidative cell damage, and also for application in rheumatoid arthritis treatment.<sup>319–322</sup> Alarifi *et al.* have evaluated MnO<sub>2</sub>NP-induced DNA damage and cytotoxic effect on human neuronal (SH-SY5Y) cells.<sup>323</sup> They found that the MnO<sub>2</sub>NPs induced ROS generation and decreased membrane potential of the mitochondria in the SH-SY5Y cells in a time and dose dependent manner. Furthermore, lipid peroxide SOD, and catalase (CAT) activities were increased with a subsequent decrease of glutathione also occurring in a dose and time dependent manner. According to Singh *et al.*, Mn<sub>3</sub>O<sub>4</sub>NPs generated by endothelial nitric oxide synthase contain multienzyme redox-activity that is shape dependent.<sup>324</sup> They found that Mn<sub>3</sub>O<sub>4</sub>NPs mimic the functions of CAT and SOD glutathione peroxidase (GPx), the cellular antioxidant enzymes. This enzyme activity by Mn<sub>3</sub>O<sub>4</sub>NPs depends on the size, morphology, and surface area of the NPs, as well as the redox properties of metal ions. Furthermore, Mn<sub>3</sub>O<sub>4</sub>NPs do not affect the level of nitric oxide in endothelial cells unlike manganese complexes that have antioxidant enzyme-like activity which change nitric oxide bioavailability. The same group has also reported that Mn<sub>3</sub>O<sub>4</sub>NPs with flower-like morphology (“nanoflowers”), and a higher ratio of Mn<sup>3+</sup>/Mn<sup>2+</sup> that was obtained by an oxidation with NaIO<sub>4</sub>, exhibit an enhanced catalytic activity compared to other materials with a lower ratio of Mn<sup>3+</sup>/Mn<sup>2+</sup>.<sup>325</sup> Environmental pH can be a key factor in controlling the switch between Fenton chemistry (low pH) and catalase activity (high pH). Tootoonchi *et al.* have developed manganese oxide nanoparticles with four different crystal structures, namely, poorly ordered (crystalline) MnO<sub>2</sub>, cryptomelane  $\alpha$ -MnO<sub>2</sub>, birnessite  $\delta$ -MnO<sub>2</sub>, and hausmannite Mn<sub>3</sub>O<sub>4</sub> for use as cytoprotective, oxygen generating agents, and to act as enzyme mimics *in vitro*.<sup>326</sup> The capability of manganese oxide nanoparticles

to produce oxygen, their rate of SOD, and their biocompatibility were all highly associated with their power to protect cells from damage. The cellular mechanisms of cytoprotective effects by these nanozymes remain to be investigated. The capability of MnO<sub>2</sub>NPs to convert H<sub>2</sub>O<sub>2</sub> was utilized by Gordijo *et al.* to fabricate an autonomous insulin delivery system with a variable release rate dependent on blood glucose concentration.<sup>327</sup> In these works, a proteinaceous membrane was created by cross-linking bovine serum albumin (BSA)-MnO<sub>2</sub>NP aggregates in the presence of poly(*N*-isopropylacrylamide-*co*-methacrylic acid) nanoparticles and the enzymes glucose oxidase (GOx) and CAT. The presence of both the MnO<sub>2</sub>NPs and CAT in the membrane enabled the immobilized GOx to trigger a pH change in the presence of glucose without inhibition by H<sub>2</sub>O<sub>2</sub> formed during the glucose oxidation. This pH change caused a reversible contraction of the poly(*N*-isopropylacrylamide-*co*-methacrylic acid) nanoparticles, thereby increasing the porosity of the membrane and increasing the rate of insulin release in proportion to glucose concentration.<sup>328</sup> Moreover, Prasad *et al.* have increased radiation therapy tumor elimination by using several MnO<sub>2</sub>NP formulations to treat hypoxia and glycolytic acidosis, two conditions commonly observed in tumor environment.<sup>329</sup>

**3.2.5. Cobalt oxide nanoparticles.** Cobalt oxide nanoparticles (Co<sub>3</sub>O<sub>4</sub>NPs) have been investigated for their potential antioxidant properties in various research studies. It has been used to create flexible supercapacitors due to their high specific capacitance and surface-to-volume ratio.<sup>330</sup> Co<sub>3</sub>O<sub>4</sub>NPs have unique catalytic, magnetic, and optical properties which also make them suitable for biomedical applications. The antioxidant-like activity of three different shapes of Co<sub>3</sub>O<sub>4</sub>NP was found to decrease in the order of nanoplates, nanorods, and nanocubes, being inversely proportional to their redox-potentials.<sup>251</sup> This result suggests that electron transfer during H<sub>2</sub>O<sub>2</sub> reduction by Co<sub>3</sub>O<sub>4</sub> might be a rate-determining step in the antioxidant activity. Furthermore, cobalt oxide nanoparticles have been investigated for scavenging of free radicals and helping to neutralize ROS like superoxide, and hydroxyl radicals.<sup>331,332</sup> In addition to their potential antioxidant activity, cobalt oxide nanoparticles may possess anti-inflammatory activity, which is directly linked to oxidative stress, materials with anti-inflammatory effects can directly contribute to antioxidant defense.<sup>333</sup> However, cobalt oxide nanoparticles induced cytotoxicity by release of Co<sup>2+</sup> ions which strongly triggered the generation of ROS, and caspase cascade in cell lines. The toxicity of the cobalt oxide nanoparticles can be minimized by surface modification approach using active agents/biopolymers or doping in nanoparticles through reducing the Co<sup>2+</sup> ions release.<sup>334</sup>

**3.2.6. Iron oxide nanoparticles.** Magnetic nanoparticles (MNPs), particularly iron oxide nanoparticles (Fe<sub>3</sub>O<sub>4</sub>NPs), have been intensively applied for drug delivery, cancer therapy, and tissue regeneration with different physicochemical properties. The redox-activity of MNPs depends on the oxidation state of iron, and a variety of physicochemical parameters including the particle's size, shape, surface chemistry, and magnetism. In a

sequential reaction that produces ROS, the oxidation states of Fe (2+ and 3+) are important.<sup>27</sup> Among many different forms of iron oxide nanoparticles, maghemite ( $\text{Fe}_2\text{O}_3$ ) and magnetite ( $\text{Fe}_3\text{O}_4$ ) are the most common. Recently, the application of these iron oxide NPs has gained great attention in cancer therapy as magnetic resonance imaging (MRI), and therapeutic agents by altering their redox status and increasing ROS levels, thus destroying cancer cells.<sup>335,336</sup> The ROS generating properties of the NPs have also been demonstrated to sensitize cardiomyocyte cells (H9c2) to oxidative stress; this effect has been suggested to enhance cancer therapies.<sup>337</sup> Considering the differential biological effects of transient ROS generation, intense oxidative insults by ROS are more cytotoxic to cancer cells compare to normal cells.<sup>338</sup> Moreover, oxidative stress generated by exogenous agents can disrupt redox homeostasis in the cell and induce an imbalanced redox condition leading to a selective cancer toxicity.<sup>339,340</sup> Recently, Torres-Herrero *et al.* have designed and synthesized the nanohybrid nanoparticles made of co-encapsulation of a prodrug converting therapeutic enzyme as HRP with nano-heater as MNPs in the silica matrix for cancer treatment.<sup>341</sup> These nanohybrid MNPs achieve heat-triggered control of glucose oxidase (GOx)-peroxidase nanoenzyme cascade reaction was recently reported for production of intracellular ROS.<sup>342</sup>

A recent study has further investigated the underlying mechanisms of anti-cancer effects induced by magnetite nanoparticles, demonstrating that ROS produced by magnetite NPs lead to mitochondrial damage and genotoxic effects in A549 cells. Mathias *et al.* have further demonstrated the cytotoxic mechanisms of magnetite-mediated ROS generation using A549 and H1299 human lung cancer cells.<sup>340</sup> The study has clearly shown that ROS generated by magnetite nanoparticles induce gene mutations, without a direct effect on cell death. Hauser *et al.* have utilized ROS produced by iron oxide nanoparticles to enhance the efficacy of radiation therapy, as a combination treatment.<sup>343</sup> In this study, they used iron oxide nanoparticles coated with TAT, a cell penetrating peptide, to avoid degradation by lysosomes after being internalized by cancer cells, enabling intracellular hydroxyl radical formation. In addition, TAT-coated MNPs have been shown to produce significantly more ROS compared to uncoated MNPs in A549 lung carcinoma cells. Combined treatment of TAT-functionalized MNPs and radiation therapy resulted in a synergistic effect due to the increased lysosomal permeability, ROS generation, and loss of mitochondrial integrity and function.<sup>344</sup> In particular, when greater amounts of superoxide anions are generated under increased cellular respiration in mitochondria, MNPs may show synergic effects on the formation of the highly reactive hydroxyl radicals as described in Fig. 8. Aranda *et al.* have also suggested that the magnetite nanoparticles might generate higher levels of ROS and oxidative stress due to magnetite possessing both  $\text{Fe}^{3+}$  and  $\text{Fe}^{2+}$  ions, while maghemite has mostly ferric iron ions ( $\text{Fe}^{3+}$ ).<sup>154</sup> For this reason, magnetite nanoparticles have been more frequently used to generate intracellular ROS.<sup>345-348</sup>

**3.2.7. Copper oxide nanoparticles.** Copper is a very interesting metal which has been applied in various fields including biomedicine, electronics, the metal industry, and for medical device development. In normal conditions, copper possesses two oxidative states, namely  $\text{Cu}^+$  and  $\text{Cu}^{2+}$ , thus it is a versatile candidate for biomedical applications. Copper oxide nanoparticles (CuONPs) have been explored for their antibacterial, angiogenic, and antitumor properties. For example, Sarkar *et al.* have biosynthesized CuONPs from copper sulfate using an (*Adiantum lunulatum*) plant extract to provide boost the enzyme-based antioxidant defenses of *Lens culinaris* seeds).<sup>349</sup> Another group, Sukumar *et al.*, have prepared environmentally-friendly rice-shaped CuONPs from the seed extract of *Caesalpinia bonduc* and evaluated their electrocatalytic properties by electrochemical measurement of riboflavin and antibacterial activity.<sup>350</sup> They found that the CuONPs have better antibacterial effects against *S. aureus* than *Aeromonas*. The effect of nanoparticle shape has also been investigated, with plate like CuONPs found to exhibit the best antibacterial activities against Gram-negative and Gram-positive bacteria compared to grain or needle shaped NPs. It was suggested that differing extents of membrane damage were the cause of this due to geometry dependent interactions with the cell surface.<sup>351</sup> Nasrollahzadeh *et al.* have demonstrated another efficient and environmentally-friendly way to synthesis CuONPs using an aqueous extraction of *Gundelia tournefortii* and have also evaluated their catalytic activity.<sup>352</sup> As a result of an energy level transition available within the ring of the cinnamoyl system, and also because of absorbance of the benzyl system, the UV-visible spectrum of *Gundelia tournefortii* extract shows specific signals of phenolics within the plant as two distinct absorbances at 385 and 235 nm, respectively, relating to  $\pi \rightarrow \pi^*$  transitions. The presence of these excited energy states demonstrates that polyphenolics are a potential source of antioxidant activity suitable for coating CuONPs. Rehana *et al.* have synthesized CuONPs using medically important plant extracts using a different chemical method for comparative evaluation of their antioxidant and anticancer activities.<sup>353</sup> They screened the performance of phytochemicals produced from leaf extracts for incorporation into CuONPs. They have also evaluated the antioxidant activity of CuONPs using ABBT, DPPP, and  $\text{H}_2\text{O}_2$  assays and found that the CuONPs formed in the presence of plant extract have a significantly higher ability to scavenge radicals compared to chemically synthesized CuONPs. Possibly, this is due to secondary metabolites from the plant extracts residing at the NP surface, including flavonoids, carbohydrates, glycosides, saponins, phenolic compounds, and tannins. CuONPs primarily generate ROS *via* two mechanisms; first, reaction at the nanoparticle surface, and second, by copper ion release and reaction.<sup>354</sup> Due to the short lifetime of ROS, the site of ROS production in both situations needs to be in close proximity to cause damage. Although these two mechanisms have suggested the details of how each component damages DNA, the exact mechanism remain unclear.<sup>355,356</sup> Angèl-Martínez *et al.* have evaluated the ROS generation ability of CuONPs and evaluated them using a DNA damage assay and

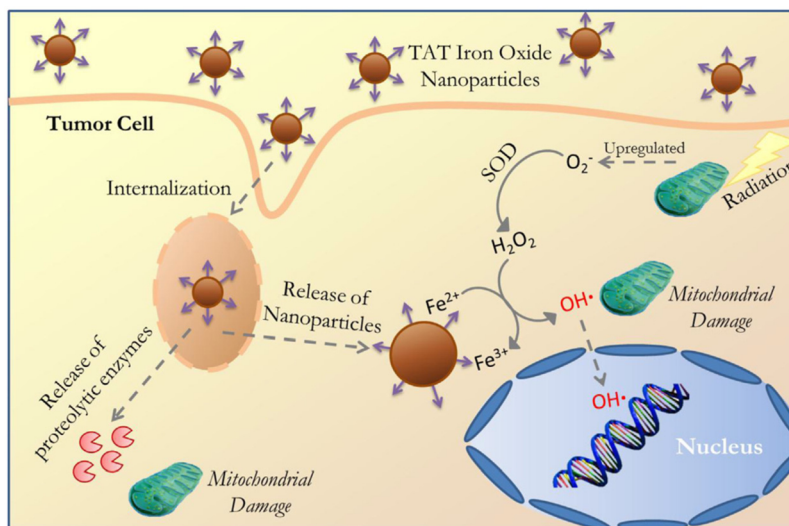


Fig. 8 Schematic illustration of the cellular internalization of TAT-conjugated iron oxide via lysosomal membrane permeabilization followed by NP and proteolytic enzyme delivery into the cytoplasm and subsequent interactions with organelles (nucleus and mitochondria) and catalytic reaction to produce the hydroxyl radical. Reproduced with permission from Hauser *et al.*<sup>344</sup> [Copyright 2016, Elsevier].

electron paramagnetic resonance (EPR) spectroscopy.<sup>354</sup> To address the question of whether ROS are generated from the particle surface or by released ions, they separated CuONPs from their supernatant containing any dissolved copper and then measure the degree of DNA damage in the presence of H<sub>2</sub>O<sub>2</sub>, ascorbate, or both. They have found that NP induced DNA damage in the presence of ascorbate was much higher than that of the dissolved copper in the supernatant and that ROS generation primarily occurs on the surface of nanoparticles. EPR analysis also suggested that the ROS generated from the surface of CuONPs in the presence of ascorbate are mainly ascorbyl, hydroxyl, and superoxide radicals. It is likely that CuONPs generate ROS through both Fenton-like reactions at the surface and through Haber–Weiss reaction by dissolved copper ions, respectively.<sup>292,357</sup>

**3.2.8. Zinc oxide nanoparticles.** Zinc is known to be an essential element in human health that activates many enzymes such as carbonic anhydrase, carboxypeptidase, and alcohol dehydrogenase.<sup>358</sup> Interestingly, zinc oxide nanoparticles (ZnONPs) have long been used in various industrial products such as paints and coating materials,<sup>359</sup> cosmetics,<sup>360</sup> plant fertilizers,<sup>361</sup> electrical devices,<sup>362</sup> drug delivery carriers,<sup>363,364</sup> as a suitable agent for bioimaging<sup>365</sup> and targeted gene therapy,<sup>366,367</sup> as sensors for detecting pollutants<sup>368</sup> and for environmental remediation.<sup>369</sup> Particularly, ZnONPs have gained tremendous attention in many biomedical applications such as target-specific delivery of anticancer drugs, imaging, and for antibacterial applications due to their low-cost synthesis, versatile properties due to variable shape, size, and morphology, biocompatibility, and antioxidant activity. The biological effects induced by ZnONPs mainly depend on the size, shape, morphology, concentration, pH, and surface chemistry of the particles. ZnONPs are also known to promote ROS production in the form of superoxide radicals and H<sub>2</sub>O<sub>2</sub> in the

absence of photochemical energy in plants.<sup>370</sup> ROS generated from ZnONPs can induce membrane lipid peroxidation subsequent to cellular damage, which is considered to be the primary reason for their plant toxicity.<sup>371</sup> Nagajyothi *et al.* have demonstrated the antioxidant and anti-inflammatory activities of ZnONPs synthesized from *Polygala tenuifolia* root extract.<sup>372</sup> They discovered that ZnONPs produced by *Polygala tenuifolia* inhibited the lipopolysaccharide (LPS)-induced synthesis of IL-1 $\beta$  and IL-6 proteins in a dosage-dependent manner, but dramatically reduced the expression of TNF- $\alpha$  at a concentration of 1 mg mL<sup>-1</sup>. However, ZnONPs have no effect on the level of anti-inflammatory related cytokines such as IL-1 $\beta$ , IL-6 and TNF- $\alpha$  in LPS treated RAW 294.7 cells and exhibited a dose dependent inhibitory effect on pro-inflammatory cytokines related to mRNA expression. The surface of green-synthesized ZnONPs is covered with phytochemicals which function as reducing agents, allowing ZnONPs to be less toxic compared to chemically synthesized ZnONPs.<sup>190</sup> Shoeb *et al.* have synthesized ZnONPs from egg albumin that show an anticandidal effect by ROS produced from ZnONPs.<sup>373</sup> They found that the anticandidal activity of ZnONPs was correlated with ROS production in a dose dependent manner which was confirmed by the protection of histidine against ROS. Moreover, ZnONPs can be easily internalized into cells *via* electrostatic interaction; once internalized, they produce excessive ROS leading to cell death.<sup>374</sup> Another beneficial effect of ZnONPs is their ability to generate ROS without light or under only visible light.<sup>375,376</sup> The antibacterial activities of ZnONPs seem to be caused by Zn<sup>2+</sup> ions being easily internalized by the cell, destroying cell organelles, DNA, and proteins. Xia and Gupta *et al.* have suggested that the ROS generation from ZnONPs occurs right at the surface of the NPs causing a subsequent change of electronic transfer in mitochondria, affecting cellular metabolism.<sup>208,377</sup>

**3.2.9. Gadolinium oxide nanoparticles.** Gadolinium oxide nanoparticles ( $\text{Gd}_2\text{O}_3\text{NPs}$ ) have been well studied for magnetic resonance imaging (MRI) application in cancer theranostics, but there has only been limited study of their antioxidant and redox-activities.<sup>378</sup> Seo *et al.* have investigated the nanoradiator effect of  $\text{Gd}_2\text{O}_3\text{NPs}$  in enhancing ROS production by radiosensitizing the high-atomic number (high- $Z$ ) nanoparticle to enhancing therapeutic treatment.<sup>379</sup> The generation of ROS in a  $\text{Gd}_2\text{O}_3\text{NPs}$  solution was measured by either monochromatic synchrotron X-rays or protons with a power of 45 MeV. They found that both photoexcitation and proton impact can enhance ROS production in a dose dependent manner, ranging from a fold change in production from 1.6–1.94 compared with radiation. Radiation therapy benefits from the strong Gd–Gd interatomic de-excitation-driven nanoradiator effect because it increases the formation of ROS by irradiated nanoparticles. Gd-based contrast agents have been reported to be cytotoxic mainly because of free Gd ions, *i.e.* those unbound from the crystal structure or incorporated into organic compounds.<sup>380</sup> This toxicity could be controlled with low doses of Gd. To improve the contrast ability (relaxivity), gadolinium content should be enhanced in multifunctional nanoparticles.<sup>381</sup>

**3.2.10. Cerium oxide nanoparticles.** Cerium oxide nanoparticles ( $\text{CeO}_2\text{NPs}$ ), also known as ceria, have gained considerable attention due to their unique catalytic activities (*i.e.* oxidant and antioxidant). The catalytic activities of  $\text{CeO}_2\text{NPs}$  are due to their different oxidation states ( $\text{Ce}(\text{IV})$ ) and ( $\text{Ce}(\text{III})$ ). In  $\text{CeO}_2\text{NPs}$ , cerium atoms are positioned in a cubic crystalline fluorite lattice structure, where  $\text{Ce}^{3+}$  and its corresponding oxygen vacancies are localized at the surface of NPs.<sup>382</sup>  $\text{CeO}_2\text{NPs}$  are very well-known antioxidants with a great potential to be therapeutic candidates in oxidative stress related diseases. The redox-reaction cycles of  $\text{CeO}_2\text{NPs}$  between  $\text{Ce}(\text{III})$  and  $\text{Ce}(\text{IV})$  oxidation states allow catalytic reactions with superoxide and  $\text{H}_2\text{O}_2$ , mimicking superoxide dismutase and catalase, the two key antioxidant enzymes which abate all noxious intracellular ROS *via* a self-regeneration mechanism. The main reasons for interest in  $\text{CeO}_2\text{NPs}$  are unique physical and chemical characteristics such as redox activities, and

oxygen buffering capacity. Furthermore, the cellular interactions, and cytotoxicity of  $\text{CeO}_2\text{NPs}$  based redox-active nanoparticles are strongly associated and dependent on surface chemistry.<sup>383</sup> Therefore,  $\text{CeO}_2\text{NPs}$  are known to be well tolerated in living organisms and could be potentially useful in treating chronic inflammation and ROS related pathologies including cancer and neurodegenerative disease.<sup>384,385</sup>

$\text{CeO}_2\text{NPs}$  are well known to act as antioxidants and to have redox-activity in tissue repair and regeneration. The relatively stable surface of peroxy/hydroperoxy species of  $\text{CeO}_2\text{NPs}$  is used for ROS generation.<sup>386,387</sup>  $\text{CeO}_2\text{NPs}$  with high surface  $\text{Ce}^{4+}/\text{Ce}^{3+}$  ratios function more efficiently as antioxidant enzyme mimics.<sup>388</sup> The redox-activities of  $\text{CeO}_2\text{NPs}$  (*i.e.*, switching oxidation state of  $\text{Ce}^{3+}$  and  $\text{Ce}^{4+}$ ) make these NPs a potential candidate for biomedical applications. The direct scavenging of  $\cdot\text{OH}$  by ceria NPs is presented in process 1 of Fig. 9(a),  $\text{NO}^\bullet$ ,  $\text{OONO}^\bullet$  chelating by  $\text{CeO}_2\text{NPs}$  have also been investigated.<sup>389–391</sup>  $\text{CeO}_2\text{NPs}$  have also shown superoxide dismutase-like effects (process 3 and 5 in Fig. 9(a)), that are associated with surface concentrations of  $\text{Ce}^{3+}$  and  $\text{Ce}^{4+}$ , pH, and chelating ligand concentrations.<sup>388,392</sup> The inflammatory cell signalling response to  $\text{CeO}_2\text{NPs}$ , and cell apoptosis upon ROS production are shown in process 4 and 6 in Fig. 9.<sup>268,393</sup>

Recently, Filippi *et al.* have demonstrated the antioxidant activity of  $\text{CeO}_2\text{NPs}$  and cerium nanorods (CNRs) in scavenging hydroxyl radicals.<sup>394</sup> They have shown that  $\text{CeO}_2\text{NPs}$  and  $\text{CeO}_2\text{NRs}$  exhibit stronger ROS scavenging activities than  $\cdot\text{OH}$  generation in phosphate buffer saline (PBS) and surrogated lung fluid (SLF). Further,  $\text{CeO}_2\text{NRs}$  have a larger surface area and higher defect density than  $\text{CeO}_2\text{NPs}$ , resulting in greater  $\cdot\text{OH}$  scavenging activity. Mahapatra *et al.* have suggested that the  $\text{CeO}_2\text{NPs}$  with different directional shapes (aspect ratios) are internalized in different rates in human dental pulp stem cells.<sup>395</sup> Nanoparticles with a smaller aspect ratio ( $\text{CeO}_2\text{NPs}$  and  $\text{CeO}_2\text{NRs}$ ) are internalized faster into the cells and are more effective at suppressing ROS either intracellularly or extracellularly upon  $\text{H}_2\text{O}_2$  treatment. Their findings suggest that special attention should be paid to the resulting particle geometry during synthesis of cerium oxide-based nanomaterials,

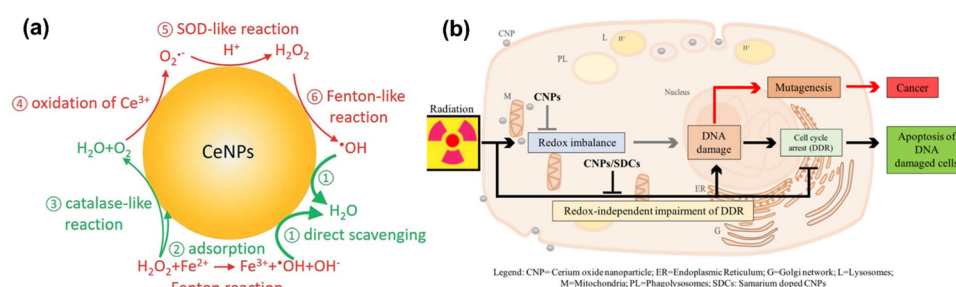


**Fig. 9** (a) Schematic illustration of Fenton reaction and reactive oxygen chemistry of ceria nanoparticles. Surface chemical reactions presented in red and green colors imply ROS generation and scavenging steps, respectively. This is a proposed model for ROS production and scavenging from ceria nanoparticles as redox-independent radio-sensitizing agents in HaCat keratinocytes cells. Reproduced with permission from Filippi *et al.*<sup>394</sup> [Copyright 2019, Royal Society of Chemistry]. (b) Schematic diagram illustrate the administrative role of ceria nanoparticles (here CNPs) to promote in a redox-independent manner strengthening of the cell DNA damage response (DDR) after exposure to radiation, weakening X-ray-induced DNA lesions on one side, and strengthening the stringency of cell cycle checkpoints and forcing damaged cells to undergo apoptosis on the other, hence inhibiting radiation-induced mutagenesis. Reproduced with permission from Corsi *et al.*<sup>386</sup> [Copyright 2018, Frontiers].

depending on their use such as for ROS-scavenging to protect from the ROS-insult environment, stem cell protection, tissue engineering and regenerative medicine applications.

Cells internalizing  $\text{CeO}_2$ NPs appear to respond more effectively to DNA damage *via* unrelated mechanisms that reduce DNA breaks, improving apoptotic outcomes.<sup>396</sup> Moreover,  $\text{CeO}_2$ NPs help cells to restore DNA integrity, the ability of which cancer cells lose during X-ray mediated mutagenesis by acting on the intimate pathways controlling survival of injured cancer cells. The radio-sensitization has no relationship with the redox-switching of  $\text{CeO}_2$  nanoparticles because it has not been affected by Sm-doping, a strategy that prevents a switch of  $\text{Ce}^{3+}/\text{Ce}^{4+}$  and provides 3+ valence by providing an antioxidant action<sup>397,398</sup> as shown in Fig. 9(b). The mechanisms of how  $\text{CeO}_2$ NPs interact with cells have been studied at cellular and molecular levels by several groups.  $\text{CeO}_2$ NPs have been suggested as cytoprotective antioxidants and free radical scavengers or oxidants but have also showed cytotoxicity.  $\text{CeO}_2$ NPs delayed cellular damage with ROS scavenging properties, resulting in an increase of cellular resistance to an exogenous ROS stimulation in oxidative stress condition.<sup>399</sup> On the contrary, the pro-oxidative effect of  $\text{CeO}_2$ NPs induces oxidative stress leading to cell death upon the cellular internalization of  $\text{CeO}_2$ NPs. Subsequently, ROS are generated from reduction of  $\text{Ce}(\text{IV})$  to  $\text{Ce}(\text{III})$ , and the dual nature of  $\text{CeO}_2$ NPs, as an antioxidant and a pro-oxidant, could be dependent on the shape, size, dose and exposure time of the nanoparticles.<sup>395,400–402</sup> Recently, Pota *et al.* have synthesized the redox-active  $\text{CeO}_2$ -based hybrid nanostructure *via* molecular combinations of organic and inorganic semiconductor for antibacterial and biomimetic radical homeostasis applications.<sup>403</sup>

### 3.3. Carbon-based nanomaterials

Carbon nanotubes (CNTs), fullerenes ( $\text{C}_{60}$ ), nanodiamonds, carbon quantum dots, graphene and its derivatives are all carbon-based nanomaterials (CBNs).<sup>25,404</sup> CBNs have unique properties including a high electrical conductivity, high mechanical strength, thermal conductivity, tunable optical behaviour, and catalytic activities which have led to significant interest in diverse fields such as biomedicine (drug delivery, tissue engineering, and regenerative medicine), energy storage, electronics, and biosensing. CBNs have recently shown a huge impact in biomedical fields, particularly applied in therapeutic delivery and cell/tissue imaging in cancer treatment. In fact, the potential use of CBNs has been reported in tissue engineering, anticancer, and anti-inflammatory treatments with their effect mainly due to ROS generation in cancer. The ROS generation by CBNs causes lysosomal and DNA damage, mitochondrial dysfunction and eventually leads to cell death *via* either apoptosis or necrosis. Moreover, CBNs have been intensively studied in pulmonary macrophage activation and inflammation, and the mechanisms of their immune suppression continue to be investigated.<sup>405,406</sup>

#### 3.3.1. Single-walled and multi-walled carbon nanotubes.

Single-walled carbon nanotubes (SWCNTs) and multi-walled

carbon nanotubes (MWCNTs) are the two types of carbon nanotube. The development of SWCNT-based cellular technologies has gained interest in nanomedicine for drug delivery, imaging, and immune response modulation.<sup>407</sup> An additional advantage of SWCNTs is their ability to avoid interfering with normal cell process, while maintaining their inherent properties. Pristine SWCNTs have toxic and negative effects on cellular responses, but functionalized SWCNTs have shown less cytotoxicity, better dispersion in aqueous solutions and better delivery to the cells.<sup>408–410</sup> In the last three decades, CBNs have been well established as a promising nanomaterial for technological and pharmaceutical applications. However, the long half-life of CBNs remains as a matter of concern in biological environments. Particularly for *in vivo* applications of CBNs, challenges remain in addressing their biodistribution that may affect their efficiency and safety. Michael *et al.* have developed a tumor-targeting SWCNT construct using covalent functionalization with multiple copies of tumor-specific antibodies, fluorescent probes, and radiometal-ion chelates.<sup>411</sup> The construct was used in human lymphoma *in vivo* model, *in vitro* flow cytometry, and cell-based immunoreactivity experiments with respect to adequate controls because it was known to react with human cancer cells. They found that the SWCNTs were degraded slowly in phagosomes, although the underlying mechanisms of graphitic degradation remain unclear. The enzymatic degradation of CNTs was tested in the presence of horseradish peroxide which can oxidize SWCNTs in the presence of a low level of  $\text{H}_2\text{O}_2$  at 4 °C in over 12 weeks of time at static conditions.<sup>412</sup> The biodegradation of CNTs has been studied using several other peroxidase enzymes including myeloperoxidase (MPO),<sup>413</sup> neutrophils and eosinophil peroxidase,<sup>414</sup> and lactoperoxidase<sup>415</sup> expressed by goblet cells in the epithelial layers of the respiratory tract. A mini review by Yang *et al.* has summarized studies on CNT biodegradation by macrophages and other factors that can influence CNTs biodegradation based on their individual characteristics and applications.<sup>416</sup> The schematic illustration of biological pathways for CNT biodegradation and ROS generation is presented in Fig. 10(a). Once CNTs are internalized into macrophages, either NADPH oxidase activates and starts the formation of  $\text{O}_2^{\cdot-}$  and then conversion of superoxide into  $\text{H}_2\text{O}_2$  by SOD, or reacts with free radical nitric oxide to produce  $\text{ONOO}^-$ . Hypochlorite is created when  $\text{H}_2\text{O}_2$  and  $\text{Cl}^-$  are combined by an enzyme like MPO. Conversely, if  $\text{Fe}^{3+}$  is present,  $\cdot\text{OH}$  is created, which attacks unsaturated carbon bonds on the side walls of CNTs and causes holes to form in the graphitic structure, ultimately leading to the degradation of CNTs into carbon dioxide.<sup>417,418</sup>

**3.3.2. Carbon-based quantum dots.** Carbon-based quantum dots (QDs) have also been explored for their antioxidant activity. Graphene quantum dots (GQDs) are well known for their electron donor and acceptor abilities and hence exhibit antioxidant activity and ROS generation under UV and visible light irradiation. The assembly of quantum dot-dye conjugates construct using peptide bridge can specifically design to recognize and interact with the breast cancer biomarkers.<sup>420</sup>

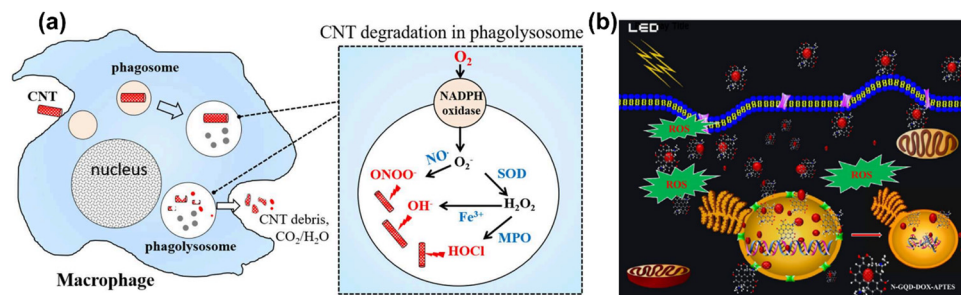


Fig. 10 (a) A scheme illustration of CNTs degradation and generation of ROS in a macrophage cell. Reproduced with permission from Yang *et al.*<sup>416</sup> [Copyright 2019, Frontiers]. (b) Light-mediated drug delivery and ROS production from GQD in breast cancer cell line MDA-MB-231 cells. Reproduced with permission from Ju *et al.*<sup>419</sup> [Copyright 2019, Wiley].

Christensen *et al.* have reported the dual nature of GQDs on the generation of singlet oxygen and ROS in an aqueous solution and radical either by chemical exposure using 2,2'-azobis (2-amidinopropane) dihydrochloride (AAPH) or by irradiation of visible light of 390–470 nm (peak 420 nm).<sup>421</sup> This study also shows that GQDs inhibit the oxidation of radical probes by decomposition of AAPH, concluding that upon external irradiation GQDs can generate ROS acting as pro-oxidants, and also scavenge chemically generated radical like antioxidants. Interestingly, Ruiz *et al.* have reported that the antioxidant ability of GQDs can be tuned with different chemical compositions and  $\text{sp}^2$ -hybridized carbon content.<sup>422</sup> They used top-down and bottom-up methods for GQDs synthesis using three different precursors namely carbon black, glucose, and pyrene with various chemical compositions, electron densities, and  $\text{sp}^2$ -hybridized carbon content. These results suggest that the GQDs with strong hydrogen donation potential and high contents of  $\text{sp}^2$ -hybridized carbon domains are the most effective radical scavengers. Recently, Nilewski *et al.* have reported that coal-derived GQDs functionalized with poly(ethylene glycol) show antioxidants abilities in chemical, electrochemical, and *in vitro* biologically stimulating conditions.<sup>423</sup> This study also showed that coal derived GQDs can quench superoxide and  $\cdot\text{OH}$ , converting superoxide into oxygen, acting as SOD mimetics. Wang *et al.* have improved GQDs by optimizing the functional groups of oxygen.<sup>424</sup> A study was performed to determine if surface oxygen functional groups had any relationship with antioxidant activity, researchers prepared GQDs with different total oxygen fractions and controlled oxygen concentrations. A GQD's antioxidant activity was affected by both its total oxygen level and types of oxygen groups. Furthermore, the transfer of hydrogen donor from the surface hydroxyl and carbonyl groups for the creation of adducts at the  $\text{sp}^2$  hybridized carbon atom site is the primary mechanism for the free radical scavenging ability of GQDs. It has been demonstrated that  $\text{C}-\text{OH}$  and  $\text{C}=\text{O}$  groups are more active than  $\text{C}-\text{O}-\text{C}$  groups for the scavenging of radical. However, different locations and chemical environments for each surface oxygen group may contribute to the scavenging actions of GQDs. Li *et al.* have reported electrochemical synthesis of phosphorus-doped GQDs and tested the particles for their free radical scavenging effects.<sup>424</sup> They found that phosphorous doping on the GQDs played a critical role in

scavenging DPPH radicals, as well as oxygen groups on the surface of GQDs. Carotenoids and other intriguing compounds with lengthy conjugated  $\text{C}=\text{C}$  chains have also been suggested as effective free radical scavengers.<sup>425</sup> Similarly, other CBNs have been thoroughly investigated for their capacity to neutralize ROS and operate as free radical scavengers. For instance, fullerene derivatives exhibit high superoxide quenching activity, which is supported by a mechanism that combines electron transfer and adduct formation.<sup>426</sup> Recently, CNT-tailored electrospun nanofibers with electrical conductivity and bi-modal nanotopography have been used for bone and neuronal tissue engineering applications.<sup>427,428</sup> Fenogilo *et al.* found that MWCNTs in aqueous solution do not generate oxygen or carbon-centered radical in the presence of  $\text{H}_2\text{O}_2$  and formate.<sup>429</sup> On the contrary, purified MWCNTs are very effective scavengers for  $\cdot\text{OH}$  and  $\text{O}_2^-$ , although the molecular mechanism is not fully understood. Galanio *et al.* have reported theoretical studies on the potential ability of SWCNTs as free radical scavengers using density functional theory calculations.<sup>430</sup> Their findings suggest that once radicals are attached to a nanotube, additional reactions can be enhanced, indicating that SWCNTs can act as free radical sponges. In case of reaction with OH radicals, subsequent additions would lead to products in which the created OH groups are distributed in clusters rather than a homogeneous spread throughout the nanotube.

**3.3.3. Graphene-based nanomaterials.** Graphene-based (2D) nanomaterials such as graphene (G), reduced graphene oxide (rGO), and few-layer graphene (FLG) have been used as a new class of potential antioxidants that combine physical barrier function with an ultra-high surface area for free radical scavenging. Moreover, graphene-based nanomaterials have also been shown to have protective characteristics to many molecular targets from oxidation by these species, and to be highly effective as  $\cdot\text{OH}$  scavengers. Qiu *et al.* have investigated the antioxidant chemistry of GO, rGO, and FLG focusing on their roles in oxygen protection technology.<sup>431</sup> They found that the  $\cdot\text{OH}$  scavenging activities were in the order FLG > rGO > GO, which is an inverse order of the total surface area of the corresponding graphene nanomaterials. Although FLG has a smaller surface area, its greater scavenging ability suggests that its main scavenging ability is due to the intact  $\text{sp}^2$ -hybridized

carbon domains on the basal surface, rather than hydroquinone or hydroxyl groups. In addition, GO is not a strong H-donor due to the non-phenolic nature of the hydroxyl groups on its surface, which reside at basal  $sp^3$ -hybridized carbon atoms, and hence do not allow radical resonance stabilization following H-donation.

Many other CBNs including fullerenes,<sup>432</sup> CNTs, carbon nanodots and metal-doped carbon nanodots,<sup>433–435</sup> GQDs,<sup>436</sup> GO,<sup>437,438</sup> rGO,<sup>439</sup> FLG<sup>431</sup> and metal functionalized GO<sup>16,165,440</sup> have been investigated for ROS and radical scavenging effects. The scavenging abilities of CBNs are due to  $sp^2$ -hybridized carbon sites, structural defects, surface electrophilic effects, H-donation from surface functional groups, and adduct formation. However, other possible factors including imperfect antioxidant mechanisms, a lack of an effective method for the regulation of antioxidants, and a low antioxidant activity need to be investigated.

ROS generation and their roles have been implicated in many disease animal models. Sharma *et al.* have performed a set of experiments to determine SWCNT toxicity in rat epithelial cells and measured ROS generation by change in fluorescence using dichlorofluorescein.<sup>441</sup> They found that the increased ROS production upon rat epithelial cell exposure to SWCNTs occurred in a dose and time dependent manner. Additionally, the decreased level of glutathione suggested a loss of cellular defense mechanisms against ROS generation in SWCNTs treated cells. The inhibition of mitochondrial function had no change on ROS levels, suggesting the role of SWCNTs in ROS production. Manna *et al.* have reported the effects of SWCNTs in human keratinocytes cells, looking at toxicity, oxidative stress and cell proliferation.<sup>442</sup> They found that the SWCNTs increased oxidative stress in keratinocytes by activating NF- $\kappa$ B pathway in a dose dependent manner. The NF- $\kappa$ B signalling seems to be activated by stress-related kinases triggered by SWCNTs in the keratinocytes. Alarifi *et al.* have reported the underlying mechanism of the toxic effects and ROS generation of MWCNTs in mouse fibroblasts (L929).<sup>443</sup> They found that the MWCNTs significantly increase ROS production, lipid peroxidation, superoxide dismutase levels, and decrease glutathione concentration. Rasras *et al.* have examined the effects of SWCNTs and MWCNTs in rat brains, in particular focusing on mitochondria. They measured ROS activity with altered levels of malondialdehyde, glutathione and mitochondrial membrane potential.<sup>444</sup> They found that both SWCNTs and MWCNTs may damage brain tissue through mitochondria by increasing oxidative stress and activating apoptosis-related cell death pathways. According to Hou *et al.* the direct photoreactivity of pristine SWCNTs is usually low under sunlight, however indirect photoreactions that generate  $\cdot OH$  may play a greater role in natural aquatic environments.<sup>445</sup> Furthermore, the reactivity of SWCNTs to  $\cdot OH$  depends on their chirality as well as the surfactant used. Singh *et al.* have demonstrated the influence of SWCNTs on multicellular chirality, a property that describes a state of directional cell migration. They also show that incubation of SWCNTs with mouse myoblasts (C2C12) and human umbilical vein endothelial cells (hUVECs) stimulated

ROS production by intra and extracellular oxidative stress in dose and time dependent manner.<sup>446</sup> They found that the SWCNTs-mediated oxidative stress leads to a loss of multicellular chirality.

Graphene itself is not considered a good candidate for biomedical applications due to its poor dispersibility in aqueous conditions such as water, phosphate buffer and culture media, however, chemically functionalized GO or rGO are good candidates for various biomedical applications.<sup>447–449</sup> GO and rGO have widely been studied in cell biology due to their outstanding biocompatibility, large surface area, and simple modification of the surface.<sup>450,451</sup> GO contains hydroxyl, carbonyl, epoxy, and carboxyl groups on the base plane and edges, which promote cell affinity and a high hydrophilicity. Due to the wrinkled nature of the carbon plane, GO may increase stem cell adherence and differentiation to the osteoblast lineage.<sup>452,453</sup> Nanosized GO sheets could serve as nanocarriers of drugs<sup>451,454,455</sup> and nucleic acids,<sup>456</sup> for gene transfection<sup>457</sup> into cells or animals<sup>458</sup> for bioimaging,<sup>459</sup> biosensing,<sup>460,461</sup> and therapeutic purposes.<sup>462</sup>

Graphene-based materials can modulate the metabolic activities of macrophages by increasing ROS levels resulting in mitochondrial membrane damage and apoptotic cell death. It is complicated and challenging to study the stability and susceptibility to different reagents of graphene-based nanomaterials. In the study of Hsieh *et al.*, the degradation rate constants of graphene-based nanomaterials have been calculated using dissolved organic carbon loss and steady-state concentrations of individual ROS as an indicator of their reactivity with OH,  $^1O_2$ , and  $O_2$ .<sup>463</sup> Their findings suggest that ROS distribution and GO reactivity with ROS requires long-term exposure of GO and rGO. A detailed review by Niu *et al.* has summarized nanocarrier-based delivery vehicles to overcome the challenge of crossing the blood–brain barrier (BBB) to cure neurodegenerative diseases.<sup>464</sup> Ju *et al.* have investigated ROS using graphene quantum dots (GQD) that function as a photosensitizer with various nitrogen atom dopant concentrations, thus achieving photodynamic therapy.<sup>419</sup> They also found that amine functionalized doxorubicin (DOX) loading on GQDs can have two functions, first, as a drug delivery carrier for nuclear targeting with photosensitizer and second, as a strong ROS generator as shown in Fig. 10(b).

**3.3.4. Silicon carbide nanomaterials.** Silicon carbide (SiC) is a compound composed of silicon (Si) and carbon (C) atoms in a 1:1 ratio, and can be considered as carbon-based nanomaterials in the sense that it contains carbon as a significant component of its structure. In crystal lattice structure, each silicon atom is covalently bonded to a carbon atom.<sup>465</sup> Recently, SiC is growing significant interests as a potential solution for enhanced energy storage and power density.<sup>466</sup> Moreover, the unique physical and chemical characteristics of SiC such as high temperature resistance, strong mechanical strength, excellent resistance to wear and oxidation, and chemical stability compared to carbon-based materials endow SiC an excellent nanomaterials for renewable energy storage, and portable electron applications.<sup>467</sup>

Silicon carbide is the second hardest-known material after diamond and is used in various industrial applications. SiC has potential applications in various fields but has been reported to have toxic effects on bacteria and mammalian cells.<sup>468,469</sup> For example, Pourchez *et al.* investigated SiC nanoparticles for impact of physico-chemical features on pro-inflammatory and pro-oxidative effects on macrophage.<sup>470</sup> They found that SiC nanoparticles generate oxidative stress in macrophages, leading to significantly enhanced and dose-dependent LDH release and pro-inflammatory response in the macrophage cell line. The cytotoxicity of SiC mostly depends on morphology of the SiC nanoparticles. Studies have shown that SiC nanostructures such as nanofibers and nanorods induce oxidative stress in *Pseudomonas putida* compared to micrometric SiC, likely by increasing the formation of highly reactive radicals and disrupting cell membrane integrity, leading to DNA damage.<sup>469</sup> Similarly, research has revealed that SiC nanowires (SiCNWs) are more toxic to hMSCs than SiC nanoparticles (SiCNPs) at the same concentration. Moreover, SiCNWs negatively impact hMSCs' cellular activities including adhesion, proliferation, migration ability, multipotency, phenotypes, and cytokine secretion. This adverse effect is likely due to an overproduction of pro-inflammatory cytokines MCP-1 and IL-8 and a deficiency in MMP-3 and C3. Furthermore, SiCNWs have a greater impact on MCP-1, IL-8, MMP-3, and C3 secretion than SiCNPs, leading to differences in cytotoxicity to hMSCs between the two.<sup>468</sup> In summary, while SiC includes carbon as a key components, it is more accurately described as a ceramic or composite material rather than carbon-based materials.

### 3.4. Nanomaterials for drug delivery

RANs have also been developed for the delivery of molecules/drugs which can cause intracellular ROS generation after internalization by cells. Mesoporous silica nanoparticles (MSNs) are frequently used in drug delivery, imaging, and many biomedical applications due to their unique physical pore structure (pore size, shape, volume, and alignment), surface area, surface chemistry, biocompatibility and biostability.<sup>239</sup> Their biomedical applications include targeted therapeutic delivery, biosensing, cell and tissue imaging, and photothermal or photodynamic therapy for cancer treatment. Both porous and non-porous silica nanoparticles can generate ROS in the form of  $\cdot\text{OH}$ ,  $\text{O}_2^-$  and  $\text{H}_2\text{O}_2$ , causing an imbalance between oxidant and antioxidant states and creating intracellular oxidative stress.<sup>471</sup> For example, Yi *et al.* have fabricated MSNs as redox-responsive short-chain gatekeeper nanoparticles for the controlled release of salicylic acid.<sup>472</sup> Redox-responsive gatekeepers such as these MSNs are openable by glutathione, an endogenous reductant in cells, and thus do not require any external/exogenous agents. The versatility of MSN surface chemistry creates huge potential for the design of new multifunctional nanocarriers for more efficient delivery. An innovative redox-responsive delivery system of multifunctional nanoparticles capped with bovine serum albumin and hyaluronic acid has been developed by Chen *et al.* for cancer drug delivery and MRI imaging.<sup>473</sup> An overview of the synthetic

process for a multifunctional MSN for redox-responsive drug delivery and MR imaging can be found in Fig. 11. Zhao *et al.* have also modified MSNs with redox-responsive oligosaccharides for targeted drug delivery using disulfide bonds that are cleavable under high concentrations of glutathione (GSH).<sup>474</sup> The covalent disulfide bond is relatively stable in the extracellular fluid and plasma, and is easily ruptured in intracellular fluid due to the increase in GSH concentration between the extracellular (2–20  $\mu\text{M}$ ), and intracellular (1–10 mM) fluids.<sup>475</sup> Surface functionalized MSNs have been tested for GSH-responsive drug release in tumors. As shown in Fig. 11(b), oligomeric hyaluronic acid functionalized multifunctional MSNs (oHA-MSN) are internalized through endocytosis. The HA-mediated CD44 interaction and GSH-triggered disulfide cleavage led to drug release in the cell after cellular uptake. Singh *et al.* have developed cerium oxide capped MSN nanocarriers as a pH-responsive drug delivery system.<sup>25</sup> In this system the cerium oxide nanoparticles are shown to facilitate the pro-oxidant properties of MSNs followed by increased ROS levels leading to the killing of cancer cells. Additionally, a DOX combination therapy with cerium oxide capped MSNs is more effective in ROS generation, demonstrating a cytotoxic synergism between the drug and nanoparticle in terms of ROS generation. The combined effect of the pH-triggered intracellular ROS therapy and chemotherapy caused by DOX-loaded cerium oxide capped MSNs is presented in Fig. 11(c). A proper range of ROS concentration seems to be critical in functioning as essential messengers to facilitate immune responses.<sup>476,477</sup> ROS can be a signal for cellular danger in the immune system by the activation of dendritic cells (DCs),<sup>478,479</sup> increasing the concentration of co-stimulating molecules like CD80 and CD86 to speed up the presentation of an antigen.<sup>480</sup> Therefore, ROS generating nanoparticles might improve the immune response.<sup>481</sup> For example, Lu *et al.* have found that mesoporous organosilica nanoparticles improve cancer immunotherapy by depleting glutathione.<sup>482</sup> They used biodegradable glutathione-depleted dendritic mesoporous organosilica nanoparticles (GDMON) with a tetrasulfide-incorporated framework to deliver an antigen protein (ovalbumin) and a toll-like receptor 9 (TLR9) agonist into antigen-presenting cells (APCs). As a result of  $-\text{S}-\text{S}/\text{GSH}$  redox chemistry, glutathione (GSH) levels are decreased intracellularly and ROS are generated, leading to the proliferation of cytotoxic T lymphocytes (CTLs) which inhibited tumor growth in B16-OVA cells, an aggressive melanoma model, described in Fig. 11(d). Overall, intracellularly generated ROS could be an oxidative stress and intracellular antioxidant system like GSH will be operated in nature.<sup>483</sup> In cells, GSH is an endogenous antioxidant neutralizing excessive ROS, which can be cytotoxic.<sup>484</sup> Farooq *et al.* have tested titania coated MSNPs with hydroxyl groups on the surface that can react with intracellular  $\text{H}_2\text{O}_2$  producing ROS, possibly contributing to biocompatibility as well as therapeutic delivery. The MSNPs generate ROS much less than dense silica nanoparticles. In addition, MSNPs exhibit less toxicity than nonporous silica nanoparticles, whose surface modification has further improved the biocompatibility.

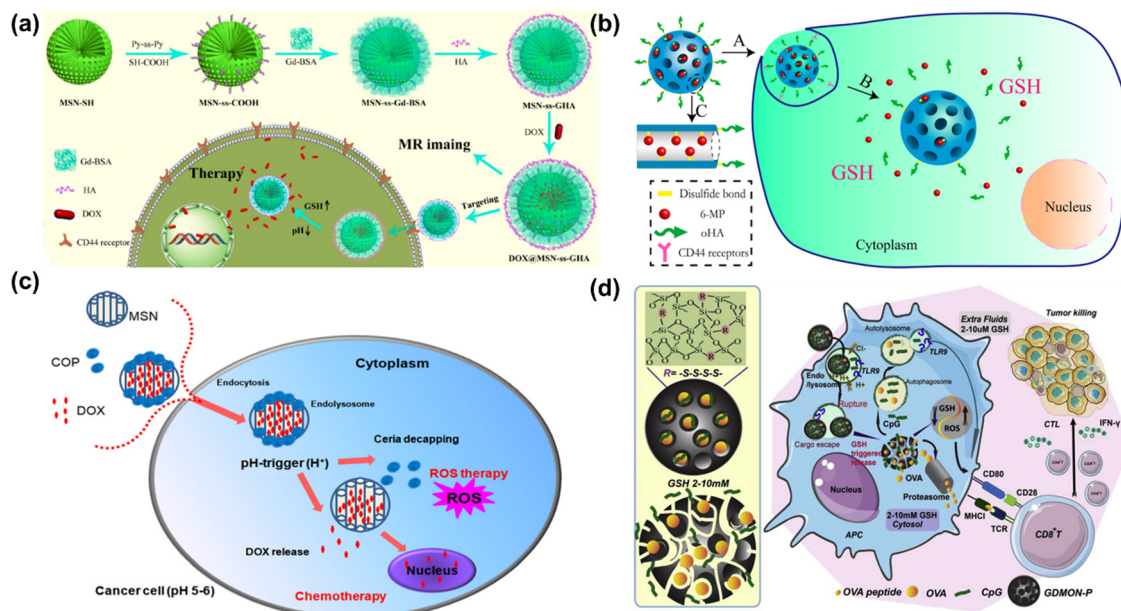


**Fig. 11** (a) Schematic diagram to illustrate the preparation method of multifunctional MSNs for redox-responsive theranostics (drug delivery and imaging). Reproduced with permission from Chen *et al.*<sup>473</sup> [Copyright 2016, American Chemical Society]. (b) Schematic diagram presenting GSH-responsive drug release in the tumor cells from MSNs; (A) cellular internalization of oHA-modified MSNs via oHA mediated CD44 interaction, and (B) GSH-activated drug release into the cell, (C) Pore structure of CMS-SS-MP/OHA. Reproduced with permission from Zhao *et al.*<sup>474</sup> [Copyright 2014, American Chemical Society]. (c) Schematic diagram illustrating the combined effect of intracellular ROS therapy and chemotherapy (doxorubicin), release from cerium oxide nanoparticles capped MSNs in cancer cells. Reproduced with permission from Singh *et al.*<sup>111</sup> [Copyright 2019, American Chemical Society]. (d) Schematic illustration of GDMON-P + OVA + CpG enhanced cancer immunotherapy, and co-delivery of an antigen protein (ovalbumin) and CpG into antigen presenting cells (APCs) and inducing endosome escape. In the cytosol of APCs, GDMON-P diminish the intracellular glutathione (GSH) level through the  $-S-S-/GSH$  redox chemistry and up-regulating the intracellular ROS production and endowing specific cytotoxic T cell (CTL) proliferation and inducing cancer cell apoptosis. Reproduced with permission from Lu *et al.*<sup>482</sup> [Copyright 2016, Elsevier].

Previous research has attributed the increase in cytoplasmic and mitochondrial ROS production during silica nanoparticles (SiNPs) exposure solely to NADPH oxidase 2 (NOX2) pathways.<sup>485</sup> However, research teams like Cui *et al.* and Joshi *et al.* reported ROS production upon exposure of cells such as macrophages and Cos7, to silica nanoparticles could also be independent from NOX2 pathways.<sup>485,486</sup> Reported results suggest that silica nanoparticles are able to generate ROS independently from NOX2 once they are in the phagosomal system contributing to the increase in cytoplasmic ROS and subsequently downstream cytotoxic pathways such as over expression of COX2, enzyme linked to a variety of inflammatory pathways, or including phagosome leakage.<sup>485,486</sup> The latter is hypothesized to happen through Fenton reaction between the free ion left on the surface of the silica particles after production of hydrogen peroxide in the phagosomes, the resulting  $\cdot OH$  radicals drive the damage of the phagosomal membrane *via* per-oxidation leaking ROS.<sup>486</sup>

In addition to mitochondrial and NOX2 mediated ROS production, other methods for ROS production induced by silica nanoparticles include peroxisomes and xanthine oxidase.<sup>487</sup> Furthermore, Petracche Voicu *et al.* have shown that silica nanoparticles induced ROS production in MRC-5 cells is also enabled *via* severe down regulation of the tripeptides glutathione (GSH), antioxidant mechanism in cells.<sup>488</sup> Moreover, the abundant hydroxyl groups on the surface of silica

nanoparticles together with topographic irregularities enhances the production of hydroxyl radicals, which in turn can interact in the chemical reactions, such as production of superoxide that get dismutated by extracellular superoxide dismutases to produce hydrogen peroxide, or with membrane NADPH oxidase systems to produce superoxide anion even before entering into the cells.<sup>488</sup>

### 3.5. Biofouling and NPs aggregation effects

Surface biofouling is a common issue with the metallic nanoparticle's therapeutics, where non-specific biomolecules bind to and accumulate at the reactive nanoparticles surface, creating a protein corona.<sup>489</sup> The formation of a protein corona has been shown to occur rapidly, to modulate nanoparticles toxicity, and to alter their uptake.<sup>490</sup> Furthermore, quantification of the effect of a protein corona on the kinetics of redox-reactions at a NPs surface has not been carried out to our knowledge. It may be the case that this accumulation reduces the chance of direct interaction between electron donor and acceptor molecules and the NPs, thereby lowering its therapeutics efficacy. This magnitude will likely be particle and environment specific, with potential for some proteins to perhaps improve electron transfer from NPs surface if they undergo in redox-reactions themselves.<sup>491</sup>

The stability of a suspension of NPs, *i.e.* the likelihood of NPs aggregation, depends on its surface chemistry and the

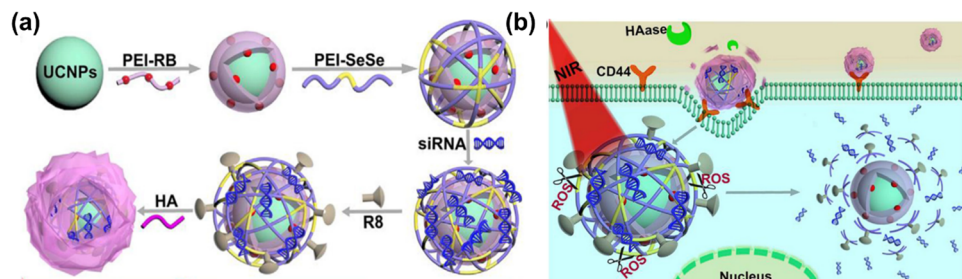


Fig. 12 (a) Schematic illustration of step-by-step preparation and surface modification of up-conversion nanoparticles (UCNP-PEI-RB-PEI-SeSe/siRNA-R8-HA) for drug delivery and imaging applications, and (b) corresponding sequential responsive disintegration of UCNPs and NIR boosted intracellular siRNA release and reactive oxygen species therapy. Reproduced with permission from He *et al.*<sup>498</sup> [Copyright 2019, Elsevier].

solvent its dispersed. The complex and dynamic physiological environments that a NP therapeutic may be exposed to during application, therefore present a great challenge in terms of retention activities. To overcome this, several passivation methods have been developed that preserve function and reduce NPs surface instabilities.<sup>492</sup> Furthermore, various surface coatings approaches including polymers, lipids, and silica-based coatings have been developed to improve the stability, and functionality. Silica-based coatings introduced significant porosity at the surfaces with sustainable benefits for drug loading and controlled release,<sup>493</sup> and lipid coating can be used to reduce cytotoxicity and improve cellular uptake due to the similarity to the cell membranes.<sup>494</sup>

### 3.6. Other types of nanomaterials

Up-conversion nanoparticles (UCNPs) are a distinct category of nanomaterials that are doped with rare earth metal atoms embedded in a crystalline structure. For example, lanthanide ( $\text{Ln}^{3+}$ ) can be used to dope nanocrystals. UCNPs are anti-Stokes type materials, which exhibit anti-Stokes optical properties. When these types of nanomaterials interact with infrared radiation (lower energy photons), they absorb and upconvert to emit in the visible light spectrum (higher energy photons) through a series of real as opposed to virtual levels, as in conventional two-photon dyes.<sup>495</sup> The UCNPs can up-convert two or more lower energy photons into one high energy photon through either sequential excitation of one emitting atom or excitation actions of two different atoms and subsequent energy transfer between co-doped rare-earth atoms.<sup>496,497</sup>

The applications of UCNPs as delivery and bioimaging agents have been explored enormously, for example He *et al.* have developed up-conversion nano-onions (UNCNs) coated with polymer, which degrade sequentially in response to NIR stimulation in the extracellular environment.<sup>28,498</sup> These UCNs have a core of UCNPs functionalized with the photosensitizer rose Bengal (RB), which is conjugated with poly ethylenimine 600 (PEI-600), followed by a ROS responsive middle layer of singlet oxygen ( ${}^1\text{O}_2$ ) sensitive diselenide bonds (PEI-SeSe) connected to siRNA and cell penetrating peptide R8 modifications, and an outer coating layer of negatively charged hyaluronic acid (HA) represented as (UCNPs-PEIRB-PEI-SeSe-R8-HA) as presented in Fig. 12(a). Electrostatically adsorbed

siRNA molecules on the middle PEI-SeSe layer were released when the UCNPs core was irradiated with light between 525 and 540 nm to activate the RB in PEI-RB's inner layer, boosting ROS production and fully decomposing the PEI-SeSe bonds as shown in Fig. 12(b). The significance of the HA coating is to prolong the circulation of the nanoparticles in the bloodstream, by preventing NP degradation during delivery process and to control UCNPs transporting to target special tumor cells *via* cell membrane receptor CD44.<sup>499</sup> The subsequent stripping of UCNPs coating upon internalization into the cells improved siRNA delivery without leaking, thus it can be an efficient strategy for NIR-assisted gene therapy.

## 4. Biomedical applications of RANs

### 4.1. Cancer

Reactive oxygen species are natural byproducts of various cellular processes including metabolism, proliferation, and differentiation. An excessive amount of ROS can damage cells by random interaction with proteins, lipids, and DNA, ultimately leading to cell death.<sup>35,500</sup> ROS are generated as an oxidative phosphorylation byproduct in mitochondria including superoxide, hydrogen peroxide ( $\text{H}_2\text{O}_2$ ) and hydroxyl ( $\text{OH}^-$ ) radicals.<sup>28,35</sup> ROS regulation is important within the cellular microenvironment and is mostly controlled by ROS-scavenging mechanisms such as superoxide dismutases (SOD1, SOD2, SOD3), peroxiredoxins, glutaredoxins, thioredoxins, glutathione peroxidase, and catalases.<sup>501,502</sup> However, in the event where these unstable radicals are uncontrolled due to a reduction of intracellular ROS-scavenging, oxidative stress can result.<sup>502</sup> Oxidative stress conditions are harmful for normal cells, and a chronic over production of ROS can induce normal cells to transform into tumor cells through genetic alterations, thus reprogramming cancer cell metabolism.<sup>110</sup>

Among the pathophysiological processes that ROS are involved in, such as genomic instability, inflammation, and metabolic reprogramming, tumorigenesis is of particular interest.<sup>35</sup> Disruption of ROS-scavenging-enzyme production can trigger several cancers signalling cascades, including cancer angiogenesis and metastasis as presented in Fig. 13. All these cellular activities mentioned above are highly dependent

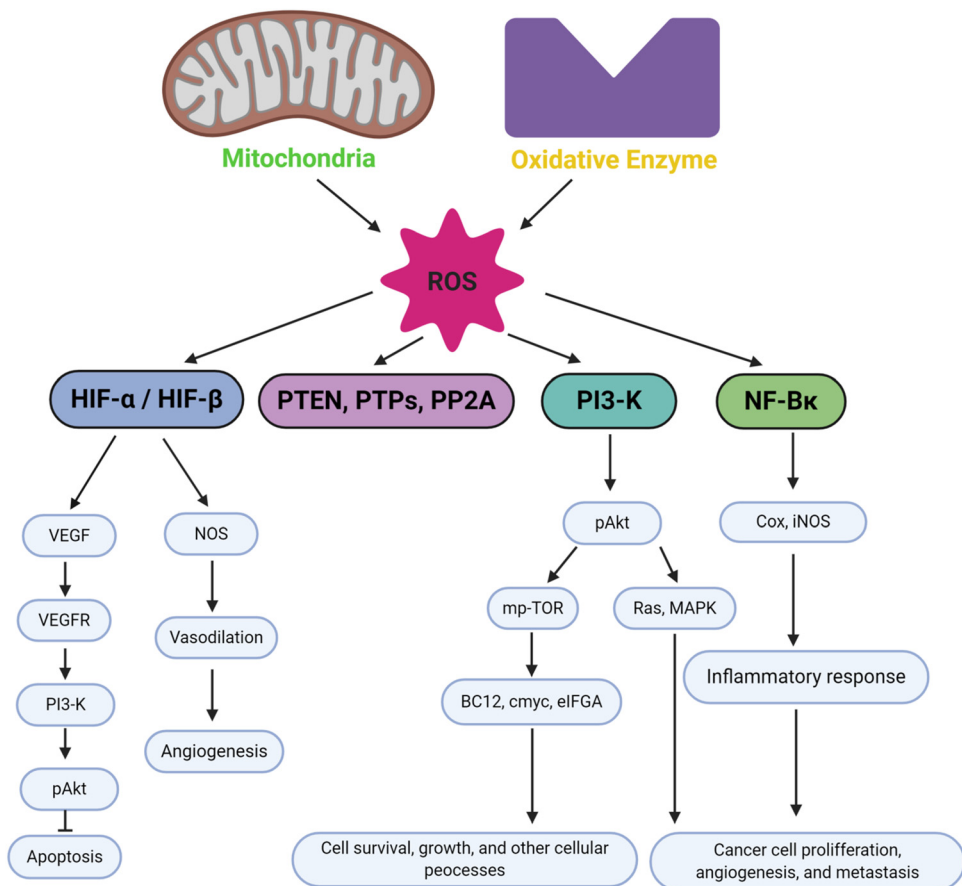


Fig. 13 The biological significance of ROS in inducing cell signalling pathways in cancer for apoptosis, angiogenesis, cell survival, inflammatory response, and cancer proliferation and metastasis. Figure created by authors using BioRender.com.

on the levels of ROS, which promote cell proliferation and survival at low levels, induce cell cycle arrest leading to cellular differentiation at intermediate levels and cause oxidative damage and DNA mutations at high levels potentially leading to cancer.<sup>501</sup>

ROS generation mainly occurs in mitochondria within the electron transport chain (ETC) in which one-electron reduction of oxygen happens at several major sites such as complexes I, II and III.<sup>35,501</sup> Complexes I and II produce  $O_2^\bullet$  in the mitochondrial matrix, and superoxide dismutase protein 2 (SOD2) will subsequently convert  $O_2^\bullet$  into  $H_2O_2$  through complex III when intermembrane  $O_2^\bullet$  is transferred to the outer mitochondrial membranes and cytosol. Subsequently,  $O_2^\bullet$  is converted into  $H_2O_2$  by superoxide dismutase protein 1 (SOD1). Another ROS production pathway utilizes nicotinamide adenine dinucleotide phosphate (NADPH) oxidases (NOX) located in the cell membrane, which activate the conversion of oxygen to  $O_2^\bullet$  via electron transfer across biological membranes, which will then be further reduced by superoxide dismutases to produce  $H_2O_2$ .<sup>35</sup>

Over the last few decades, surface functionalized metal nanoparticles, lipids particles, liposomes particles, quantum dots, and dendrimers have been extensively applied for anti-cancer drug delivery and imaging applications.<sup>503</sup> The oxidative

nature of ROS generated by NPs is very useful in anticancer therapy to suppress and eliminate cancerous cells. The activation of ROS is highly dependent on the redox-related application, such as photodynamic therapy (PDT), chemodynamic therapy (CDT), radiation therapy (RT), sonodynamic therapy (SDT), controlled drug release (CDR) *etc.*, as well as the functionalities of the nanoparticles. Meanwhile nanoparticles containing prooxidant can be internalized into cancer cells followed by ROS generation within mitochondria with subsequent activation of tumor necrotic factor and other transcription factors, which finally lead to adenosine triphosphate depletion and cell necrosis.<sup>503</sup> Alternatively, cancer cells can be killed by cell cycle arrest *via* disruptions of the mitochondrial membrane, which will further increase ROS levels, exceeding body defense system, and activate effector caspases.<sup>504,505</sup>

Chen *et al.* have reported the mechanism of plasmon enhanced PDT based on photosensitizers (PS) that generate ROS to enhance cancer therapeutic efficiency. The PS used in the study are upconversion nanoparticles conjugated with gold nanorods that convert near-infrared (NIR) light to visible light and then excite surface plasmon resonance (SPR) locally to generate cytotoxic ROS.<sup>506</sup> During this process, apoptotic cell death *via* caspases-3 activation occurs followed by the release of cytochrome *c* from mitochondria upon ROS production as

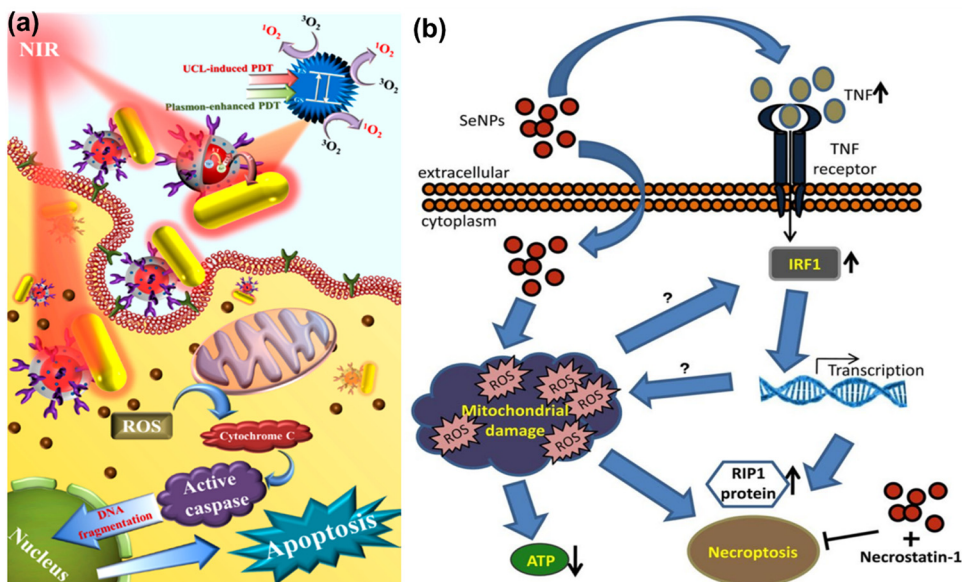


**Fig. 14** (a) Cell apoptosis pathway of plasmon-enhanced PDT treatment using upconversion nanoparticles conjugated with gold nanorods. Reproduced with permission from Chen *et al.*<sup>506</sup> [Copyright 2016, American Chemical Society]. (b) Selenium nanoparticles induced ROS-mediated necroptosis in PC-3 cells. Reproduced with permission from Sonkusre *et al.*<sup>503</sup> [Copyright 2017, Springer].

shown in Fig. 14(a). A similar study performed by Sonkusre *et al.*<sup>503</sup> involved selenium induced necroptosis reported in PC-3 cells, where the nanoparticle activates TNF and the transcription factor IRF1, leading to ROS-mediated necroptosis through RIP1 protein as illustrated in Fig. 14(b). Selenium nanoparticles (SeNPs) have been widely studied as they show strong anticancer activity and excellent biocompatibility in a physiological environment.<sup>503</sup> Several forms of SeNP such as chemically synthesized SeNP, sol-gel synthesized SeNPs, and co-precipitated SeNPs have been reported.<sup>504</sup> It has been demonstrated that chemically functionalized SeNPs inhibit cell growth by suppressing the transcription and translation of androgen receptors, leading to a loss of androgen receptors *via* phosphorylation, ubiquitination and Akt/Mdm2 degradation pathways.<sup>507,508</sup> Meanwhile transferrin-conjugated SeNP increases intracellular ROS and activates MAPKs pathways inducing p52-mediated apoptosis. Glucose incorporated into SeNPs is also known to induce cell apoptosis.

Recently, Zhuang *et al.* have reported that SeNPs enhanced the permeability and retention (EPR) of NP in the cancer area, thus inhibiting tumor growth more effectively. In addition, SeNPs accumulate within the cancer causing a drastic increase of ROS and oxidative stress, thus activating cell-death pathways.<sup>509</sup> It is of interest that SeNPs coated with human serum albumin (HSA) show enhanced mitochondrial targeting compared to unmodified SeNPs. Alternatively, Chan *et al.* have investigated the potential combination of SeNPs seeded with iodine-125 ( ${}^{125}\text{I}$ ) for chemo-radiotherapy application to be more effective and safer to target cancer.<sup>510</sup> Sensitizer based SeNPs have shown Auger-electron effect and Compton effect by generating a high concentration of intracellular ROS with only low-dosages for long-term activation, regulating p53-mediated DNA

damage apoptotic signalling pathways and MAPKs phosphorylation to prevent cancer cell growth.<sup>510</sup>

#### 4.2. Neurodegenerative diseases

Neurodegenerative diseases are a heterogeneous group of disorders including, Parkinson disease, Huntington diseases (HD), Alzheimer's disease (AD), epilepsy, multiple sclerosis (MS), amyotrophic lateral sclerosis (ALS), and strokes,<sup>511–514</sup> defined by a decrease in the number of neurons and glial activation.<sup>515,516</sup> Oxidative stress has been considered as a central and crucial element in the onset of these neurodegenerative conditions. Some important and comprehensive reviews have summarized ROS in neurodegenerative diseases in detail.<sup>514,517–519</sup> The brain is far more vulnerable to excessively generated ROS than other tissues because of its high oxygen requirement and peroxidation vulnerability.

The most common type of senile dementia is Alzheimer's disease (AD), which is characterized by the presence of intracellular tangles of beta amyloid (A $\beta$ ) peptides and extracellular amyloid plaques made of hyperphosphorylated tau proteins.<sup>520,521</sup> Numerous studies have reported the relationship between ROS and amyloid plaques. High levels of ROS can induce an inflammatory response, hyperphosphorylation of tau and neural dysfunction. Thus, it has been a long therapeutic strategy for AD to find drugs to inhibit the formation of plaques and tangles and to reduce the inflammation response. In this context, Yin *et al.* have created sialic acid-modified selenium nanoparticles incorporating a highly effective blood-brain barrier-penetrating peptide known as B6 (referred to as B6-SA-SeNPs). These nanoparticles serve as a synthetic selenoprotein analog, designed for Alzheimer's disease therapy.<sup>522</sup> The results of their *in vitro* experiments suggest that B6-SA-SeNPs exhibit effectiveness not only in preventing the aggregation and

promoting the disaggregation of A $\beta$ , but also have the capacity to shield PC12 cells from A $\beta$ -induced damage. Moreover, they claimed the developed nanoparticles cross the blood-brain-barrier in an *in vitro* system of PC12 cells. In order to prevent metal-induced A $\beta$  aggregation, Yang *et al.* developed modified selenium/ruthenium nanoparticles (Se/Ru NPs) containing L-cysteine.<sup>523</sup> Se/Ru NPs suppress a Zn<sup>2+</sup> – amyloid mediated ROS generation process, thus reducing neurotoxicity in PC12 cells. A significant reduction in intracellular peptide aggregates was observed when spherical NPs with varying surface charges were used. NPs containing Ru also inhibit the random coiling or sheeting of A $\beta$  that disrupts the alpha helical structure of amyloid plaques. Additionally, Se/RuNPs decrease A $\beta_{40}$  fibrillation intracellularly, independent from lysosomal pathways. The release of borneol (Bor), which occurs when mesoporous nanoselenium (MNSe) reacts with blood or intracellular esterase, enables the nanosystem to cross the BBB.<sup>524</sup>

At the beginning stages of AD, the buildup of A $\beta$  causes a surge in oxidative stress, which in turn causes mitochondrial malfunction and energy failure.<sup>517,525</sup> A decline in dopaminergic input into the brain's nigrostriatal dopaminergic pathways and a specific neuronal loss of dopaminergic neurons in the substantia nigra pars compacta (SNc) are characteristics of the neurodegenerative disorder Parkinson's disease (PD).<sup>526–528</sup> A genetic mutation of the Huntingtin (HTT) gene on chromosome 4 (4p63) results in HD, which is characterized by progressive loss of function in the brain and muscle, loss of neurons, uncontrollable movements, loss of intellectual ability, and emotional disorders.<sup>529</sup> These neurodegenerative disorders share common pathological mechanisms including protein aggregation, oxidative damage, and mitochondrial dysfunction. Many of the genes involved in these neurodegenerative diseases are associated with mitochondrial function.<sup>530</sup> Therefore, it is vital to understand the underlying mechanism of mitochondrial dysfunctions when proposing RAN treatments for NDs. In addition to mitochondrial dysfunction, other cellular processes have recently been investigated for ROS generation. Activation of the peroxisome and endoplasmic reticulum, neuroinflammation, genetic mutation, and antioxidant depletion can induce ROS formation in the cell with subsequent loss of neurons by lipid peroxidation, and DNA or protein oxidation.<sup>531</sup>

Many studies have shown the roles of ROS in the development of neurodegenerative disorders.<sup>530–532</sup> Although ROS might not be the main key factor in all events of progression of the disease developments, ROS generation in oxidative stress conditions could be a common boosting influence on cell damage. Considering that many good antioxidant candidates cannot cross the BBB, nanoparticles with antioxidant properties would be a good option for antioxidant delivery.<sup>533</sup> Recently cerium oxide nanoparticles have been intensively studied in antioxidant delivery applications. A systematic representation of CeO<sub>2</sub>NPs and their inherent antioxidant characteristics for use as efficient neurodegeneration therapies is presented in Fig. 15(a). ROS scavenging from the injured area of the brain is critically aided by the low reduction potential of CeO<sub>2</sub>NPs and the coexistence of mixed valence states. Moreover, CeO<sub>2</sub>NPs can

cross the BBB due to their nanoscale size. Considering the important role of oxidative stress, regulation of ROS concentrations is a promising treatment mechanism for the early stages of neurodegenerative disease. In this respect, numerous compounds that have antioxidant properties such as GSH, vitamin C, vitamin E and coenzyme Q10 have been studied for their potential to constrict neurodegenerative side effects in concert with NPs or using various delivery vehicles.<sup>532</sup>

Other RANs have also been investigated for neurodegenerative disease treatment. For example, Zhou *et al.* created a thermo-responsive hollow ruthenium flower-like system to maintain the release of nerve growth factor (NGF) and prevent tau hyperphosphorylation and neuronal death, offering a potential therapeutic for AD treatment.<sup>535</sup> The thermally controlled drug delivery system of NGF-PCM@Ru NPs not only prolonged NGF circulation time but also penetrated the BBB and inhibited tau-related AD pathogenesis *via* NIR irradiation as presented in Fig. 15(b). In another study, Kwon *et al.* developed three forms of functionalized ceria NPs for ROS scavenging in Parkinson's disease, which inhibited microglial activation, lipid peroxidation, and restored tyrosine hydroxylase expression.<sup>536</sup> The three differently functionalized NPs, also varying in size, were localized to different subcellular parts when delivered to the cell. ROS can be detected in mitochondria, intracellularly, and extracellularly as presented in Fig. 15(c), all these ROS play a distinctive role in pathological conditions. This study represents the first biomedical application of NPs for clearing reactive oxygen by-products in Parkinson's disease demonstrating their potential as new therapeutic targets. In the future, this concept could be implemented in various neuronal disorders associated with ROS including cancer, cardiovascular diseases, and sepsis. Zhang *et al.* have developed biocompatible MnFe<sub>2</sub>O<sub>4</sub> NPs and applied them to chelate the 74 glutamine repeats (Htt(Q74)) of mutant huntingtin protein (Htt), the key disease factor in Huntington disease.<sup>537</sup> Instead of triggering the autophagy pathway, Zhang's group found that MnFe<sub>2</sub>O<sub>4</sub>NPs facilitated Htt(Q74) degradation through the ubiquitin-proteasome system (UPS). In contrast to p62/SQSTM1, MnFe<sub>2</sub>O<sub>4</sub>NPs improved the ubiquitination of GFP-Htt(Q74) associated with the Lys 48 (K48) ubiquitin chain through the ubiquitin receptor. Further, they evaluated the potential efficacy of MnFe<sub>2</sub>O<sub>4</sub>NPs in Htt protein clearance and explored the underlying mechanism for protein degradation using Neuro 2A, a neural cell line stably expressing GFP-tagged mutant Htt aggregates with 74 polyQ tracts (mHtt-GFP-Q74) Fig. 15(d). This suggests that MnFe<sub>2</sub>O<sub>4</sub>NPs are good candidate nanoparticles in nanomedicine therapy for HD.

Interestingly, exosomes, extracellular vesicles (~30–120 nm) that are secreted by cells, have also been used for drug delivery as they can also cross the BBB.<sup>538</sup> It has been discovered that exosomes significantly contribute to the pathways leading to dementia. For instance, they contribute to the buildup of A $\beta$  and the development of amyloid plaques in the brains of AD patients. Furthermore, exosomes transfer pathological protein aggregates containing  $\alpha$ -synuclein to the CNS, contributing to PD.<sup>539</sup> The biggest hurdle for RAN-based AD treatment is the

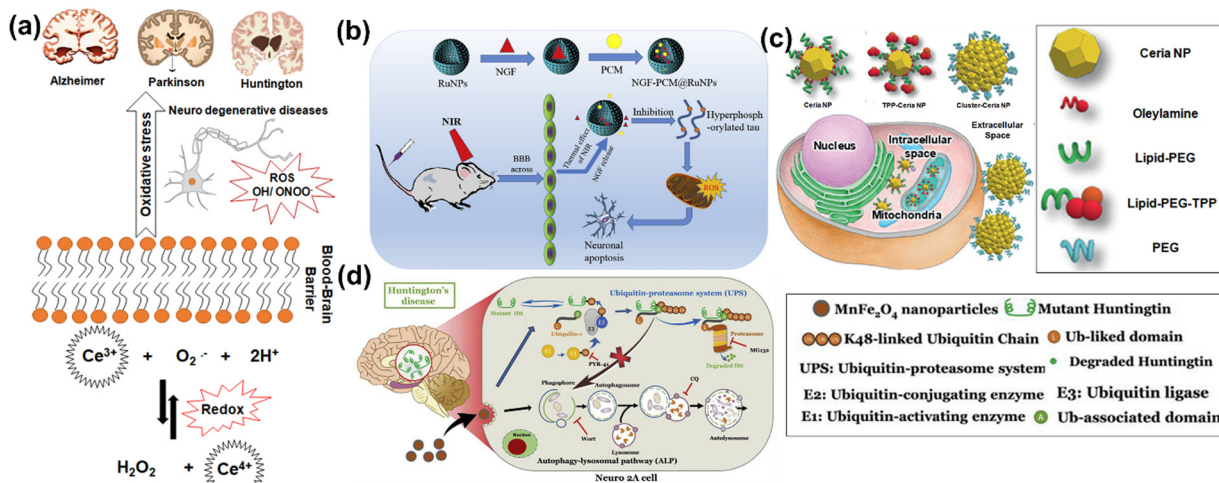


**Fig. 15** (a) Relationship between oxidative stress and neurodegenerative diseases; illustrating NP effect (cerium chosen randomly to illustrate oxidation reduction reactions). Reproduced with permission from Naz *et al.*<sup>534</sup> [Copyright 2017, Future Medicine LTD]. (b) Schematic illustration of synthesis of RuNPs, their loading with nerve growth factor (NGF) and further phase change material (PCM) to create (NGF@PCM-Ru) NPs for drug delivery through the BBB under NIR-radiation *in vivo* and projection of thermos-responsive RuNPs to AD mice model, which subsequently down-regulated the ROS production and mitigation of neuronal damage by inhibiting tau hyperphosphorylation. Reproduced with permission from Zhou *et al.*<sup>535</sup> [Copyright 2020, Elsevier]. (c) Three different functionalized ceria nanoparticles and their cellular localization-dependent ROS scavenging in Parkinson's disease. Reproduced with permission from Kwon *et al.*<sup>536</sup> [Copyright 2018, Wiley]. (d) Schematic illustration of MnFe<sub>2</sub>O<sub>4</sub> nanoparticles cellular internalization and accelerated clearance of mutant huntingtin (Htt) selectively through ubiquitin-proteasome system (UPS) in Huntington's disease. The rapid clearance of mutant Htt using MnFe<sub>2</sub>O<sub>4</sub>NPs via UPS rather than autophagy-lysosomal pathway (ALP). Among the enhanced degradation of Htt by UPS, K48-linked polyubiquitin chains target substrates to the proteasome and Ubiquilin-1 is the chosen ubiquitin receptor for mediating the cargo delivery. Reproduced with permission from Zhang *et al.*<sup>537</sup> [Copyright 2019, Elsevier].

potential side-effects arising from their short and long-term use. The gradual accumulation of NPs may be harmful with serious side effects in the body; therefore, it will be necessary to optimize the conditions of their use for therapy.

A recent study highlights the potential of graphene-based acid quantum dots (GAQDs) as a new therapeutic tool in treating neurodegenerative diseases. GAQDs have shown effectively reduce ROS by 50% at a concentration of 100  $\mu\text{g mL}^{-1}$  when exposed to a free radical generator. Moreover, GAQDs demonstrated a 70% suppression of hen egg-white lysozyme fibril production at a 5  $\text{mg mL}^{-1}$  concentration. In experiments using human neuroblastoma-derived SHSY-5Y cells, GAQDs were found to be biocompatible and capable of protecting cells from rotenone-induced apoptosis.<sup>540</sup>

RANs-based nanoparticles coated with biological membranes combine synthetic and biological elements were developed to improve targeting and therapeutic effectiveness. For example, Lin *et al.* developed drug-loaded hybrid cell-membrane liposomes that allow for multi-drug therapy and precise targeting of inflammatory brain lesion.<sup>541</sup> This hybridization technique involved loading of two small molecule medications (rapamycin and TPPU) and combining a platelet membrane with a membrane expressing a high level of CCR2. *In vitro*, cell death was prevented by the autophagy enhancer rapamycin and the soluble epoxide hydrolase (sEH) inhibitor TPPU, which also improved cognitive function in AD model mice, reduced amyloid plaque levels in their brains, and decreased neuroinflammation.

L-Molybdenum disulfide quantum dots ( $\text{L-MoS}_2$  QDs), along with a carrier material and a surface coating, were utilized as the main component to address neuronal loss in AD. The  $\text{L-MoS}_2$  QDs were more effective in inducing neural stem cells (NSCs) neuronal development when exposed to CPL NIR radiation. Moreover, when injected *in vivo* into the tail vein of AD mice, the  $\text{L-MoS}_2$  QDs had complementary effects such as the photothermal clearance of  $\text{A}\beta$  plaques, the production of  $\text{H}_2$ , which eliminated ROS, mitochondrial protection, and an overall improvement of the brain microenvironment.<sup>542</sup>

Combining ROS scavengers with nanomaterials exhibiting photothermal properties has emerged as a recent treatment for Alzheimer's disease. Song *et al.* developed Prussian blue nanomaterials (PBK NPs) with outstanding antioxidant and photothermal properties. The PBK NPs displayed activities similar to multiple antioxidant enzymes, such as peroxidase, superoxide dismutase, and catalase, which can help eliminate excessive ROS and alleviate oxidative stress. When subjected to near-infrared irradiation, the PBK NPs generated localized heat, effectively breaking down  $\text{A}\beta$  fibrils *in vitro*. Furthermore, modifying the PBK NPs with CKLVFFAED peptide enhanced their ability to penetrate the blood-brain barrier and target  $\text{A}\beta$ . Results from *in vivo* studies demonstrated that the PBK NPs disintegrated  $\text{A}\beta$  plaques and reduced neuroinflammation in an AD mouse model.<sup>543</sup> A systematic summary of therapeutic roles of RANs in various diseases are presented (Table 3).

**Table 3** Summary of the latest publications based on RANs nanoparticles and their therapeutic application using ROS in neurodegenerative diseases

ROS active NMs	Application methods/surface modifications	Brief outcomes in biomedical applications	Ref.
CeO <sub>2</sub> NPs	Reverse micelle methods	<ul style="list-style-type: none"> <li>• CeO<sub>2</sub>NPs reduced neuronal apoptosis by altering BDNF signalling, and decreased A<math>\beta</math>-aggregation in Alzheimer's disease.</li> <li>• CeO<sub>2</sub>NPs also displayed a successful reduction of manganese induced neuronal death in PD.</li> </ul>	534
CeO <sub>2</sub> NPs	Yeast model of Parkinson's Disease	<ul style="list-style-type: none"> <li>• The ideal amount of CeO<sub>2</sub>NPs has been shown to significantly diminish the harm caused by <math>\alpha</math>-synuclein-related toxicity, primarily stemming from the buildup of <math>\alpha</math>-synuclein in the cytoplasm, which leads to the repositioning of <math>\alpha</math>-synuclein to the plasma membrane upon the application of NPs.</li> <li>• CeO<sub>2</sub>NPs have demonstrated their ability to mitigate mitochondrial dysfunction induced by <math>\alpha</math>-synuclein and reduce the levels of reactive oxygen species (ROS) in yeast cells.</li> <li>• Through the adsorption of <math>\alpha</math>-synuclein onto their surface, CeO<sub>2</sub>NPs effectively function as a stable inhibitor of <math>\alpha</math>-synuclein's harmful effects rather than a radical scavenger suggested that CeO<sub>2</sub>NPs may interact co-ordinately with <math>\alpha</math>-syn <i>in vivo</i>.</li> </ul>	544
CeO <sub>2</sub> NPs	Citrate-EDTA stabilizations to CeO <sub>2</sub> NPs Murine model of ALS (SOD1G93A transgenic mice)	<ul style="list-style-type: none"> <li>• The study found that administering 20 mg kg<sup>-1</sup> of CeO<sub>2</sub>NPs intravenously twice per week increased the lifespan of SOD1G93A transgenic mice, a model for ALS.</li> <li>• Even when treatment was initiated at the onset of muscle weakness, the mice survived longer.</li> <li>• Both male and female mice benefited equally from CeO<sub>2</sub>NPs treatment suggests that CeO<sub>2</sub>NPs act as redox-agents that lower ROS levels, making them a promising therapeutic option.</li> </ul>	545
Se-incorporated clioquinol compounds SeNPs	Neuroblastoma Transgenic Huntington Disease (HD) models of <i>Caenorhabditis elegans</i>	<ul style="list-style-type: none"> <li>• Showed protective properties against the oxidation and aggregation of A<math>\beta</math> induced by Cu(II).</li> <li>• Nano-Se has been found to reduce neuronal death in a dose-dependent manner and provide protection against neuronal dysfunction.</li> <li>• In a HD model, treatment with Nano-Se resulted in decreased levels of ROS and HTT aggregation, indicating that Nano-Se functions as an antioxidant by regulating the expression of the histone deacetylase family and reducing polyQ aggregation.</li> </ul>	251 546
OX26-PEG-Se NPs	To targeting the transferrin receptor. – <i>in vivo</i>	<ul style="list-style-type: none"> <li>• Se nanoparticles coated with a polyethylene glycol (PEG) layer and treated with a monoclonal antibody (OX26)</li> <li>• The injection of OX26-PEG-SeNPs into the peritoneal cavity reduced brain edema in Wistar rats with ischemic cerebral stroke.</li> </ul>	257
Fe <sub>3</sub> O <sub>4</sub> NPs AgNPs Triphenylphosphonium-conjugated ceria (TPP-ceria)	Coated with (NIPAm-AA) and modified oleic acid/chronic Parkinson disease model NP-protein complex, protein-corona formation by incubating human plasma Hydrolytic sol-gel, metal chelators or DSPE-PEG coatings	<ul style="list-style-type: none"> <li>• Reduction of apoptosis and <math>\alpha</math>-syn toxicity and showed neurorepair effect <i>in vitro</i> and <i>in vivo</i> models of PD.</li> <li>• Exposure to AgNPs may activate pathways associated with neurotoxicity and neurodegeneration.</li> <li>• The results indicated that these nanoparticles successfully decreased the buildup of mitochondrial ROS caused by A<math>\beta</math> in the U373 astrocyte cell line, implying that TPP-ceria NPs could potentially alleviate brain inflammation by lowering mitochondrial ROS levels.</li> </ul>	340 464 547
Gd3N@C80 encapsulated NP	Colloidal stability in a polymer solution	<ul style="list-style-type: none"> <li>• The nano-contrast agent for MRI is designed to possess colloidal stability, ROS-scavenging ability, and long-term circulation ability, making it an excellent choice for clinical diagnosis.</li> </ul>	549
MSNP	Lipoprotein receptor (LDLR) (conjugating and PLA coating)	<ul style="list-style-type: none"> <li>• The use of LDLR peptides significantly improved the transcytosis of MSNPs and facilitated their passage through the BBB.</li> <li>• Additionally, PLA-coated MSNPs were able to release resveratrol (antioxidant) in response to artificially induced superoxide released by activated microglia. This released resveratrol effectively reduced oxidative stress.</li> <li>• When mice orally consumed these particles, they not only prevented the accumulation of A<math>\beta</math>, but also significantly improved both spatial and non-spatial memory.</li> </ul>	550 551
PEG- <i>b</i> -poly[4-(2,2,6,6-tetramethylpiperidine-1-oxyl)aminomethylstyrene] (PEG- <i>b</i> -PMNT)	2,2,6,6-Tetramethylpiperidine-1-oxyl (TEMPO) added as side chain-oral intake to Alzheimer disease (AD) mice model		

Table 3 (continued)

ROS active NMs	Application methods/surface modifications	Brief outcomes in biomedical applications	Ref.
RuNPs	NGF loading, phase change material (PCM) presenting to AD mice	<ul style="list-style-type: none"> <li>• Additionally, the particles enhanced neuronal densities in the cortex and hippocampus by reducing the activity of glutathione peroxidase and superoxide dismutase. Furthermore, the levels of A<math>\beta</math> (1–40), A<math>\beta</math> (1–42) and gamma (<math>\gamma</math>)-secretase were reduced, ultimately leading to a reduction in A<math>\beta</math> plaque.</li> <li>• The nanocomposites showed excellent choice for biosafety in AD treatment due to its good biocompatibility and high stability.</li> <li>• With the aid of RuNPs' photothermal activity, cross-BBB movement and brain penetration was improved under NIR irradiation, leading to enhanced circulation efficiency <i>in vivo</i>.</li> <li>• The researcher found that modified RuNPs had the ability to effectively inhibit hyperphosphorylation of tau, reduced oxidative stress, and reduced tau aggregation, restore nerve damage, and alleviate cognitive impairment in AD mice.</li> </ul>	535
AuNPs	1-Methyl-4-phenyl-1,2,3,6-tetrahydropyridine (MPTP) induced rat models with PD.	<ul style="list-style-type: none"> <li>• AuNPs can effectively reduce motor disorders, oxidative stress, and inflammatory cytokines, as well as inhibit TLR/NF-<math>\kappa</math>B signalling in rats with PD.</li> <li>• Additionally, the authors observed that MPTP administration in the brain increased ROS generation, while treatment with AuNPs was able to scavenge ROS in a dose-dependent manners.</li> </ul>	552

#### 4.3. Infection and inflammation

Acute or chronic pathogenic infections by bacteria, viruses and parasites are a primary cause of human morbidity and mortality. During infection, overproduction of ROS can occur. This occurs most notably in infections caused by blood-borne viruses such as human immunodeficiency virus (HIV), hepatitis (B, C and D), influenza A, respiratory syncytial virus, Epstein-Barr virus and others.<sup>553</sup> In liver diseases, production of ROS associated with transcriptional activation of some cytokines and growth factors leads to hepatic damage. Additionally, viral infections downregulate glutathione (GSH) in liver cells, leading to the oxidation of DNA, lipids and proteins, and the cascade of these events contributes to the development of liver cirrhosis and hepatocellular carcinoma.<sup>554</sup> There are antioxidant strategies to react with ROS produced from the electron transport chain, including the production of non-enzymatic ROS scavengers [GSH and NAD(P)H] and antioxidant enzymes [superoxide dismutase, catalase and family members of peroxidase].<sup>555</sup> However, temporary imbalance between antioxidants and ROS can alter cellular signalling pathways, which could be reversed by nanoparticles encapsulated with antioxidants to treat liver diseases.

The versatile properties of nanoceria make it an ideal antibacterial solution against both Gram-negative and Gram-positive bacteria by generating ROS. It acts as an antioxidant in healthy cells, protecting them under normal physiological pH, while also acting as a pro-oxidant in cancer cells under low pH environments, which may lead to the death of cancer cells. Furthermore, nanoceria has been successfully utilized as a carrier for targeted drug and gene delivery in both *in vitro* and *in vivo* models. Besides, nanoceria is known to be a good candidate as an anti-diabetic, anti-inflammatory agent with

protective effects against diabetes pathophysiology associated with a decrease in ROS concentration in diabetic patients. Nanoceria is also actively studied in the field of tissue engineering.<sup>556,557</sup>

ROS have two faces in normal cell responses, such that they are important in host defense, but paradoxically inhibit inflammation and immune response.<sup>558,559</sup> In non-infectious hyper-inflammatory conditions such as chronic granulomatous disease (CGD), there are both high and low levels of ROS in the inflammatory responses.<sup>558</sup> The lack of ROS generation by the NOX2 complex is known to be associated with a high incidence of autoimmune disease in CGD patients. A deficiency in NOX2 can lead to hyperinflammation and increased immune activation, which may have some benefits. In CGD mice, heightened inflammation has been shown to protect against pulmonary infection caused by influenza.<sup>404,560</sup> The association between NOX2-dependent ROS generation deficiency and increased inflammation is unexpected and requires further investigation.

Oxidative stress arises when the production of reactive ROS surpasses the capacity of antioxidant defense mechanisms, potentially resulting in the development of various diseases. Hydrogen peroxide (H<sub>2</sub>O<sub>2</sub>) is a widely seen and long-lasting form of ROS that has been linked to various physiological processes including inflammation, cellular malfunction, and apoptosis. These factors ultimately have a role in the development of tissue and organ damage.<sup>561</sup> Cellular DNA damage arises from a combination of intrinsic and extrinsic causes, encompassing ionizing radiation, chemical intake, light exposure, and radical generated during oxygen metabolism. The presence of these external stimuli leads to the production of radical, which in turn initiates a pathway that causes damage to DNA, resulting in a total of 465 instances of such damage.<sup>562</sup>

The phenomenon of DNA damage, commonly referred to as genotoxicity, is of great importance within the field of nanomaterials. Although the development of non-cytotoxic therapies is challenging, DNA damage offers a promising avenue for the creation of anti-cancer medications.<sup>563</sup> ROS generation has been recognized as a crucial determinant in the modulation of the cellular response to chemotherapy or radiotherapy, exerting its influence on the downstream signalling pathways involved in cell survival and death.

The role of ROS in the DNA damage response is complicated and can be revealing in different ways. It is of utmost significance to distinguish between the occurrence of DNA damage resulting from oxidative stress and the following initiation of DNA damage repair (DDR). Additionally, it is crucial to consider the influence of ROS on the regulation of DDR components, encompassing both signalling and effectors. Multiple studies have indicated that the dysregulation of ROS plays a substantial role in the development of cancer, as well as in the resistance to chemotherapy and radiation therapy.<sup>564</sup> The presence of active nanoparticles in the presence of ROS can result in the induction of DNA damage by the production of a hydroxyl radical ( $\text{HO}^\bullet$ ). This radical interacts with DNA molecules, leading to the formation of a specific DNA lesion called 8-hydroxy-2'-deoxyguanosine (8-OHdG). Ultimately, this process contributes to the occurrence of DNA damage.<sup>565</sup> The excessive generation of radical can induce oxidative stress and inflammation, hence contributing to the development of numerous diseases.<sup>566</sup> Certain nanoparticles, namely copper, copper oxide, iron, silver,  $\text{TiO}_2$ , and nickel, exhibit pronounced toxicity. Even at low concentrations, exposure to these NPs can induce DNA damage and elicit the expression of inflammatory markers. These particles induce cellular apoptosis and inflammation through the generation of ROS, primarily targeting mitochondria and pro-oxidant enzymes.<sup>567</sup> The utilization of various nanomaterials has been found to result in toxicity associated with the formation of ROS in multiple biological systems, such as human erythrocytes, skin fibroblasts, and various tumor cells.<sup>568</sup> The mitochondria play a pivotal role in the production of ROS that are linked to nanoparticles. Previous studies have demonstrated that NPs have the capability to stimulate NADPH-associated enzymes, resulting in the depolarization of the mitochondrial membrane and the disruption of the electron transport chain.<sup>208,569</sup> This inhibition of a key metabolic process would increase the quantity of ROS in cells by allowing electron transfer from respiratory carriers to oxygen.<sup>570</sup> The mechanism implicated in NP-induced ROS production and factors affecting the ROS generation in cells are presented in Fig. 16.

There are several other diseases such as diabetes, osteoarthritis (OA), rheumatoid arthritis (RA), glaucoma, hearing loss, atherosclerosis, hypertension, restenosis, ischemia/reperfusion injury, and pulmonary and liver fibrosis that are highly affected by ROS. A potentially more favorable strategy for achieving therapeutic efficacy involves the targeted inhibition of enzymes responsible for the generation of reactive oxygen species. The occurrence of excessive formation of ROS is observed in several

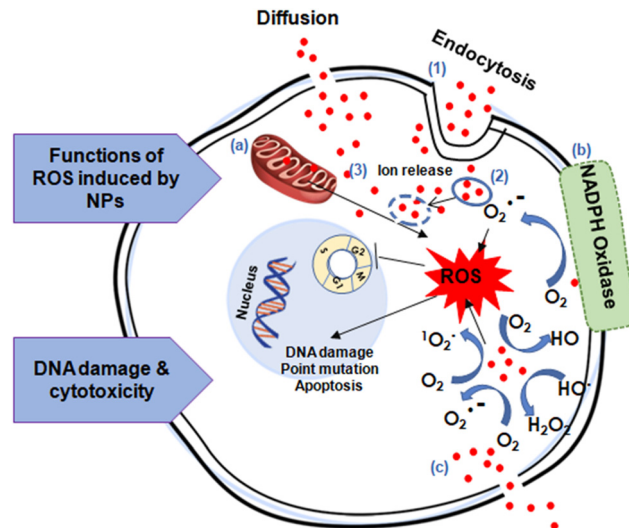


Fig. 16 Schematic illustration of the cellular mechanisms associated with NP-induced ROS production. The nanoparticles can be internalized into the cell by (1) endocytosis; (2) which then accumulate through formation of endocytosis vesicles, and finally (3) the ions release from nanoparticles into the cell. ROS generation by NPs is mainly dependent on (a) interaction of nanoparticles with the mitochondria; (b) interaction of nanoparticles with NADPH oxidase; and (c) the physicochemical factors of the nanoparticles including size, shape, photoreactive properties, and the surface chemistry of the particles. These factors play an important role and lead to ROS generation and its severe consequences, including DNA and cell membrane damage, and cell apoptosis. Figure created by authors using BioRender.com.

clinical states. Additionally, there exists a genetic factor that influences the likelihood of ROS generation, as supported by research.<sup>571</sup>

With over 170 million people worldwide affected, diabetes is a metabolic inflammatory disease that poses a significant threat to public health. Despite efforts to control the disease, its complications can only be slowed down rather than halted completely. The primary characteristic of diabetes is hyperglycemia, which initiates various metabolic signalling pathways that cause inflammation, cell death, and eventually lead to diabetic complications. The activation of diacylglycerol (DAG)-protein kinase C pathways by hyperglycemia is well-known to trigger a specific metabolic route. This signalling pathway is gaining more attention for its ability to regulate angiogenesis, reduce oxidative stress and prevent cellular death.<sup>572</sup> It is widely believed that the disparity between the generation and removal of ROS and the resulting oxidative stress, induced by elevated blood glucose levels (hyperglycemia), is the primary factor contributing to the development of diabetic complications.<sup>573</sup> In addition to hyperglycemia and ROS, Toll-like receptor 4 (TLR 4) activation can also trigger apoptosis. To control cardiac apoptosis in diabetes, researchers have found that silencing the TLR 4 gene or upregulating its expression in diabetic mice can be effective. This ultimately results in the reduction of oxidative stress and suppression of caspase 3 in cardiomyocytes.<sup>573</sup> As a result, controlling ROS generation

and TLR 4 downregulation may play a crucial role in managing diabetic complications.

Osteoarthritis is a degenerative joint condition that mostly impacts the geriatric population and is a significant contributor to functional impairment. The condition is distinguished by alterations in bone cells, resulting in softness, ulceration, fibrillation, degradation of articular cartilage, sclerosis of subchondral bone, inflammation of the synovial membrane, and the development of osteophytes and subchondral cysts. The mitochondria in OA produce an excessive amount of reactive oxygen species, leading to the oxidation of proteins. This oxidative process alters cell signalling pathways, favouring catabolic signalling, and ultimately contributing to cell death. A recent study has indicated that an elevated amount of ROS can interfere with the signalling pathways of IRS-1-PI-3 kinase-Akt, which is crucial for the integration of anabolic and catabolic signalling and the promotion of cell survival.<sup>574</sup> The activation of Akt is hindered in OA chondrocytes and normal cells under oxidative stress, resulting in a decrease in matrix formation and an increase in vulnerability to cell death. Reactive oxygen species are mostly generated at minimal levels within articular chondrocytes, predominantly through the activity of NADPH oxidase. These entities play a significant role in the intracellular signalling processes that are involved in

maintaining the equilibrium of cartilage. They achieve this by regulating many aspects such as chondrocyte death, gene expression, synthesis of the extracellular matrix (ECM), and cytokine production breakdown.<sup>575-577</sup> Patients diagnosed with osteoarthritis have heightened levels of ROS generation and experience an increase in oxidative stress.<sup>578,579</sup> The impact of interleukin-1 (IL-1) on DNA damage induced by ROS is significantly greater in cartilage afflicted by OA compared to healthy cartilage.<sup>580</sup>

Rheumatoid arthritis (RA) is a pathological condition characterized by the immune system's aberrant response, resulting in the degradation of several bodily structures, including joints, synovial tissue, cartilage, bone, and ligaments.<sup>581-583</sup> HLA-DR-1 and HLA-DR-4 major histocompatibility complex (MHC) class II molecules exhibit a strong correlation with RA susceptibility in the human population. Additionally, DBA/1 and B10 strains have also been implicated in this association. The mice strains had I-Ag and I-Ar haplotypes, rendering them significantly vulnerable to collagen-induced arthritis (CIA), which serves as an experimental model for rheumatoid arthritis. The development of CIA in mice is associated with the expression of a limited T-cell receptor (TCR).<sup>584-586</sup> The spontaneous development of arthritis in inbred mouse strains can be attributed to several factors, such as the expression of T cell receptor or

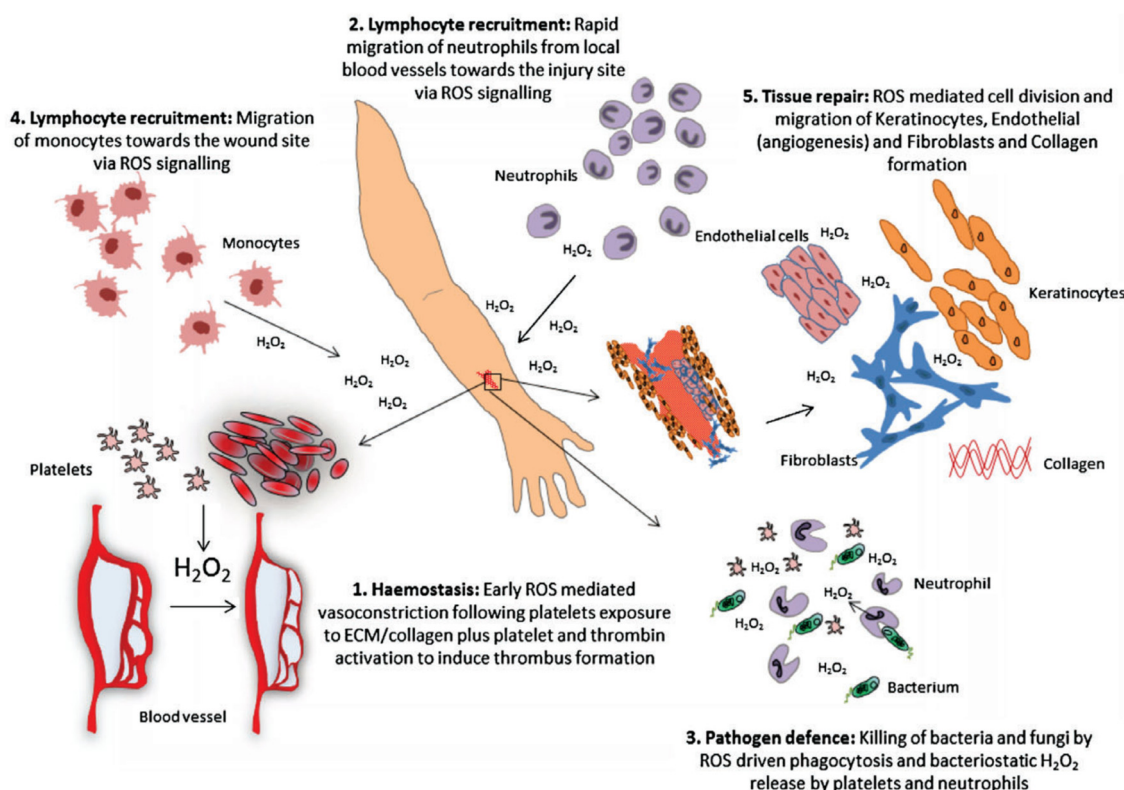


**Fig. 17** Schematic diagram illustrates the various role of ROS throughout severe wound healing conditions (i.e., homeostatic, level of ROS); (i) at early-stage, ROS help to reduce the blood flow and cell-signalling for thrombus formation, (ii) activated local neutrophils associated to blood vessels accumulate at the wound site for protection from bacteria, (iii) ROS produced by phagocytosis processes inhibit bacterial growth and help signal support for wound response, (iv) this helps to recruit immunocytes (monocytes) and help them to migrate towards to injury site to prevent attack invading pathogens, (v) at final stage, ROS stimulate endothelial cell differentiation and migration for blood vessel formation, and fibroblast differentiation and migration for new extracellular matrix formation and tissue regeneration. Reproduced with permission from Dunnill *et al.*<sup>593</sup> [Copyright 2015, Wiley].

TNF- $\alpha$ , as well as mutations in ZAP70 or Ncf1. There is a potential for these strains to have arthropathy, especially when exposed to specific environmental factors such as hormone imbalances, stress, or infections.<sup>587,588</sup> There is a potential for these strains to have arthropathy, especially when exposed to specific environmental factors such as hormone imbalances, stress, or infections.<sup>589,590</sup> Ncf1 is a constituent of the phagocyte NADPH oxidase complex, which plays a crucial role in modulating the magnitude of oxidative burst within phagocytes. Research has demonstrated that reduced levels of ROS generated by the NADPH oxidase complex have been found to exacerbate arthritis, inflammation, and immunological responses, contradicting commonly held beliefs.<sup>591</sup>

#### 4.4. Tissue regeneration

Tissue regeneration is a dynamic process, which mainly includes cell migration and tissue reformation through morphogenesis followed by vigorous cell proliferation activity which commonly occurs at the traumatic or infected sites.<sup>592</sup> There are complicated mechanisms underlying tissue regeneration including activation of specific cells or certain signalling molecules required for the effective recovery of injured tissues. Thus, it is important to understand intracellular and extracellular mechanisms with key mediators in tissue regeneration.<sup>593,594</sup>

Radical have been implicated as an initiator of tissue damage in various diseases, such as skin aging, cardiovascular disease, chronic diabetic wounds and so on.<sup>592,595</sup> Oxidative stress due to an imbalance of oxidative and antioxidative byproducts contributes to the development of the diseases mentioned above. On the other hand, free radical species can be beneficial, acting as a mediator in cellular signalling for tissue regeneration, in particular when there is a high demand for mitochondrial production of adenosine triphosphate (ATP) during tissue renewal.<sup>593</sup> ROS act as secondary messenger-signalling molecules that induce a respiratory chain reaction *via* oxidation and reduction.<sup>348,593</sup> There are various signalling pathways reported to be involved in the ROS-mediated tissue regeneration response, such as Jun N-terminal kinase (JNK) and p38 mitogen-activated protein kinases (MAPK).<sup>596</sup> ROS also play a role in regulating vasoconstriction and vasodilation, the important events in vascularization, an event that accompanies tissue regeneration.<sup>593</sup> Nitric oxide, which belongs to reactive nitrogen species, reacts with a number of molecules including ROS to regulate a vascular relaxation.<sup>593</sup> Essentially cells and molecules including macrophages, fibroblasts, platelets, keratinocytes and endothelial cells utilize these radicals to facilitate a healing response. Initial release of ROS activates vasoconstriction and reduces local cell signalling to enable thrombus formation. An antibacterial environment is then created after blood vessel-bound neutrophils are recruited to the injury site as shown in Fig. 17. Subsequently more ROS are released by phagocytosis to prevent the growth of bacteria and induce vital signals to other immunocytes in response to the pathogens at the wound site, including monocytes.<sup>593</sup> These further stimulate endothelial cell division and migration for new ECM

formation, which subsequently promotes keratinocyte proliferation and migration by activating angiogenesis and fibroblast division and migration.<sup>593</sup>

ROS responsive nanoparticles can play a vital role in responding to oxidative stress in a physiological environment. Under such conditions, the nanoparticles are targeted to the injury site as they exhibit either switchable solubility or the ability to degrade chemical bonds to create an oxidative microenvironment.<sup>596</sup> Their functionalities are highly dependent on the types of ROS being targeted, material structure/characteristics, and exposure time.<sup>596</sup> Wang *et al.* have reported a novel bioactive chitosan nanoparticle-loaded calcium alginate hydrogel for wound healing.<sup>597</sup> Apart from inducing an antibacterial environment even at a very low dosage, the formulation also facilitated proliferation and migration of vascular endothelial cells (VEC) *via* massive production of ROS that subsequently assisted in metastasis and neovascularization creating an effective wound healing effect.<sup>597</sup> Tang *et al.* have demonstrated a ROS-reactive nanomaterial poly-(1,4-phenyleneacetone dimethylene thioketal) loaded with stromal cell-derived factor-1 $\alpha$  (SDF-1 $\alpha$ ). The loaded nanoparticle is reported able to respond to ROS by delivering drugs to inflammatory tissues accumulated with large amount of ROS, which subsequently attracts BMSCs, triggering vascularisation and healing.<sup>598</sup> The role of RANs in various cellular functions including DNA damage and cytotoxicity are presented (Table 4).

## 5. Conclusions and current and potential future clinical directions

The unique features of RANs such as intrinsic ROS production as well as their physicochemical properties such as particle shape, size, dimensions, surface chemical functionality, surface area, and imaging ability make them a promising nanoplatform for future application in biomedicine. The physical and chemical engineering of RANs has significantly changed their ability to generate ROS and provide control over pathological conditions. Furthermore, recent engineering of NPs has also helped to reduce their potential cytotoxicity, thereby improving the biosafety of NPs for therapeutic applications. Thanks to the advancement of nanoscience and nanotechnology, there are now many immense tools to synthesize various types of NPs and explore them as ROS-based therapeutic candidates in *in vitro* and *in vivo* applications.

ROS is an essential biochemical component in various pathological conditions, ranging from tissue injury/damage, infection/inflammation, tissue regeneration, cancer, OA, and neurodegenerative disease. Furthermore, ROS also plays a crucial multifunctional role in cell biology including cell signalling, cell viability, proliferation, differentiation, and cell apoptosis. As a result, controlling and treating diseases by regulating the excess or deficiency of ROS in tissue/organ/body using RANs in the form of ROS generating or scavenging NPs, is possible. However, concerns about potential toxicities and the ability to target specific cells are significant. Some RANs may

Table 4 Summary of the role of RANs in DNA damage and cytotoxicity, based on recent studies

RANs	Application methods/surface modifications	Brief outcomes	Ref.
Fe <sub>3</sub> O <sub>4</sub> and Ag NPs	Low-toxic concentration of deferoxamine (DFO) pre-treatment – applied <i>in vitro</i> HepG2 cells	<ul style="list-style-type: none"> <li>The toxicity of AgNPs was reduced by using iron as a chelator.</li> <li>AgNPs induced mitochondrial collapse, and O<sub>2</sub>•– was produced and quickly dismutated to H<sub>2</sub>O<sub>2</sub>.</li> <li>In the presence of iron ions, H<sub>2</sub>O<sub>2</sub> underwent a Fenton reaction, resulting in the production of an extremely reactive hydroxyl radical (•OH).</li> <li>However, pre-treating AgNP-exposed cells with DFO significantly reduced the induction of DNA damage.</li> </ul>	565
TiOxNPs and (PAA-TiOxNPs)	Polyacrylic acid-(PAA) modification	<ul style="list-style-type: none"> <li><i>In vitro</i>, the absorption of PAA-TiOxNPs increased DNA damage and led to greater cytotoxicity when exposed to X-ray irradiation.</li> <li>In combination with X-ray treatment PAA-TiOxNPs had a significantly more powerful effect on inhibiting tumor growth than either treatment alone.</li> </ul>	599
Polyvinylpyrrolidone (PVP) + iron oxide nanoparticles	<i>S. aromaticum</i> flower bud extract loading	<ul style="list-style-type: none"> <li>The application of nanoparticles to the MCF-7 breast cancer cell line has resulted in a notable increase in the accumulation within the sub-G1 phase, hence leading to the initiation of apoptosis.</li> <li>The augmentation in the quantity of nanoparticles resulted in a concomitant elevation in the enzymatic activity of caspase-3, caspase-8, and caspase-9.</li> <li>Besides, the introduction of functionalized iron nanoparticles (FeNPs) led to the initiation of oxidative stress, which subsequently triggered the creation of ROS and promoted death in MCF-7 cells.</li> <li>These findings underscore the promising prospects of using functionalized FeNPs in the field of cancer therapy.</li> </ul>	600
Cu/CuONPs	Produced by chemical reductions	<ul style="list-style-type: none"> <li>The toxicity of Cu/CuONPs was assessed by evaluating their effects on human lung carcinoma cell line (A549) and human lung normal cell line (WI-38).</li> <li>The IC<sub>50</sub> values of Cu/CuONPs were applied to both cell types, resulting in DNA damage and the generation of reactive oxygen species.</li> <li>The potential utility of investigating the toxicological impacts of Cu/CuONPs on mature A549 cells lies in the development of targeted therapeutic delivery systems for certain cancer cell types.</li> </ul>	601
SiNPs	Suspended in DI and applied to murine neuroblastoma cell line: Neuro-2a	<ul style="list-style-type: none"> <li>The research conducted demonstrated that exposure to SiNPs resulted in a notable elevation of ROS levels within cellular structures.</li> <li>Nevertheless, prior administration of the antioxidant <i>N</i>-acetylcysteine (NAC) successfully mitigated the generation of ROS and the subsequent decline in cell viability, occurrence of apoptotic events, and activation of molecules associated with endoplasmic reticulum (ER) stress.</li> <li>The findings provide evidence that ROS plays a pivotal role in the harmful effects generated by silicon nanoparticles (SiNPs).</li> <li>This involvement of ROS leads to the activation of ER stress and subsequent initiation of apoptosis, finally culminating in the demise of neuronal cells.</li> </ul>	602
ZnONPs	Dispersed into the culture media and up-taken by HEK-293 cells	<ul style="list-style-type: none"> <li>The concentration of ZnONPs has caused an excessive increase in ROS and O<sub>2</sub> species, leading to impaired cellular oxidative stress management.</li> <li>The expression of TET-methylcytosine dioxygenase genes has significantly increased, while DNA-methyltransferases (DNMTs) expression remains unchanged.</li> <li>ZnONPs can cause a significant increase in ROS, resulting in various structural and functional abnormalities in cells.</li> </ul>	603
CeO <sub>2</sub> NPs	Cellular internalization of nanoceria to the THP-1 cells	<ul style="list-style-type: none"> <li>The study found that nanoceria has powerful antioxidant properties, as shown by its ability to scavenge radical in mammalian cells.</li> <li>This suggests that nanoceria may be a promising treatment for conditions related to inflammation and oxidative stress.</li> </ul>	566
AuNPs	Three types of 3–4 nm AuNPs on human A549 cells	<ul style="list-style-type: none"> <li>After 24 hours, cells were found to have agglomerated AuNP, but this did not affect cell viability or inflammation.</li> <li>Although no increase in ROS production was observed, however, intracellular glutathione levels decreased over time, indicating oxidative stress.</li> <li>Furthermore, all three types of AuNPs caused DNA damage, with the strongest genotoxic effect observed for positively charged AuNP I.</li> <li>However, despite the significant DNA damage caused by single exposure to AuNP I, A549 cells were able to recover and repair the damage over time.</li> </ul>	604

Table 4 (continued)

RANs	Application methods/surface modifications	Brief outcomes	Ref.
TiO <sub>2</sub> NPs	Different concentration NPs orally presented to male rats	<ul style="list-style-type: none"> <li>The administration of escalating doses of TiO<sub>2</sub>NPs was observed to induce elevated levels of cytotoxicity, oxidative stress, and apoptosis in both Caco-2 and HepG2 cell lines.</li> <li>Additionally, it was shown that the inclusion of TiO<sub>2</sub>NPs resulted in a notable reduction in the activity of antioxidant enzymes and the expression of related genes, such as SOD, CAT, and GPx.</li> <li>Furthermore, the levels of glutathione (GSH) and the overall capacity for antioxidant activity (TAC) were also found to be diminished.</li> <li>The investigation revealed that the presence of TiO<sub>2</sub>NPs induced gene expressions associated with apoptosis and inflammatory pathways, along with caspase-3 activity in both the intestinal and hepatic tissues.</li> </ul>	605
SeNPs	Hepatocellular carcinoma rat model (HCC)	<ul style="list-style-type: none"> <li>The co-administration of doxorubicin and SeNPs resulted in a notable decrease in chromosomal abnormalities, micronuclei formation, and DNA damage in male rats with hepatocellular carcinoma (HCC) when compared to the administration of doxorubicin alone.</li> <li>The research demonstrated that the presence of NM300K AgNPs resulted in heightened production of ROS and elevated levels of oxidative stress, predominantly inside the intestinal lumen.</li> <li>To conduct a more comprehensive examination of the relative toxicity of these NPs in comparison to AgNO<sub>3</sub>, the research employed SOD-1 and two biosensors, namely HyPer and GRX.</li> <li>The findings of the study demonstrated that even at low concentrations, NM300K AgNPs induced cellular redox-potential instability and suggested the occurrence of oxidative stress.</li> <li>Furthermore, the data consistently demonstrated discernible variations in behavior between the two forms of Ag, namely in relation to uptake, retention, toxic effects, and patterns of oxidative stress.</li> </ul>	606
AgNPs and AgNO <sub>3</sub>	Nematode <i>Caenorhabditis elegans</i>	<ul style="list-style-type: none"> <li>The research demonstrated that the presence of NM300K AgNPs resulted in heightened production of ROS and elevated levels of oxidative stress, predominantly inside the intestinal lumen.</li> <li>To conduct a more comprehensive examination of the relative toxicity of these NPs in comparison to AgNO<sub>3</sub>, the research employed SOD-1 and two biosensors, namely HyPer and GRX.</li> <li>The findings of the study demonstrated that even at low concentrations, NM300K AgNPs induced cellular redox-potential instability and suggested the occurrence of oxidative stress.</li> <li>Furthermore, the data consistently demonstrated discernible variations in behavior between the two forms of Ag, namely in relation to uptake, retention, toxic effects, and patterns of oxidative stress.</li> </ul>	607
Bi <sub>2</sub> O <sub>3</sub> NPs	<i>In vitro</i> human breast cancer (MCF-7) cells	<ul style="list-style-type: none"> <li>This study aimed to examine the impact of Bi<sub>2</sub>O<sub>3</sub>NPs on MCF-7 cells, with a specific focus on evaluating its cytotoxicity and induction of apoptosis.</li> <li>The findings indicated that the presence of Bi<sub>2</sub>O<sub>3</sub>NPs resulted in a decrease in cell viability and induced damage to the cell membrane, with the extent of these effects being directly proportional to the dosage administered, and cell cycle was observed, along with the induction of oxidative stress responses.</li> <li>This was demonstrated by the heightened production of ROS, elevated levels of lipid peroxidation, decreased GSH levels, and diminished activity of the SOD enzyme.</li> <li>Additionally, the investigation revealed that Bi<sub>2</sub>O<sub>3</sub>NPs triggered apoptosis <i>via</i> the mitochondrial route, as evidenced by a decrease in mitochondrial membrane potential (MMP) and an elevated expression ratio of bax/bcl-2 genes.</li> <li>In general, the results underscore the possible cytotoxic properties of Bi<sub>2</sub>O<sub>3</sub>NPs on MCF-7 cells.</li> </ul>	608

not be inherently biocompatible, and their introduction into the body could lead to adverse reactions such as inflammation, oxidative stress, or cellular damage. Moreover, some RANs release toxic ions or molecules during their redox-reactions, causing harm to cells or tissues. For example, certain metals used in nanoparticles formulations could pose toxicity risks. Additionally, if these nanoparticles are not effectively cleared from the body, they can accumulate in the organs such as the liver, spleen, kidneys, and leads to the potential toxicity over time. Furthermore, RANs face biological barriers, such as the blood brain or endothelial barriers in tumors, which can limit their ability to reach target cells or tissues. Therefore, precisely targeting RANs to specific cells is also a challenge for RANs.

Targeted application of redox-active nanoparticles in cells, tissues, or within the body requires advanced design and engineering to lower the energy barriers of ROS associated catalytic reactions within location specific conditions to

regulate the favorable *in vivo* ROS-based therapeutic effect. However, these local *in vivo* physiological conditions (pH, temperature) can also trigger the ROS catalytic reactions by exciting the energy level of NPs, and thus can have severe consequences on health. Further exploration of the generation or scavenging of ROS by NPs and their associated cellular and molecular mechanisms is therefore required. A thorough understanding of these mechanisms will help significantly in efforts to engineer NPs with appropriate physicochemical functionalities.

Advancements in nanotechnology, biomaterials, and biomedical engineering are pushing towards overcoming challenges in medicine and unlocking the full potential of RANs. For instance, multifunctional nanoparticles adorned with targeting ligands and responsive moieties are making precision delivery of therapeutic agents to diseased tissues a reality. These strategies could enhance treatment efficacy while reducing

the off-target effects and systemic toxicity. In future, developed RANs may respond to specific stimuli, prompting controlled drug release at the target site, which could improve treatment efficacy while minimizing side effects. Multi-therapeutic agent delivery is also promising, holding the potential to overcome drug resistance and improve treatment outcomes. Lastly, RANs with intrinsic fluorescence or luminescence properties could be used for minimally invasive *in vivo* bioimaging and biosensing, enabling early disease detection, monitoring, and personalized treatment approaches. Future redox-active nanomaterials will likely exhibit improved biodistribution, biodegradability, and clearance from the body, reducing the long-term accumulation and potential toxicity. Biocompatible degradation products could also be engineered to ensure safe elimination *via* renal or hepatobiliary pathways.

A common concern across the various nanomedicine modalities is their potential adverse effects on human health and safety. While RANs hold promises in preclinical studies for disease prevention and treatment, however their clinical applications remain limited, with research predominantly focused on *in vitro* studies and animal experiments. These models do not fully replicate human pathological conditions, particularly metastatic tumors, posing challenges in accurately mimicking the cellular or tissue damage caused by oxidative stress in physiological conditions.<sup>609</sup> Moreover, the lack of clinical trial results is a major factor restricting the clinical translation of RANs. One of the key challenges includes inadequate methods for evaluating biocompatibility, which require a deeper understanding of toxicity mechanisms and enhanced *in vivo* cytotoxicity detection. This is mainly due to conventional antioxidants possess a double-edged sword effect.<sup>610</sup> They suffer from low bioavailability due to poor gut absorption and nonspecific distribution, which reduces their local concentration and often leads to a failure in neutralizing excess free radicals.<sup>611</sup> Conversely, high local concentrations can disrupt crucial ROS-mediated signalling pathways necessary for cell function and, in some cases, act as prooxidants, exacerbating oxidative damage.<sup>610,611</sup> Additionally, they lack reusability, as they become inactive after neutralizing ROS through self-oxidation.<sup>611</sup> Hence, to develop a comprehensive biocompatibility evaluation index, systemic toxicity testing must be performed, emphasizing the retention of nanomaterials in vital organs like the liver and kidneys, coupled with *in vitro* biosafety evaluations using human cell lines, which are also essential for advancing clinical trials.<sup>609</sup>

Advancements in nanotechnology offer various methods for modifying nanomaterials, such as using small molecules, polymers, antibodies, or nucleic acids, for targeted delivery by attaching cell-specific ligands that bind to receptors overexpressed in particular tissues.<sup>612</sup> For example, nanomaterials capped with folate can precisely target cancer cells, which have higher folate receptor expression than normal cells, allowing for controlled local concentrations and maintaining cellular redox balance.<sup>611</sup> Although nanomaterials may exhibit inherent properties such as ideal size, shape, hydrophobicity, rigidity, and composition, influencing biodistribution within the body,

another important challenge is that redox-active nanodrugs, despite their longer-lasting effects and reduced side effects compared to traditional drugs, currently lack sufficient therapeutic efficacy for widespread clinical use, partly due to high design costs.<sup>609</sup> These costs are associated with the complex structures of redox nanodrugs, especially those involved in multifunctional nanoplateform therapy systems. Additionally, RANs with strong permeability and retention effects often have low drug delivery efficiencies, highlighting the need for precise controlled release capabilities.<sup>609</sup> While these nanoparticles show promise in diagnostics and bioassays, their therapeutic application faces challenges, including their use in topical or injectable solutions and implants. Some, like citrate-functionalized Mn<sub>3</sub>O<sub>4</sub>NPs, have shown success in preclinical trials, but others need further animal testing to confirm the efficacy observed *in vitro*.<sup>611</sup> Injected nanoparticles must have minimal side effects and efficient excretion pathways, as certain materials like gold cannot be metabolized and must be excreted *via* urine or faeces.<sup>613</sup> Their interaction with biological fluids and the need for precise targeting without causing toxicity are crucial considerations. Although simpler nanoparticle designs have paved the way for initial attempts, more complex structures pose significant translational challenges. Despite these complexities, progress has led to FDA-approved nanomedicines.<sup>614</sup> However, more research on catalytic activity, therapeutic efficacy, and safety is needed to advance clinical applications effectively.<sup>611</sup>

In essence, addressing these challenges by selecting more cost-effective redox-responsive nanomaterials and improving synthesis methods can enhance their practicality and efficacy. Ultimately, it is crucial to understand comprehensively how these nanomaterials induce unintended effects on the immune and nervous systems. This necessitates a shift from descriptive toxicology to predictive toxicology.<sup>615</sup> Given the diverse array of nanomaterial types and formulations, individual assessments for each are not feasible. Therefore, employing predictive toxicology models alongside high-content cellular screening emerges as a practical and promising approach to evaluate nanomaterial toxicity in humans, gradually making them applicable in clinical medicine.<sup>616</sup>

Overall, the field of redox-active nanomaterials in medicine will rely heavily on cross-disciplinary collaboration, inventive nanomaterial design, fabrication techniques, and thorough preclinical and clinical testing to guarantee both safety and effectiveness. With ongoing improvements in our comprehension of nanoscale phenomena and biological mechanisms, RANs are poised to transform personalized medicine in areas such as diagnostics tools, imaging technologies, drug administration, and therapeutic interventions.

## Data availability

The data that support the finding of this review study are openly available and collected from the published research articles, review papers with permission of publishers.

## Conflicts of interest

The authors declare that they have no financial interests or personal conflict of interest.

## Acknowledgements

The authors would like to acknowledge the Engineering and Physical Science Research Council (EPSRC), the UK for empower program at University of Bristol under grant no. EP/T020792/1, and the National Research Foundation (NRF; 2021R1A5A2022318, RS-2024-00348908, and RS-2023-00220408) of Republic of Korea. The Biotechnology and Biological Science Research Council (BBSRC) London Interdisciplinary Bioscience PhD Consortium (LIDO; BB/M009513/1).

## References

- 1 B. Perillo, M. Di Donato, A. Pezone, E. Di Zazzo, P. Giovannelli, G. Galasso, G. Castoria and A. Migliaccio, *Exp. Mol. Med.*, 2020, **52**, 192–203.
- 2 H. Sies and D. P. Jones, *Nat. Rev. Mol. Cell Biol.*, 2020, **21**, 363–383.
- 3 C.-S. Lee, R. K. Singh, H. S. Hwang, N.-H. Lee, A. G. Kurian, J.-H. Lee, H. S. Kim, M. Lee and H.-W. Kim, *Prog. Mater. Sci.*, 2023, **135**, 101087.
- 4 J. Bi, J. Zhang, Y. Ren, Z. Du, Q. Li, Y. Wang, S. Wei, L. Yang, J. Zhang, C. Liu, Y. Lv and R. Wu, *Redox Biol.*, 2019, **20**, 296–306.
- 5 F. Pagliari, C. Mandoli, G. Forte, E. Magnani, S. Pagliari, G. Nardone, S. Licoccia, M. Minieri, P. Di Nardo and E. Traversa, *ACS Nano*, 2012, **6**, 3767–3775.
- 6 T. Zhou, E. R. Prather, D. E. Garrison and L. Zuo, *Int. J. Mol. Sci.*, 2018, **19**(2), 417.
- 7 N. Solovyev, E. Drobyshev, G. Bjørklund, Y. Dubrovskii, R. Lysiuk and M. P. Rayman, *Free Radicals Biol. Med.*, 2018, **127**, 124–133.
- 8 M. P. Murphy, H. Bayir, V. Belousov, C. J. Chang, K. J. A. Davies, M. J. Davies, T. P. Dick, T. Finkel, H. J. Forman, Y. Janssen-Heininger, D. Gems, V. E. Kagan, B. Kalyanaraman, N.-G. Larsson, G. L. Milne, T. Nyström, H. E. Poulsen, R. Radi, H. Van Remmen, P. T. Schumacker, P. J. Thornalley, S. Toyokuni, C. C. Winterbourn, H. Yin and B. Halliwell, *Nat. Metab.*, 2022, **4**, 651–662.
- 9 A. Marino, M. Battaglini, N. Moles and G. Ciofani, *ACS Omega*, 2022, **7**, 25974–25990.
- 10 S. Mollazadeh, M. Mackiewicz and M. Yazdimamaghani, *Mater. Sci. Eng., C*, 2021, **118**, 111536.
- 11 L. Han, X.-Y. Zhang, Y.-L. Wang, X. Li, X.-H. Yang, M. Huang, K. Hu, L.-H. Li and Y. Wei, *J. Controlled Release*, 2017, **259**, 40–52.
- 12 Y. Liu, P. Bhattacharai, Z. Dai and X. Chen, *Chem. Soc. Rev.*, 2019, **48**, 2053–2108.
- 13 M. Hao, B. Chen, X. Zhao, N. Zhao and F.-J. Xu, *Mater. Chem. Front.*, 2020, **4**, 2571–2609.
- 14 A. Moazzen, N. Öztinen, E. Ak-Sakalli and M. Koşar, *Helijon*, 2022, **8**, e10467.
- 15 Q. Guo, S. Ji, Q. Yue, L. Wang, J. Liu and J. Jia, *Anal. Chem.*, 2009, **81**, 5381–5389.
- 16 G. Goncalves, P. A. A. P. Marques, C. M. Granadeiro, H. I. S. Nogueira, M. K. Singh and J. Grácio, *Chem. Mater.*, 2009, **21**, 4796–4802.
- 17 J. Bai Aswathanarayanan, R. Rai Vittal and U. Muddegowda, *Artif. Cells, Nanomed., Biotechnol.*, 2018, **46**, 1444–1451.
- 18 S. Franco-Ulloa, D. Guarnieri, L. Riccardi, P. P. Pompa and M. De Vivo, *J. Chem. Theory Comput.*, 2021, **17**, 4512–4523.
- 19 Z. Nie, K. J. Liu, C.-J. Zhong, L.-F. Wang, Y. Yang, Q. Tian and Y. Liu, *Free Radicals Biol. Med.*, 2007, **43**, 1243–1254.
- 20 S. M. Ansar, S. Chakraborty and C. L. Kitchens, *Nanomaterials*, 2018, **8**, 339.
- 21 T. Yasukawa, H. Miyamura and S. Kobayashi, *ACS Catal.*, 2016, **6**, 7979–7988.
- 22 K. N. L. Hoang, S. M. McClain, S. M. Meyer, C. A. Jalomo, N. B. Forney and C. J. Murphy, *Chem. Commun.*, 2022, **58**, 9728–9741.
- 23 P. Vardakas, I. A. Kartsonakis, I. D. Kyriazis, P. Kainourgios, A. F. A. Trompeta, C. A. Charitidis and D. Kouretas, *Environ. Res.*, 2023, **220**, 115156.
- 24 Y. González-García, E. R. López-Vargas, G. Cadenas-Pliego, A. Benavides-Mendoza, S. González-Morales, A. Robledo-Olivio, Á. G. Alpuche-Solís and A. Juárez-Maldonado, *Int. J. Mol. Sci.*, 2019, **20**, 5858.
- 25 K. D. Patel, R. K. Singh and H.-W. Kim, *Mater. Horiz.*, 2019, **6**, 434–469.
- 26 I. L. Medintz, H. T. Uyeda, E. R. Goldman and H. Mattoussi, *Nat. Mater.*, 2005, **4**, 435–446.
- 27 C. M. Sims, S. K. Hanna, D. A. Heller, C. P. Horoszko, M. E. Johnson, A. R. Montoro Bustos, V. Reipa, K. R. Riley and B. C. Nelson, *Nanoscale*, 2017, **9**, 15226–15251.
- 28 B. Yang, Y. Chen and J. Shi, *Chem. Rev.*, 2019, **119**, 4881–4985.
- 29 Y. Nosaka and A. Y. Nosaka, *Chem. Rev.*, 2017, **117**, 11302–11336.
- 30 X. Shi, Y. Tian, S. Zhai, Y. Liu, S. Chu and Z. Xiong, *Front. Chem.*, 2023, **11**, 1115440.
- 31 P. Chen, W. Zhang, X. Fan, X. Shi, Y. Jiang, L. Yan, H. Li, C. Wang, L. Han, X. Lu and C. Ou, *Nano Today*, 2024, **55**, 102157.
- 32 P. H. Hoet, B. Nemery and D. Napierska, *Nano Today*, 2013, **8**, 223–227.
- 33 H. Sies, *Redox Biol.*, 2015, **4**, 180–183.
- 34 A. Costa, A. Scholer-Dahirel and F. Mechta-Grigoriou, *Semin. Cancer Biol.*, 2014, **25**, 23–32.
- 35 S. H. Yoo, H.-W. Kim and J. H. Lee, *J. Tissue Eng.*, 2022, **13**, 1–14, DOI: [10.1177/20417314221083414](https://doi.org/10.1177/20417314221083414).
- 36 Y. Vakrat-Haglili, L. Weiner, V. Brumfeld, A. Brandis, Y. Salomon, B. McLlroy, B. C. Wilson, A. Pawlak, M. Rozanowska, T. Sarna and A. Scherz, *J. Am. Chem. Soc.*, 2005, **127**, 6487–6497.
- 37 M. Wang, M. Chang, C. Li, Q. Chen, Z. Hou, B. Xing and J. Lin, *Adv. Mater.*, 2022, **34**, 2106010.

38 Y. Lin, X. Chen, C. Yu, G. Xu, X. Nie, Y. Cheng, Y. Luan and Q. Song, *Acta Biomater.*, 2023, **159**, 300–311.

39 M. Sharifi-Rad, N. V. Anil Kumar, P. Zucca, E. M. Varoni, L. Dini, E. Panzarini, J. Rajkovic, P. V. Tsouh Fokou, E. Azzini, I. Peluso, A. Prakash Mishra, M. Nigam, Y. El Rayess, M. E. Beyrouthy, L. Polito, M. Iriti, N. Martins, M. Martorell, A. O. Docea, W. N. Setzer, D. Calina, W. C. Cho and J. Sharifi-Rad, *Front. Physiol.*, 2020, **11**, 694.

40 E. Birben, U. M. Sahiner, C. Sackesen, S. Erzurum and O. Kalayci, *World Allergy Organ. J.*, 2012, **5**, 9–19.

41 C. M. C. Andrés, J. M. Pérez de la Lastra, C. Andrés Juan, F. J. Plou and E. Pérez-Lebeña, *Int. J. Mol. Sci.*, 2023, **24**, 1841.

42 J. Fujii, T. Homma and T. Osaki, *Antioxidants*, 2022, **11**, 501.

43 B. Lipinski and E. Pretorius, *Hematology*, 2012, **17**, 241–247.

44 B. Lipinski, *Oxid. Med. Cell. Longevity*, 2011, **2011**, 809696.

45 S. Adhikari, R. Crehuet, J. M. Anglada, J. S. Francisco and Y. Xia, *Proc. Natl. Acad. Sci. U. S. A.*, 2020, **117**, 18216–18223.

46 P. Chaudhary, P. Janmeda, A. O. Docea, B. Yeskaliyeva, A. F. Abdull Razis, B. Modu, D. Calina and J. Sharifi-Rad, *Front. Chem.*, 2023, **11**, 1158198.

47 L. M. Smith, H. M. Aitken and M. L. Coote, *Acc. Chem. Res.*, 2018, **51**, 2006–2013.

48 J. Helberg and D. A. Pratt, *Chem. Soc. Rev.*, 2021, **50**, 7343–7358.

49 C. von Sonntag, in *Mechanisms of DNA Damage and Repair: Implications for Carcinogenesis and Risk Assessment*, ed. M. G. Simic, L. Grossman, A. C. Upton and D. S. Bergtold, Springer, US, Boston, MA, 1986, pp. 51–59, DOI: [10.1007/978-1-4615-9462-8\\_6](https://doi.org/10.1007/978-1-4615-9462-8_6).

50 K. Jomova, R. Raptova, S. Y. Alomar, S. H. Alwasel, E. Nepovimova, K. Kuca and M. Valko, *Arch. Toxicol.*, 2023, **97**, 2499–2574.

51 K. Wang, W. Mao, X. Song, M. Chen, W. Feng, B. Peng and Y. Chen, *Chem. Soc. Rev.*, 2023, **52**, 6957–7035.

52 V. Nayak, K. R. B. Singh, A. K. Singh and R. P. Singh, *New J. Chem.*, 2021, **45**, 2849–2878.

53 F. Collin, *Int. J. Mol. Sci.*, 2019, **20**(10), 2407.

54 D. D. Saraev, Z. Wu, H.-Y. H. Kim, N. A. Porter and D. A. Pratt, *ACS Chem. Biol.*, 2023, **18**, 2073–2081.

55 L. K. Folkes, S. Bartesaghi, M. Trujillo, P. Wardman and R. Radi, *Int. J. Mol. Sci.*, 2022, **23**, 1797.

56 E. Illés, A. Mizrahi, V. Marks and D. Meyerstein, *Free Radicals Biol. Med.*, 2019, **131**, 1–6.

57 R. Luc and C. Vergely, *Int. J. Biomed. Sci.*, 2008, **4**, 255–259.

58 A. M. Fleming and C. J. Burrows, *Chem. Soc. Rev.*, 2020, **49**, 6524–6528.

59 R. Xiao, Y. Meng, Y. Fu, S. Waclawek, Z. Wei, R. Spinney, D. D. Dionysiou, W. Zeng and W. P. Hu, *Chem. Eng. J.*, 2023, **474**, 145245.

60 L. Wojnárovits, T. Tóth and E. Takács, *Sci. Total Environ.*, 2020, **717**, 137219.

61 S. M. Andrabi, N. S. Sharma, A. Karan, S. M. S. Shahriar, B. Cordon, B. Ma and J. Xie, *Adv. Sci.*, 2023, **10**, 2303259.

62 M. K. Chug and E. J. Brisbois, *ACS Mater. Au*, 2022, **2**, 525–551.

63 Y. Deng, F. Jia, S. Chen, Z. Shen, Q. Jin, G. Fu and J. Ji, *Biomaterials*, 2018, **187**, 55–65.

64 E. Lubos, D. E. Handy and J. Loscalzo, *Front. Biosci.-Landmark*, 2008, **13**, 5323–5344.

65 C. Schöneich, *Molecules*, 2019, **24**(23), 4357.

66 Y. M. Lee, W. He and Y.-C. Liou, *Cell Death Dis.*, 2021, **12**, 58.

67 T. Nauser, W. H. Koppenol and C. Schöneich, *Free Radicals Biol. Med.*, 2015, **80**, 158–163.

68 D. M. Lynch and E. M. Scanlan, *Molecules*, 2020, **25**, 3094.

69 M. Janků, L. Luhová and M. Petřivalský, *Antioxidants*, 2019, **8**, 105.

70 T. Kietzmann, A. Petry, A. Shvetsova, J. M. Gerhold and A. Görlich, *Br. J. Pharmacol.*, 2017, **174**, 1533–1554.

71 B. Chance, H. Sies and A. Boveris, *Physiol. Rev.*, 1979, **59**, 527–605.

72 J. F. Turrens, *J. Physiol.*, 2003, **552**, 335–344.

73 R. Z. Zhao, S. Jiang, L. Zhang and Z. B. Yu, *Int. J. Mol. Med.*, 2019, **44**, 3–15.

74 H. Y. Chung, G. S. Lee, S. H. Nam, J. H. Lee, J. P. Han, S. Song, G.-D. Kim, C. Jung, D. Y. Hyeon, D. Hwang, B.-O. Choi and S. C. Yeom, *Brain*, 2024, **147**, 2114–2127.

75 S. Lenzen, V. I. Lushchak and F. Scholz, *Arch. Toxicol.*, 2022, **96**, 1915–1920.

76 J. P. Crow and J. S. Beckman, in *The Role of Nitric Oxide in Physiology and Pathophysiology*, ed. H. Koprowski and H. Maeda, Springer Berlin Heidelberg, Berlin, Heidelberg, 1995, pp. 57–73, DOI: [10.1007/978-3-642-79130-7\\_7](https://doi.org/10.1007/978-3-642-79130-7_7).

77 R. Radi, *Proc. Natl. Acad. Sci. U. S. A.*, 2018, **115**, 5839–5848.

78 C. M. C. Andrés, J. M. Pérez de la Lastra, C. Andrés Juan, F. J. Plou and E. Pérez-Lebeña, *Int. J. Mol. Sci.*, 2023, **24**, 1841.

79 R. Campos Chisté, M. Freitas, A. Zerlotti Mercadante and E. Fernandes, *Curr. Med. Chem.*, 2015, **22**, 4234–4256.

80 J. H. Kramer, B. F. Dickens, V. Mišík and W. B. Weglicki, *J. Mol. Cell. Cardiol.*, 1995, **27**, 371–381.

81 N. A. Popova, G. M. Sysoeva, V. P. Nikolin, V. I. Kaledin, E. V. Tretyakov, M. V. Edeeva, S. M. Balakhnin, E. L. Lushnikova, G. Audran and S. Mark, *Bull. Exp. Biol. Med.*, 2017, **164**, 49–53.

82 D. S. Dimić, D. A. Milenović, E. H. Avdović, J. Nakarada, J. M. Dimitrić Marković and Z. S. Marković, *Chem. Eng. J.*, 2021, **424**, 130331.

83 Z. Hao, J. Ma, C. Miao, Y. Song, L. Lian, S. Yan and W. Song, *Environ. Sci. Technol.*, 2020, **54**, 10118–10127.

84 D. B. Medinas, G. Cerchiaro, D. F. Trindade and O. Augusto, *IUBMB Life*, 2007, **59**, 255–262.

85 B. N. Gantner, K. M. LaFond and M. G. Bonini, *Redox Biol.*, 2020, **34**, 101550.

86 Y. Liu, G. Fiskum and D. Schubert, *J. Neurochem.*, 2002, **80**, 780–787.

87 S. Chenna, W. J. H. Koopman, J. H. M. Prehn and N. M. C. Connolly, *Am. J. Physiol.: Cell Physiol.*, 2022, **323**, C69–C83.

88 Z. Yang and D. J. Klionsky, *Curr. Opin. Cell Biol.*, 2010, **22**, 124–131.

89 V. P. Tan and S. Miyamoto, *J. Mol. Cell. Cardiol.*, 2016, **95**, 31–41.

90 C. C. Dibble and B. D. Manning, *Nat. Cell Biol.*, 2013, **15**, 555–564.

91 G. Filomeni, D. De Zio and F. Cecconi, *Cell Death Differ.*, 2015, **22**, 377–388.

92 G. Filomeni, D. De Zio and F. Cecconi, *Cell Death Differ.*, 2015, **22**, 377–388.

93 B. Groatl and U. Jakob, *Biochim. Biophys. Acta, Proteins Proteomics*, 2014, **1844**, 1335–1343.

94 T. M. Buttke and P. A. Sandstrom, *Immunol. Today*, 1994, **15**, 7–10.

95 A. Nugud, D. Sandeep and A. T. El-Serafi, *J. Adv. Res.*, 2018, **14**, 73–79.

96 Z. Ghanbari Movahed, M. Rastegari-Pouyani, M. H. Mohammadi and K. Mansouri, *Biomed. Pharmacother.*, 2019, **112**, 108690.

97 R. Bhowmick and R. R. Sarkar, *PLoS One*, 2020, **15**, e0235204.

98 C. E. Murry, M. H. Soonpaa, H. Reinecke, H. Nakajima, H. O. Nakajima, M. Rubart, K. B. S. Pasumarthi, J. Ismail Virag, S. H. Bartelmez, V. Poppa, G. Bradford, J. D. Dowell, D. A. Williams and L. J. Field, *Nature*, 2004, **428**, 664–668.

99 R. D. Unwin, D. L. Smith, D. Blinco, C. L. Wilson, C. J. Miller, C. A. Evans, E. Jaworska, S. A. Baldwin, K. Barnes and A. Pierce, *Blood*, 2006, **107**, 4687–4694.

100 J. M. Funes, M. Quintero, S. Henderson, D. Martinez, U. Qureshi, C. Westwood, M. O. Clements, D. Bourboulia, R. B. Pedley and S. Moncada, *Proc. Natl. Acad. Sci. U. S. A.*, 2007, **104**, 6223–6228.

101 J.-H. Paik, Z. Ding, R. Narurkar, S. Ramkissoon, F. Muller, W. S. Kamoun, S.-S. Chae, H. Zheng, H. Ying and J. Mahoney, *Cell Stem Cell*, 2009, **5**, 540–553.

102 F. Kocabas, J. Zheng, S. Thet, N. G. Copeland, N. A. Jenkins, R. J. DeBerardinis, C. Zhang and H. A. Sadek, *Blood*, 2012, **120**, 4963–4972.

103 T. Suda, K. Takubo and G. L. Semenza, *Cell Stem Cell*, 2011, **9**, 298–310.

104 J. M. Ryu, H. J. Lee, Y. H. Jung, K. H. Lee, D. I. Kim, J. Y. Kim, S. H. Ko, G. E. Choi, I. I. Chai, E. J. Song, J. Y. Oh, S.-J. Lee and H. J. Han, *Int. J. Stem Cells*, 2015, **8**, 24–35.

105 M. L. Circu and T. Y. Aw, *Free Radical Biol. Med.*, 2010, **48**, 749–762.

106 S. V. Avery, *Biochem. J.*, 2011, **434**, 201–210.

107 P. Storz, *Front. Biosci.*, 2005, **10**, 1881–1896.

108 D. Trachootham, Y. Zhou, H. Zhang, Y. Demizu, Z. Chen, H. Pelicano, P. J. Chiao, G. Achanta, R. B. Arlinghaus, J. Liu and P. Huang, *Cancer Cell*, 2006, **10**, 241–252.

109 M. Azmanova and A. Pitto-Barry, *ChemBioChem*, 2022, **23**, e202100641.

110 E. Panieri and M. M. Santoro, *Cell Death Dis.*, 2016, **7**, e2253–e2253.

111 R. K. Singh, K. D. Patel, C. Mahapatra, S. P. Parthiban, T.-H. Kim and H.-W. Kim, *ACS Appl. Mater. Interfaces*, 2019, **11**, 288–299.

112 G. Y. Liou and P. Storz, *Free Radical Res.*, 2010, **44**, 479–496.

113 P. Storz, in *Oxidative Stress and Redox Regulation*, ed. U. Jakob and D. Reichmann, Springer, Netherlands, Dordrecht, 2013, pp. 427–447, DOI: [10.1007/978-94-007-5787-5\\_15](https://doi.org/10.1007/978-94-007-5787-5_15).

114 S. Shibuya, Y. Ozawa, K. Watanabe, N. Izuo, T. Toda, K. Yokote and T. Shimizu, *PLoS One*, 2014, **9**, e109288.

115 D. Yang, S. G. Elner, Z.-M. Bian, G. O. Till, H. R. Petty and V. M. Elner, *Exp. Eye Res.*, 2007, **85**, 462–472.

116 J. Krstic, D. Trivanovic, S. Mojsilovic and J. F. Santibanez, *Oxid. Med. Cell. Longevity*, 2015, **2015**, 654594.

117 L. E. Huang, J. Gu, M. Schau and H. F. Bunn, *Proc. Natl. Acad. Sci. U. S. A.*, 1998, **95**, 7987–7992.

118 M. R. Abid, K. C. Spokes, S.-C. Shih and W. C. Aird, *J. Biol. Chem.*, 2007, **282**, 35373–35385.

119 Y. Higaki, T. Mikami, N. Fujii, M. F. Hirshman, K. Koyama, T. Seino, K. Tanaka and L. J. Goodyear, *Am. J. Physiol.: Endocrinol. Metab.*, 2008, **294**, E889–E897.

120 T. Minamoto, M. Mai and Z. Ronai, *Cancer Detect. Prev.*, 2000, **24**, 1–12.

121 T. Minamoto, A. V. Ougolkov and M. Mai, *Expert Rev. Mol. Diagn.*, 2002, **2**, 565–575.

122 D. Ferraro, S. Corso, E. Fasano, E. Panieri, R. Santangelo, S. Borrello, S. Giordano, G. Pani and T. Galeotti, *Oncogene*, 2006, **25**, 3689–3698.

123 V. Chavda, B. Chaurasia, K. Garg, H. Deora, G. E. Umana, P. Palmisciano, G. Scalia and B. Lu, *Brain Disord.*, 2022, **5**, 100029.

124 B. S. Berlett and E. R. Stadtman, *J. Biol. Chem.*, 1997, **272**, 20313–20316.

125 M. Mittal, M. R. Siddiqui, K. Tran, S. P. Reddy and A. B. Malik, *Antioxid. Redox Signaling*, 2014, **20**, 1126–1167.

126 S. Salzano, P. Checconi, E.-M. Hanschmann, C. H. Lillig, L. D. Bowler, P. Chan, D. Vaudry, M. Mengozzi, L. Coppo, S. Sacre, K. R. Atkuri, B. Sahaf, L. A. Herzenberg, L. A. Herzenberg, L. Mullen and P. Ghezzi, *Proc. Natl. Acad. Sci. U. S. A.*, 2014, **111**, 12157–12162.

127 M. Schäfer and S. Werner, *Pharmacol. Res.*, 2008, **58**, 165–171.

128 I. Liguori, G. Russo, F. Curcio, G. Bulli, L. Aran, D. Della-Morte, G. Gargiulo, G. Testa, F. Cacciatore, D. Bonaduce and P. Abete, *Clin. Interventions Aging*, 2018, **13**, 757–772.

129 M. Cano Sanchez, S. Lancel, E. Boulanger and R. Neviere, *Antioxidants*, 2018, **7**(8), 98.

130 R. Moseley, J. E. Stewart, P. Stephens, R. J. Waddington and D. W. Thomas, *Br. J. Dermatol.*, 2004, **150**, 401–413.

131 C. Caspersen, N. Wang, J. Yao, A. Sosunov, X. Chen, J. W. Lustbader, H. W. Xu, D. Stern, G. McKhann and S. D. Yan, *FASEB J.*, 2005, **19**, 2040–2041.

132 C. S. Casley, L. Canevari, J. M. Land, J. B. Clark and M. A. Sharpe, *J. Neurochem.*, 2002, **80**, 91–100.

133 L. S. Forno, *J. Neuropathol. Exp. Neurol.*, 1996, **55**, 259–272.

134 M. G. Spillantini, R. A. Crowther, R. Jakes, M. Hasegawa and M. Goedert, *Proc. Natl. Acad. Sci. U. S. A.*, 1998, **95**, 6469–6473.

135 E. M. Valente, P. M. Abou-Sleiman, V. Caputo, M. M. K. Muqit, K. Harvey, S. Gispert, Z. Ali, D. Del Turco, A. R. Bentivoglio, D. G. Healy, A. Albanese, R. Nussbaum, R. González-Maldonado, T. Deller, S. Salvi, P. Cortelli, W. P. Gilks, D. S. Latchman, R. J. Harvey, B. Dallapiccola, G. Auburger and N. W. Wood, *Science*, 2004, **304**, 1158–1160.

136 W. C. Nichols, N. Pankratz, D. Hernandez, C. Paisán-Ruiz, S. Jain, C. A. Halter, V. E. Michaels, T. Reed, A. Rudolph, C. W. Shults, A. Singleton and T. Foroud, *Lancet*, 2005, **365**, 410–412.

137 B. Xiao, J.-Y. Goh, L. Xiao, H. Xian, K.-L. Lim and Y.-C. Liou, *J. Biol. Chem.*, 2017, **292**, 16697–16708.

138 W. J. Szlachcic, P. M. Switonski, W. J. Krzyzosiak, M. Figlerowicz and M. Figiel, *Dis. Models Mech.*, 2015, **8**, 1047.

139 F. O. Walker, *Lancet*, 2007, **369**, 218–228.

140 B. Rotblat, A. L. Southwell, D. E. Ehrnhoefer, N. H. Skotte, M. Metzler, S. Franciosi, G. Leprivier, S. P. Somasekharan, A. Barokas, Y. Deng, T. Tang, J. Mathers, N. Cetinbas, M. Daugaard, B. Kwok, L. Li, C. J. Carnie, D. Fink, R. Nitsch, J. D. Galpin, C. A. Ahern, G. Melino, J. M. Penninger, M. R. Hayden and P. H. Sorensen, *Proc. Natl. Acad. Sci. U. S. A.*, 2014, **111**, 3032–3037.

141 A. Johri and M. F. Beal, *Biochim. Biophys. Acta, Mol. Basis Dis.*, 2012, **1822**, 664–674.

142 C. Giorgi, S. Marchi, I. C. M. Simoes, Z. Ren, G. Morciano, M. Perrone, P. Patalas-Krawczyk, S. Borchard, P. Jędrak, K. Pierzynowska, J. Szymański, D. Q. Wang, P. Portincasa, G. Węgrzyn, H. Zischka, P. Dobrzym, M. Bonora, J. Duszynski, A. Rimessi, A. Karkucinska-Wieckowska, A. Dobrzym, G. Szabadkai, B. Zavan, P. J. Oliveira, V. A. Sardao, P. Pinton and M. R. Wieckowski, *Int. Rev. Cell Mol. Biol.*, 2018, **340**, 209–344.

143 A. N. Kolodkin, R. P. Sharma, A. M. Colangelo, A. Ignatenko, F. Martorana, D. Jennen, J. J. Briedé, N. Brady, M. Barberis, T. D. G. A. Mondeel, M. Papa, V. Kumar, B. Peters, A. Skupin, L. Alberghina, R. Balling and H. V. Westerhoff, *NPJ Syst. Biol. Appl.*, 2020, **6**, 34.

144 G.-Y. Liou and P. Storz, *Free Radical Res.*, 2010, **44**, 479–496.

145 M. I. Anik, N. Mahmud, A. A. Masud, M. I. Khan, M. N. Islam, S. Uddin and M. K. Hossain, *ACS Appl. Bio Mater.*, 2022, **5**, 4028–4054.

146 J. M. Lü, P. H. Lin, Q. Yao and C. Chen, *J. Cell. Mol. Med.*, 2010, **14**, 840–860.

147 L. W. Zheng, H. Chung and Y.-S. Kim, *Food Res. Int.*, 2015, **75**, 328–336.

148 K. U. Ingold and D. A. Pratt, *Chem. Rev.*, 2014, **114**, 9022–9046.

149 N. R. Perron and J. L. Brumaghim, *Cell Biochem. Biophys.*, 2009, **53**, 75–100.

150 J. Lu and A. Holmgren, *Free Radicals Biol. Med.*, 2014, **66**, 75–87.

151 M. D. Brand, C. Affourtit, T. C. Esteves, K. Green, A. J. Lambert, S. Miwa, J. L. Pakay and N. Parker, *Free Radical Biol. Med.*, 2004, **37**, 755–767.

152 R. Amorati and L. Valgimigli, *Free Radical Res.*, 2015, **49**, 633–649.

153 L. Valgimigli, A. Baschieri and R. Amorati, *J. Mater. Chem. B*, 2018, **6**, 2036–2051.

154 A. Aranda, L. Sequedo, L. Tolosa, G. Quintas, E. Burello, J. V. Castell and L. Gombau, *Toxicol. In Vitro*, 2013, **27**, 954–963.

155 D. Yu, Y. Zha, Z. Zhong, Y. Ruan, Z. Li, L. Sun and S. Hou, *Sens. Actuators, B*, 2021, **339**, 129878.

156 A. Kessler, P. Huang, E. Blomberg and I. Odnevall, *Chem. Res. Toxicol.*, 2023, **36**, 1891–1900.

157 T. M. Potter, B. W. Neun and S. T. Stern, in *Characterization of Nanoparticles Intended for Drug Delivery*, ed. S. E. McNeil, Humana Press, Totowa, NJ, 2011, pp. 181–189, DOI: [10.1007/978-1-60327-198-1\\_19](https://doi.org/10.1007/978-1-60327-198-1_19).

158 S. Sadeghian, G. A. Kojouri and A. Mohebbi, *Biol. Trace Elem. Res.*, 2012, **146**, 302–308.

159 W. Zhang, J. Gao, L. Lu, T. Bold, X. Li, S. Wang, Z. Chang, J. Chen, X. Kong, Y. Zheng, M. Zhang and J. Tang, *NanoImpact*, 2021, **23**, 100338.

160 C. Jiang, C. Zhang, J. Song, X. Ji and W. Wang, *Spectrochim. Acta, Part A*, 2021, **250**, 119316.

161 Y. Jv, B. Li and R. Cao, *Chem. Commun.*, 2010, **46**, 8017–8019.

162 W. He, X. Han, H. Jia, J. Cai, Y. Zhou and Z. Zheng, *Sci. Rep.*, 2017, **7**, 40103.

163 S.-B. He, L. Yang, X.-L. Lin, L.-M. Chen, H.-P. Peng, H.-H. Deng, X.-H. Xia and W. Chen, *Talanta*, 2020, **211**, 120707.

164 G.-J. Cao, X. Jiang, H. Zhang, T. R. Croley and J.-J. Yin, *RSC Adv.*, 2017, **7**, 52210–52217.

165 S. V. Otari, M. Kumar, M. Z. Anwar, N. D. Thorat, S. K. S. Patel, D. Lee, J. H. Lee, J.-K. Lee, Y. C. Kang and L. Zhang, *Sci. Rep.*, 2017, **7**, 10980.

166 A. K. Keshari, R. Srivastava, P. Singh, V. B. Yadav and G. Nath, *J. Ayurveda Integr. Med.*, 2020, **11**, 37–44.

167 R. Prasad, *J. Nanopart.*, 2014, **2014**, 1–8.

168 P. V. AshaRani, G. Low Kah Mun, M. P. Hande and S. Valiyaveettil, *ACS Nano*, 2009, **3**, 279–290.

169 A. Manke, L. Wang and Y. Rojanasakul, *BioMed Res. Int.*, 2013, **2013**, 942916.

170 K. D. Patel, A. K. Patel, P. Sawadkar, B. Singh and A. W. Perriman, in *Multifunctional And Targeted Theranostic Nanomedicines: Formulation, Design And Applications*, ed. K. Jain and N. K. Jain, Springer Nature, Singapore, 2023, pp. 97–117, DOI: [10.1007/978-981-99-0538-6\\_5](https://doi.org/10.1007/978-981-99-0538-6_5).

171 A. Onodera, F. Nishiumi, K. Kakiguchi, A. Tanaka, N. Tanabe, A. Honma, K. Yayama, Y. Yoshioka, K. Nakahira, S. Yonemura, I. Yanagihara, Y. Tsutsumi and Y. Kawai, *Toxicol. Rep.*, 2015, **2**, 574–579.

172 C. Carlson, S. M. Hussain, A. M. Schrand, L. K. Braydich-Stolle, K. L. Hess, R. L. Jones and J. J. Schlager, *J. Phys. Chem. B*, 2008, **112**, 13608–13619.

173 M. A. Elfaky, A. Sirwi, S. H. Ismail, H. H. Awad and S. S. Gad, *Curr. Issues Mol. Biol.*, 2022, **44**, 2923–2938.

174 B. Dąbrowska-Bouta, G. Sulkowski, W. Strużyński and L. Strużyńska, *Neurotoxic. Res.*, 2019, **35**, 495–504.

175 Y. Qing, L. Cheng, R. Li, G. Liu, Y. Zhang, X. Tang, J. Wang, H. Liu and Y. Qin, *Int. J. Nanomed.*, 2018, **13**, 3311–3327.

176 Y.-H. Hsin, C.-F. Chen, S. Huang, T.-S. Shih, P.-S. Lai and P. J. Chueh, *Toxicol. Lett.*, 2008, **179**, 130–139.

177 M. J. Piao, K. A. Kang, I. K. Lee, H. S. Kim, S. Kim, J. Y. Choi, J. Choi and J. W. Hyun, *Toxicol. Lett.*, 2011, **201**, 92–100.

178 D. He, A. M. Jones, S. Garg, A. N. Pham and T. D. Waite, *J. Phys. Chem. C*, 2011, **115**, 5461–5468.

179 D. He, S. Garg and T. D. Waite, *Langmuir*, 2012, **28**, 10266–10275.

180 E. Mendis, N. Rajapakse, H.-G. Byun and S.-K. Kim, *Life Sci.*, 2005, **77**, 2166–2178.

181 Q. Chang, L. Yan, M. Chen, H. He and J. Qu, *Langmuir*, 2007, **23**, 11197–11199.

182 Y. Inoue, M. Hoshino, H. Takahashi, T. Noguchi, T. Murata, Y. Kanzaki, H. Hamashima and M. Sasatsu, *J. Inorg. Biochem.*, 2002, **92**, 37–42.

183 J. R. Hom, R. A. Quintanilla, D. L. Hoffman, K. L. de Mesy Bentley, J. D. Molkentin, S.-S. Sheu and G. A. Porter Jr., *Dev. Cell*, 2011, **21**, 469–478.

184 A. Henglein, *J. Phys. Chem.*, 1979, **83**, 2209–2216.

185 A. Henglein and J. Lilie, *J. Am. Chem. Soc.*, 1981, **103**, 1059–1066.

186 L. Z. Flores-López, H. Espinoza-Gómez and R. Somanathan, *J. Appl. Toxicol.*, 2019, **39**, 16–26.

187 M. E. Hamdy, M. Del Carlo, H. A. Hussein, T. A. Salah, A. H. El-Deeb, M. M. Emara, G. Pezzoni and D. Compagnone, *J. Nanobiotechnol.*, 2018, **16**, 48.

188 M. U. Farooq, V. Novosad, E. A. Rozhkov, H. Wali, A. Ali, A. A. Fateh, P. B. Neogi, A. Neogi and Z. Wang, *Sci. Rep.*, 2018, **8**, 2907.

189 Y. Liu, W. Ma and J. Wang, *Curr. Pharm. Des.*, 2018, **24**, 2719–2728.

190 P. C. Nagajyothi, T. V. M. Sreekanth, C. O. Tettey, Y. I. Jun and S. H. Mook, *Bioorg. Med. Chem. Lett.*, 2014, **24**, 4298–4303.

191 P. Lau, N. Bidin, S. Islam, W. Shukri, N. Zakaria, N. Musa and G. Krishnan, *Lasers Surg. Med.*, 2017, **49**, 380–386.

192 M. G. Arafa, R. F. El-Kased and M. M. Elmazar, *Sci. Rep.*, 2018, **8**, 13674.

193 D. A. Giljohann, D. S. Seferos, W. L. Daniel, M. D. Massich, P. C. Patel and C. A. Mirkin, *Angew. Chem., Int. Ed.*, 2010, **49**, 3280–3294.

194 R. G. Saratale, I. Karuppusamy, G. D. Saratale, A. Pugazhendhi, G. Kumar, Y. Park, G. S. Ghodake, R. N. Bharagava, J. R. Banu and H. S. Shin, *Colloids Surf., B*, 2018, **170**, 20–35.

195 N. A. Sutan, D. S. Manolescu, I. Fierascu, A. M. Neblea, C. Sutan, C. Duceu, L. C. Soare, D. Negrean, S. M. Avramescu and R. C. Fierascu, *Mater. Sci. Eng., C*, 2018, **93**, 746–758.

196 M. I. Din, F. Arshad, Z. Hussain and M. Mukhtar, *Nanoscale Res. Lett.*, 2017, **12**, 638.

197 H. Joy Prabu and I. Johnson, *Karbala Int. J. Mod. Sci.*, 2015, **1**, 237–246.

198 K. B. Ayaz Ahmed, S. Subramanian, A. Sivasubramanian, G. Veerappan and A. Veerappan, *Spectrochim. Acta, Part A*, 2014, **130**, 54–58.

199 N. Y. Stozhko, M. A. Bukharinova, E. I. Khamzina, A. V. Tarasov, M. B. Vidrevich and K. Z. Brainina, *Nanomaterials*, 2019, **9**, 1655.

200 M. Hamelian, K. Varmira and H. Veisi, *J. Photochem. Photobiol., B*, 2018, **184**, 71–79.

201 F. G. Milanezi, L. M. Meireles, M. M. de Christo Scherer, J. P. de Oliveira, A. R. da Silva, M. L. de Araujo, D. C. Endringer, M. Fronza, M. C. C. Guimarães and R. Scherer, *Saudi Pharm. J.*, 2019, **27**, 968–974.

202 L. M. Nieves, K. Mossburg, J. C. Hsu, A. D. A. Maidment and D. P. Cormode, *Nanoscale*, 2021, **13**, 19306–19323.

203 Y. Mantri, B. Davidi, J. E. Lemaster, A. Hariri and J. V. Jokerst, *Nanoscale*, 2020, **12**, 10511–10520.

204 N. Sarfraz and I. Khan, *Chem. – Asian J.*, 2021, **16**, 720–742.

205 I. B. Becerril-Castro, I. Calderon, N. Pazos-Perez, L. Guerrini, F. Schulz, N. Feliu, I. Chakraborty, V. Giannini, W. J. Parak and R. A. Alvarez-Puebla, *Analysis Sensing*, 2022, **2**, e202200005.

206 J. K. Patra, G. Das, L. F. Fraceto, E. V. R. Campos, M. D. P. Rodriguez-Torres, L. S. Acosta-Torres, L. A. Diaz-Torres, R. Grillo, M. K. Swamy, S. Sharma, S. Habtemariam and H.-S. Shin, *J. Nanobiotechnol.*, 2018, **16**, 71.

207 G. Ajnai, A. Chiu, T. Kan, C.-C. Cheng, T.-H. Tsai and J. Chang, *J. Exp. Clin. Med.*, 2014, **6**, 172–178.

208 T. Xia, M. Kovochich, J. Brant, M. Hotze, J. Sempf, T. Oberley, C. Sioutas, J. I. Yeh, M. R. Wiesner and A. E. Nel, *Nano Lett.*, 2006, **6**, 1794–1807.

209 T. Xia, M. Kovochich, M. Liong, L. Madler, B. Gilbert, H. Shi, J. I. Yeh, J. I. Zink and A. E. Nel, *ACS Nano*, 2008, **2**, 2121–2134.

210 A. Sasidharan and N. A. Monteiro-Riviere, *Wiley Interdiscip. Rev.: Nanomed. Nanobiotechnol.*, 2015, **7**, 779–796.

211 M. Holzinger, A. Le Goff and S. Cosnier, *Front. Chem.*, 2014, **2**, 63.

212 I. Willner, R. Baron and B. Willner, *Biosens. Bioelectron.*, 2007, **22**, 1841–1852.

213 K. Lee, H. Lee, K. W. Lee and T. G. Park, *Biomaterials*, 2011, **32**, 2556–2565.

214 Y. Higashi, J. Mazumder, H. Yoshikawa, M. Saito and E. Tamiya, *Anal. Chem.*, 2018, **90**, 5773–5780.

215 H. Niu, R. Yuan, Y. Chai, L. Mao, Y. Yuan, Y. Zhuo, S. Yuan and X. Yang, *Biosens. Bioelectron.*, 2011, **26**, 3175–3180.

216 L. Mao, R. Yuan, Y. Chai, Y. Zhuo and Y. Xiang, *Biosens. Bioelectron.*, 2011, **26**, 4204–4208.

217 Y. Cui, Y. Zhao, Y. Tian, W. Zhang, X. Lü and X. Jiang, *Biomaterials*, 2012, **33**, 2327–2333.

218 H. Lee and D. G. Lee, *Colloids Surf., B*, 2018, **167**, 1–7.

219 Q. Zhang, V. M. Hitchins, A. M. Schrand, S. M. Hussain and P. L. Goering, *Nanotoxicology*, 2011, **5**, 284–295.

220 D. Mateo, P. Morales, A. Ávalos and A. I. Haza, *Toxicol. Mech. Methods*, 2014, **24**, 161–172.

221 A. Watanabe, M. Kajita, J. Kim, A. Kanayama, K. Takahashi, T. Mashino and Y. Miyamoto, *Nanotechnology*, 2009, **20**, 455105.

222 K. Tahir, S. Nazir, A. Ahmad, B. Li, S. A. Ali Shah, A. U. Khan, G. M. Khan, Q. U. Khan, Z. U. Haq Khan and F. U. Khan, *RSC Adv.*, 2016, **6**, 85903–85916.

223 N. A. S. Ismail, J. X. Lee and F. Yusof, *Antioxidants*, 2022, **11**, 986.

224 A. F. Elhusseiny and H. H. A. M. Hassan, *Spectrochim. Acta, Part A*, 2013, **103**, 232–245.

225 A. J. Kora and L. Rastogi, *Arabian J. Chem.*, 2018, **11**, 1097–1106.

226 L. N. Lewis and N. Lewis, *J. Am. Chem. Soc.*, 1986, **108**, 7228–7231.

227 A. Roucoux, J. Schulz and H. Patin, *Chem. Rev.*, 2002, **102**, 3757–3778.

228 Y. Yoshihisa, Q.-L. Zhao, M. A. Hassan, Z.-L. Wei, M. Furuichi, Y. Miyamoto, T. Kondo and T. Shimizu, *Free Radical Res.*, 2011, **45**, 326–335.

229 Y. Yoshihisa, A. Honda, Q.-L. Zhao, T. Makino, R. Abe, K. Matsui, H. Shimizu, Y. Miyamoto, T. Kondo and T. Shimizu, *Exp. Dermatol.*, 2010, **19**, 1000–1006.

230 P. K. Gupta and L. Mishra, *Nanoscale Adv.*, 2020, **2**, 1774–1791.

231 C. Mu, K. E. Prosser, S. Harrypersad, G. A. MacNeil, R. Panchmatia, J. R. Thompson, S. Sinha, J. J. Warren and C. J. Walsby, *Inorg. Chem.*, 2018, **57**, 15247–15261.

232 S. K. Srivastava and M. Constanti, *J. Nanopart. Res.*, 2012, **14**, 831.

233 G. J. Cao, X. Jiang, H. Zhang, J. Zheng, T. R. Croley and J. J. Yin, *J. Environ. Sci. Health, Part C: Environ. Carcinog. Ecotoxicol. Rev.*, 2017, **35**, 223–238.

234 R. Boyd, *Nat. Chem.*, 2011, **3**, 570.

235 M. E. Weeks, *J. Chem. Educ.*, 1932, **9**, 474.

236 M. Kieliszek, I. Bano and H. Zare, *Biol. Trace Elem. Res.*, 2022, **200**, 971–987.

237 J. Zhao, R. Zhou, K. Hui, Y. Yang, Q. Zhang, Y. Ci, L. Shi, C. Xu, F. Huang and Y. Hu, *Oncotarget*, 2017, **8**, 18832–18847.

238 B. Lipinski, *Anticancer Agents Med. Chem.*, 2017, **17**, 658–661.

239 F. Maiyo and M. Singh, *Nanomedicine*, 2017, **12**, 1075–1089.

240 J. C. Avery and P. R. Hoffmann, *Nutrients*, 2018, **10**, 1203.

241 R. A. Sunde and A. M. Raines, *Adv. Nutr.*, 2011, **2**, 138–150.

242 Y. Wang, W. Kong, L. Wang, J. Z. Zhang, Y. Li, X. Liu and Y. Li, *Phys. Chem. Chem. Phys.*, 2019, **21**, 1336–1343.

243 O. K. Chun, A. Floegel, S. J. Chung, C. E. Chung, W. O. Song and S. I. Koo, *J. Nutr.*, 2010, **140**, 317–324.

244 A. P. Kipp, D. Strohm, R. Brigelius-Flohe, L. Schomburg, A. Bechthold, E. Leschik-Bonnet and H. Heseker, *J. Trace Elem. Med. Biol.*, 2015, **32**, 195–199.

245 Z. Huang, A. H. Rose and P. R. Hoffmann, *Antioxid. Redox Signaling*, 2012, **16**, 705–743.

246 H. Gill and G. Walker, *Nutr. Diet.*, 2008, **65**, S41–S47.

247 K. H. Winther, M. P. Rayman, S. J. Bonnema and L. Hegedüs, *Nat. Rev. Endocrinol.*, 2020, **16**, 165–176.

248 T. Nauser, S. Dockheer, R. Kissner and W. H. Koppenol, *Biochemistry*, 2006, **45**, 6038–6043.

249 N. K. Kildahl, *J. Chem. Educ.*, 1995, **72**, 423.

250 S. Zhai, X. Hu, Y. Hu, B. Wu and D. Xing, *Biomaterials*, 2017, **121**, 41–54.

251 J. Mu, L. Zhang, M. Zhao and Y. Wang, *ACS Appl. Mater. Interfaces*, 2014, **6**, 7090–7098.

252 X. Miao, W. Cao, W. Zheng, J. Wang, X. Zhang, J. Gao, C. Yang, D. Kong, H. Xu, L. Wang and Z. Yang, *Angew. Chem., Int. Ed.*, 2013, **52**, 7781–7785.

253 O. Brodin, S. Eksborg, M. Wallenberg, C. Asker-Hagelberg, E. H. Larsen, D. Mohlkert, C. Lenneby-Helleday, H. Jacobsson, S. Linder, S. Misra and M. Björnstedt, *Nutrients*, 2015, **7**, 4978–4994.

254 S. J. Knox, P. Jayachandran, C. A. Keeling, K. J. Stevens, N. Sandhu, S. L. Stamps-DeAnda, R. Savic, L. Shura, M. K. Buyyounouski and K. Grimes, *Transl. Oncol.*, 2019, **12**, 1525–1531.

255 H. K. Rooprai, I. Kyriazis, R. K. Nuttall, D. R. Edwards, D. Zicha, D. Aubyn, D. Davies, R. Gullan and G. J. Pilkington, *Int. J. Oncol.*, 2007, **30**, 1263–1271.

256 S. Y. Cui, H. Jin, S. J. Kim, A. P. Kumar and Y. I. Lee, *J. Biochem.*, 2008, **143**, 685–693.

257 H. Amani, R. Habibey, F. Shokri, S. J. Hajmiresmail, O. Akhavan, A. Mashaghi and H. Pazoki-Toroudi, *Sci. Rep.*, 2019, **9**, 6044.

258 E. H. Lo, T. Dalkara and M. A. Moskowitz, *Nat. Rev. Neurosci.*, 2003, **4**, 399–414.

259 S. Yang, J. Sun, P. He, X. Deng, Z. Wang, C. Hu, G. Ding and X. Xie, *Chem. Mater.*, 2015, **27**, 2004–2011.

260 H. W. Tan, H.-Y. Mo, A. T. Y. Lau and Y.-M. Xu, *Int. J. Mol. Sci.*, 2018, **20**, 75.

261 S. Khandelwal, M. Boylan, J. E. Spallholz and L. Gollahan, *Int. J. Mol. Sci.*, 2018, **19**(11), 3352.

262 C. M. Weekley, J. B. Aitken, S. Vogt, L. A. Finney, D. J. Paterson, M. D. de Jonge, D. L. Howard, P. K. Witting, I. F. Musgrave and H. H. Harris, *J. Am. Chem. Soc.*, 2011, **133**, 18272–18279.

263 Y. Wang, J. Wang, H. Hao, M. Cai, S. Wang, J. Ma, Y. Li, C. Mao and S. Zhang, *ACS Nano*, 2016, **10**, 9927–9937.

264 T. Li, F. Li, W. Xiang, Y. Yi, Y. Chen, L. Cheng, Z. Liu and H. Xu, *ACS Appl. Mater. Interfaces*, 2016, **8**, 22106–22112.

265 W. Zheng, T. Yin, Q. Chen, X. Qin, X. Huang, S. Zhao, T. Xu, L. Chen and J. Liu, *Acta Biomater.*, 2016, **31**, 197–210.

266 W. Zheng, C. Cao, Y. Liu, Q. Yu, C. Zheng, D. Sun, X. Ren and J. Liu, *Acta Biomater.*, 2015, **11**, 368–380.

267 J. Sun, C. Wei, Y. Liu, W. Xie, M. Xu, H. Zhou and J. Liu, *Biomaterials*, 2019, **197**, 417–431.

268 M. S. Wason, J. Colon, S. Das, S. Seal, J. Turkson, J. Zhao and C. H. Baker, *Nanomedicine*, 2013, **9**, 558–569.

269 J.-D. Cafun, K. O. Kvashnina, E. Casals, V. F. Puntes and P. Glatzel, *ACS Nano*, 2013, **7**, 10726–10732.

270 N. Sutradhar, A. Sinhamahapatra, S. K. Pahari, P. Pal, H. C. Bajaj, I. Mukhopadhyay and A. B. Panda, *J. Phys. Chem. C*, 2011, **115**, 12308–12316.

271 R. Dobrucka, *Iran. J. Sci. Technol., Trans. A: Sci.*, 2018, **42**, 547–555.

272 N. John Sushma, D. Prathyusha, G. Swathi, T. Madhavi, B. Deva Prasad Raju, K. Mallikarjuna and H.-S. Kim, *Appl. Nanosci.*, 2016, **6**, 437–444.

273 G. Kiranmai and A. R. Reddy, *Toxicol. Ind. Health*, 2013, **29**, 897–903.

274 Y.-C. Kuo, S.-P. Lin, C.-W. Lin, Y.-C. Tsai, T.-S. Wu and I. L. Hsiao, *ACS Appl. Nano Mater.*, 2023, **6**, 19915–19925.

275 A. Sinha and S. K. Khare, *Bioresour. Technol.*, 2011, **102**, 4281–4284.

276 A. M. Allahverdiyev, E. S. Abamor, M. Bagirova and M. Rafailovich, *Future Microbiol.*, 2011, **6**, 933–940.

277 J. Matena, S. Petersen, M. Gieseke, A. Kampmann, M. Teske, M. Beyerbach, H. Escobar, H. Haferkamp, N.-C. Gellrich and I. Nolte, *Int. J. Mol. Sci.*, 2015, **16**, 7478.

278 O. Lucaciu, O. Soritău, D. Gheban, D. R. Ciucă, O. Virtic, A. Vulpoi, N. Dirzu, R. Cămpian, G. Băciuț, C. Popa, S. Simon, P. Berce, M. Băciuț and B. Crisan, *BMC Biotechnol.*, 2015, **15**, 1–18.

279 D. Kuroda, M. Niinomi, M. Morinaga, Y. Kato and T. Yashiro, *Mater. Sci. Eng. A*, 1998, **243**, 244–249.

280 B. J. Farrell, B. I. Prilutsky, J. M. Ritter, S. Kelley, K. Popat and M. Pitkin, *J. Biomed. Mater. Res., Part A*, 2014, **102**, 1305–1315.

281 T. K. Ahn, D. H. Lee, T. S. Kim, G. C. Jang, S. Choi, J. B. Oh, G. Ye and S. Lee, *Adv. Exp. Med. Biol.*, 2018, **1077**, 355–368.

282 F. U. Rehman, C. Zhao, H. Jiang and X. Wang, *Biomater. Sci.*, 2016, **4**, 40–54.

283 M. Song, R. Zhang, Y. Dai, F. Gao, H. Chi, G. Lv, B. Chen and X. Wang, *Biomaterials*, 2006, **27**, 4230–4238.

284 J. Wei, H. Shi, M. Zhou, D. Song, Y. Zhang, X. Pan, J. Zhou and T. Wang, *Appl. Catal., A*, 2015, **499**, 101–108.

285 R. Cai, Y. Kubota, T. Shuin, H. Sakai, K. Hashimoto and A. Fujishima, *Cancer Res.*, 1992, **52**, 2346–2348.

286 N. Lagopati, E.-P. Tsilibary, P. Falaras, P. Papazafiri, E. A. Pavlatou, E. Kotsopoulou and P. Kitsiou, *Int. J. Nanomed.*, 2014, **9**, 3219–3230.

287 P. Boffetta, V. Gaborieau, L. Nadon, M. F. Parent, E. Weiderpass and J. Siemiatycki, *Scand. J. Work, Environ. Health*, 2001, **27**, 227–232.

288 Y. Wang, H. Cui, J. Zhou, F. Li, J. Wang, M. Chen and Q. Liu, *Environ. Sci. Pollut. Res.*, 2015, **22**, 5519–5530.

289 K. Niska, K. Pyszka, C. Tukaj, M. Wozniak, M. W. Radomski and I. Inklelewicz-Stepniak, *Int. J. Nanomed.*, 2015, **10**, 1095–1107.

290 S. K. Verma, E. Jha, P. K. Panda, A. Thirumurugan, S. K. S. Parashar, S. Patro and M. Suar, *ACS Omega*, 2018, **3**, 1244–1262.

291 C. Jin, Y. Tang, F. G. Yang, X. L. Li, S. Xu, X. Y. Fan, Y. Y. Huang and Y. J. Yang, *Biol. Trace Elem. Res.*, 2011, **141**, 3–15.

292 C. Angelé-Martínez, C. Goodman and J. Brumaghim, *Metalloomics*, 2014, **6**, 1358–1381.

293 X. Chen and S. S. Mao, *Chem. Rev.*, 2007, **107**, 2891–2959.

294 P.-C. Maness, S. Smolinski, D. M. Blake, Z. Huang, E. J. Wolfrum and W. A. Jacoby, *Appl. Environ. Microbiol.*, 1999, **65**, 4094–4098.

295 J. Cai, J. Peng, J. Feng, R. Li, P. Ren, X. Zang, Z. Wu, Y. Lu, L. Luo, Z. Hu, J. Wang, X. Dai, P. Zhao, J. Wang, M. Yan, J. Liu, R. Deng and D. Wang, *Nat. Commun.*, 2023, **14**, 3643.

296 J. Chu, Z. Kong, D. Lu, W. Zhang, X. Wang, Y. Yu, S. Li, X. Wang, S. Xiong and J. Ma, *Mater. Lett.*, 2016, **166**, 179–182.

297 J. Kysar and P. K. Sekhar, *Appl. Nanosci.*, 2016, **6**, 959–964.

298 A. Liu, M. Ichihara, I. Honma and H. Zhou, *Electrochem. Commun.*, 2007, **9**, 1766–1771.

299 R. Berenguer, M. O. Guerrero-Pérez, I. Guzmán, J. Rodríguez-Mirasol and T. Cordero, *ACS Omega*, 2017, **2**, 7739–7745.

300 K. K. Dey, S. Jha, A. Kumar, G. Gupta, A. K. Srivastava and P. P. Ingole, *Electrochim. Acta*, 2019, **312**, 89–99.

301 R. K. Sharma, P. Kumar and G. B. Reddy, *J. Alloys Compd.*, 2015, **638**, 289–297.

302 X. Zhou, G. Wu, J. Wu, H. Yang, J. Wang and G. Gao, *Phys. Chem. Chem. Phys.*, 2014, **16**, 3973–3982.

303 S. Pang, G. Li and Z. Zhang, *Macromol. Rapid Commun.*, 2005, **26**, 1262–1265.

304 J. Zhu, L. Cao, Y. Wu, Y. Gong, Z. Liu, H. E. Hoster, Y. Zhang, S. Zhang, S. Yang, Q. Yan, P. M. Ajayan and R. Vajtai, *Nano Lett.*, 2013, **13**, 5408–5413.

305 A. Makarevich, O. Makarevich, A. Ivanov, D. Sharovarov, A. Eliseev, V. Amelichev, O. Boytsova, A. Gorodetsky, M. Navarro-Cía and A. Kaul, *CrystEngComm*, 2020, **22**, 2612–2620.

306 A. Pan, H. B. Wu, L. Yu, T. Zhu and X. W. Lou, *ACS Appl. Mater. Interfaces*, 2012, **4**, 3874–3879.

307 F. Natalio, R. André, A. F. Hartog, B. Stoll, K. P. Jochum, R. Wever and W. Tremel, *Nat. Nanotechnol.*, 2012, **7**, 530–535.

308 A. A. Vernekar, D. Sinha, S. Srivastava, P. U. Paramasivam, P. D'Silva and G. Mugesha, *Nat. Commun.*, 2014, **5**, 5301.

309 S. Das, A. Roy, A. K. Barui, M. M. A. Alabbasi, M. Kuncha, R. Sistla, B. Sreedhar and C. R. Patra, *Nanoscale*, 2020, **12**, 7604–7621.

310 B. L. Zhu, Q. Qiherima, L. Lv and X. J. Wang, *Key Eng. Mater.*, 2012, **492**, 264–267.

311 Y. Du and Y. Zhang, *J. Exp. Nanosci.*, 2014, **9**, 120–125.

312 S. Rong, P. Zhang, F. Liu and Y. Yang, *ACS Catal.*, 2018, **8**, 3435–3446.

313 T. Soejima, K. Nishizawa and R. Isoda, *J. Colloid Interface Sci.*, 2018, **510**, 272–279.

314 V. Kumar, K. Singh, S. Panwar and S. K. Mehta, *Int. Nano Lett.*, 2017, **7**, 123–131.

315 J. Shin, R. M. Anisur, M. K. Ko, G. H. Im, J. H. Lee and I. S. Lee, *Angew. Chem., Int. Ed.*, 2009, **48**, 321–324.

316 Y. Chen, H. Chen, S. Zhang, F. Chen, S. Sun, Q. He, M. Ma, X. Wang, H. Wu, L. Zhang, L. Zhang and J. Shi, *Biomaterials*, 2012, **33**, 2388–2398.

317 H. Zhang, F. Xu, J. Xue, S. Chen, J. Wang and Y. Yang, *Sci. Rep.*, 2020, **10**, 6067.

318 S. Fairose, S. Ernest and Ashna, *Mater. Today: Proc.*, 2017, **4**, 12085–12093.

319 Y. Zhang, L. Chen, R. Sun, R. Lv, T. Du, Y. Li, X. Zhang, R. Sheng and Y. Qi, *ACS Biomater. Sci. Eng.*, 2022, **8**, 638–648.

320 J. Kim, H. Y. Kim, S. Y. Song, S.-H. Go, H. S. Sohn, S. Baik, M. Soh, K. Kim, D. Kim, H.-C. Kim, N. Lee, B.-S. Kim and T. Hyeon, *ACS Nano*, 2019, **13**, 3206–3217.

321 Y. Wu, Z. Zhou, M. Zhang, S. Li, M. Sun and Z. Song, *J. Nanobiotechnol.*, 2023, **21**, 432.

322 F. Qian, Z. Huang, W. Liu, Y. Liu and X. He, *J. Biomed. Mater. Res., Part A*, 2023, **111**, 1678–1691.

323 S. Alarifi, D. Ali and S. Alkahtani, *BioMed Res. Int.*, 2017, **2017**, 5478790.

324 N. Singh, M. Geethika, S. M. Eswarappa and G. Mugesh, *Chem. – Eur. J.*, 2018, **24**, 8393–8403.

325 N. Singh, M. A. Savanur, S. Srivastava, P. D'Silva and G. Mugesh, *Nanoscale*, 2019, **11**, 3855–3863.

326 M. H. Tootoonchi, M. Hashempour, P. L. Blackwelder and C. A. Fraker, *Acta Biomater.*, 2017, **59**, 327–337.

327 C. R. Gordijo, K. Koulajian, A. J. Shuhendler, L. D. Bonifacio, H. Y. Huang, S. Chiang, G. A. Ozin, A. Giacca and X. Y. Wu, *Adv. Funct. Mater.*, 2011, **21**, 73–82.

328 C. R. Gordijo, A. J. Shuhendler and X. Y. Wu, *Adv. Funct. Mater.*, 2010, **20**, 1404–1412.

329 P. Prasad, C. R. Gordijo, A. Z. Abbasi, A. Maeda, A. Ip, A. M. Rauth, R. S. DaCosta and X. Y. Wu, *ACS Nano*, 2014, **8**, 3202–3212.

330 I. Rabani, J. Yoo, H.-S. Kim, D. V. Lam, S. Hussain, K. Karuppasamy and Y.-S. Seo, *Nanoscale*, 2021, **13**, 355–370.

331 R. Shanmuganathan, S. Sathiyavimal, Q. Hoang Le, M. M. Al-Ansari, L. A. Al-Humaid, G. K. Jhanani, J. Lee and S. Barathi, *Environ. Res.*, 2023, **236**, 116747.

332 D. Das and B. J. Saikia, *Chem. Phys. Impact*, 2023, **6**, 100137.

333 L. Díez-Tercero, L. M. Delgado, E. Bosch-Rué and R. A. Perez, *Sci. Rep.*, 2021, **11**, 11707.

334 N. Mandakhbayar, Y. Ji, A. El-Fiqi, K. D. Patel, D. S. Yoon, K. Dashnyam, O. Bayaraa, G. Jin, K. Tsogtbaatar, T.-H. Kim, J.-H. Lee and H.-W. Kim, *Bioact. Mater.*, 2024, **31**, 298–311.

335 S. E. Kim, L. Zhang, K. Ma, M. Riegman, F. Chen, I. Ingold, M. Conrad, M. Z. Turker, M. Gao, X. Jiang, S. Monette, M. Pauliah, M. Gonen, P. Zanzonico, T. Quinn, U. Wiesner, M. S. Bradbury and M. Overholtzer, *Nat. Nanotechnol.*, 2016, **11**, 977–985.

336 L. Jiang, N. Kon, T. Li, S. J. Wang, T. Su, H. Hibshoosh, R. Baer and W. Gu, *Nature*, 2015, **520**, 57–62.

337 C. Luo, Y. Li, L. Yang, X. Wang, J. Long and J. Liu, *Arch. Toxicol.*, 2015, **89**, 357–369.

338 Y. Ichikawa, M. Ghanefar, M. Bayeva, R. Wu, A. Khechaduri, S. V. Naga Prasad, R. K. Mutharasan, T. J. Naik and H. Ardehali, *J. Clin. Invest.*, 2014, **124**, 617–630.

339 L. S. Lin, J. Song, L. Song, K. Ke, Y. Liu, Z. Zhou, Z. Shen, J. Li, Z. Yang, W. Tang, G. Niu, H. H. Yang and X. Chen, *Angew. Chem., Int. Ed.*, 2018, **57**, 4902–4906.

340 S. Niu, L. K. Zhang, L. Zhang, S. Zhuang, X. Zhan, W. Y. Chen, S. Du, L. Yin, R. You, C. H. Li and Y. Q. Guan, *Theranostics*, 2017, **7**, 344–356.

341 B. Torres-Herrero, I. Armenia, M. Alleva, L. Asín, S. Correa, C. Ortiz, Y. Fernández-Afonso, L. Gutiérrez, J. M. de la Fuente, L. Betancor and V. Grazú, *ACS Nano*, 2023, **17**, 12358–12373.

342 Y. Zhang, Y. Wang, Q. Zhou, X. Chen, W. Jiao, G. Li, M. Peng, X. Liu, Y. He and H. Fan, *ACS Appl. Mater. Interfaces*, 2021, **13**, 52395–52405.

343 Y. Hao, Z. Dong, M. Chen, Y. Chao, Z. Liu, L. Feng, Y. Hao, Z. L. Dong, M. C. Chen, Y. Chao, Z. Liu and L. Z. Feng, *Biomaterials*, 2020, **228**, 119568.

344 A. K. Hauser, M. I. Mitov, E. F. Daley, R. C. McGarry, K. W. Anderson and J. Z. Hilt, *Biomaterials*, 2016, **105**, 127–135.

345 M. I. Khan, A. Mohammad, G. Patil, S. A. H. Naqvi, L. K. S. Chauhan and I. Ahmad, *Biomaterials*, 2012, **33**, 1477–1488.

346 J. Liu, L. Wang, J. Cao, Y. Huang, Y. Lin, X. Wu, Z. Wang, F. Zhang, X. Xu and G. Liu, *Nanoscale*, 2014, **6**, 9025–9033.

347 E.-J. Park, D.-H. Choi, Y. Kim, E.-W. Lee, J. Song, M.-H. Cho, J.-H. Kim and S.-W. Kim, *Toxicol. In Vitro*, 2014, **28**, 1402–1412.

348 H. Y. Tan, N. Wang, S. Li, M. Hong, X. Wang and Y. Feng, *Oxid. Med. Cell. Longevity*, 2016, **2016**, 2795090.

349 J. Sarkar, N. Chakraborty, A. Chatterjee, A. Bhattacharjee, D. Dasgupta and K. Acharya, *Nanomaterials*, 2020, **10**(2), 312.

350 S. Sukumar, A. Rudrasenan and D. Padmanabhan Nambiar, *ACS Omega*, 2020, **5**, 1040–1051.

351 A. Ananth, S. Dharaneehdaran, M.-S. Heo and Y. S. Mok, *Chem. Eng. J.*, 2015, **262**, 179–188.

352 M. Nasrollahzadeh, M. Maham and S. Mohammad Sajadi, *J. Colloid Interface Sci.*, 2015, **455**, 245–253.

353 D. Rehana, D. Mahendiran, R. S. Kumar and A. K. Rahiman, *Biomed. Pharmacother.*, 2017, **89**, 1067–1077.

354 C. Angelé-Martínez, K. V. T. Nguyen, F. S. Ameer, J. N. Anker and J. L. Brumaghim, *Nanotoxicology*, 2017, **11**, 278–288.

355 A. M. Studer, L. K. Limbach, L. Van Duc, F. Krumeich, E. K. Athanassiou, L. C. Gerber, H. Moch and W. J. Stark, *Toxicol. Lett.*, 2010, **197**, 169–174.

356 H. L. Karlsson, P. Cronholm, J. Gustafsson and L. Möller, *Chem. Res. Toxicol.*, 2008, **21**, 1726–1732.

357 J. P. Kehrer, *Toxicology*, 2000, **149**, 43–50.

358 H. Ashrafizadeh, S. R. Abtahi and A. A. Oroojan, *Diabetes Metab. Syndr.*, 2020, **14**, 443–445.

359 B. Stieberova, M. Zilka, M. Ticha, F. Freiberg, P. Caramazana-González, J. McKechnie and E. Lester, *ACS Sustainable Chem. Eng.*, 2017, **5**, 2493–2500.

360 S. Y. Kim, S. H. Jeong, E. Y. Lee, Y.-H. Park, H. C. Bae, Y. S. Jang, E. H. Maeng, M.-K. Kim and S. W. Son, *J. Toxicol. Environ. Health Sci.*, 2011, **3**, 258–261.

361 C. García-Gómez, A. Obrador, D. González, M. Babín and M. D. Fernández, *Sci. Total Environ.*, 2017, **589**, 11–24.

362 Y. K. Mishra and R. Adelung, *Mater. Today*, 2018, **21**, 631–651.

363 M. Martínez-Carmona, Y. Gun'ko and M. Vallet-Regí, *Nanomaterials*, 2018, **8**, 268.

364 J. W. Rasmussen, E. Martinez, P. Louka and D. G. Wingett, *Expert Opin. Drug Delivery*, 2010, **7**, 1063–1077.

365 R. Lahri, M. Rahman, M. Wright, P. Kosmas and M. Thanou, *Med. Phys.*, 2018, **45**, 3820–3830.

366 P. Ruenraroengsak, D. Kiryushko, I. G. Theodorou, M. M. Klosowski, E. R. Taylor, T. Niriella, C. Palmieri, E. Yagüe, M. P. Ryan, R. C. Coombes, F. Xie and A. E. Porter, *Nanoscale*, 2019, **11**, 12858–12870.

367 J. Wang, J. S. Lee, D. Kim and L. Zhu, *ACS Appl. Mater. Interfaces*, 2017, **9**, 39971–39984.

368 S. Chaudhary, A. Umar, K. K. Bhasin and S. Baskoutas, *Materials*, 2018, **11**(2), 287.

369 J. Singh, T. Dutta, K.-H. Kim, M. Rawat, P. Samddar and P. Kumar, *J. Nanobiotechnol.*, 2018, **16**, 84.

370 J. A. Hernandez-Viezcas, H. Castillo-Michel, A. D. Servin, J. R. Peralta-Videa and J. L. Gardea-Torresdey, *Chem. Eng. J.*, 2011, **170**, 346–352.

371 G. Chichiriccò and A. Poma, *Nanomaterials*, 2015, **5**(2), 851–873.

372 P. C. Nagajyothi, S. J. Cha, I. J. Yang, T. V. M. Sreekanth, K. J. Kim and H. M. Shin, *J. Photochem. Photobiol. B*, 2015, **146**, 10–17.

373 M. Shoeb, B. R. Singh, J. A. Khan, W. Khan, B. N. Singh, H. B. Singh and A. H. Naqvi, *Adv. Nat. Sci.*, 2013, **4**, 035015.

374 J.-H. Li, X.-R. Liu, Y. Zhang, F.-F. Tian, G.-Y. Zhao, Q.-L.-Y. Yu, F.-L. Jiang and Y. Liu, *Toxicol. Res.*, 2012, **1**, 137–144.

375 W. M. U. Daniels, J. Hendricks, R. Salie and S. J. van Rensburg, *Metab. Brain Dis.*, 2004, **19**, 79–88.

376 X. Xu, D. Chen, Z. Yi, M. Jiang, L. Wang, Z. Zhou, X. Fan, Y. Wang and D. Hui, *Langmuir*, 2013, **29**, 5573–5580.

377 J. Gupta and D. Bahadur, *ACS Omega*, 2018, **3**, 2956–2965.

378 M. Ahrén, L. Selegård, A. Klasson, F. Söderlind, N. Abrikossova, C. Skoglund, T. Bengtsson, M. Engström, P.-O. Käll and K. Uvdal, *Langmuir*, 2010, **26**, 5753–5762.

379 S. J. Seo, S. M. Han, J. H. Cho, K. Hyodo, A. Zaboronok, H. You, K. Peach, M. A. Hill and J. K. Kim, *Radiat. Environ. Biophys.*, 2015, **54**, 423–431.

380 D. J. Todd and J. Kay, *Curr. Rheumatol. Rep.*, 2008, **10**, 195–204.

381 P. Sharma, S. Brown, G. Walter, S. Santra and B. Moudgil, *Adv. Colloid Interface Sci.*, 2006, **123–126**, 471–485.

382 A. Trovarelli and P. Fornasiero, *Catalysis by Ceria and Related Materials*, 2013, DOI: [10.1142/9781848169647\\_fmatter](https://doi.org/10.1142/9781848169647_fmatter).

383 J. M. Dowding, S. Das, A. Kumar, T. Dosani, R. McCormack, A. Gupta, T. X. T. Sayle, D. C. Sayle, L. von Kalm, S. Seal and W. T. Self, *ACS Nano*, 2013, **7**, 4855–4868.

384 I. Celardo, J. Z. Pedersen, E. Traversa and L. Ghibelli, *Nanoscale*, 2011, **3**, 1411–1420.

385 M. S. Lord, J. F. Berret, S. Singh, A. Vinu and A. S. Karakoti, *Small*, 2021, **17**, 2102342.

386 F. Corsi, F. Caputo, E. Traversa and L. Ghibelli, *Front. Oncol.*, 2018, **8**, 309.

387 D. Damatov and J. M. Mayer, *Chem. Commun.*, 2016, **52**, 10281–10284.

388 B. C. Nelson, M. E. Johnson, M. L. Walker, K. R. Riley and C. M. Sims, *Antioxidants*, 2016, **5**(2), 15.

389 J. M. Dowding, S. Seal and W. T. Self, *Drug Delivery Transl. Res.*, 2013, **3**, 375–379.

390 W. He, Y. Liu, W. G. Wamer and J.-J. Yin, *J. Food Drug Anal.*, 2014, **22**, 49–63.

391 Y. Xue, Q. Luan, D. Yang, X. Yao and K. Zhou, *J. Phys. Chem. C*, 2011, **115**, 4433–4438.

392 V. Patel, M. Singh, E. L. H. Mayes, A. Martinez, V. Shutthanandan, V. Bansal, S. Singh and A. S. Karakoti, *Chem. Commun.*, 2018, **54**, 13973–13976.

393 A. Srinivas, P. J. Rao, G. Selvam, P. B. Murthy and P. N. Reddy, *Toxicol. Lett.*, 2011, **205**, 105–115.

394 A. Filippi, F. Liu, J. Wilson, S. Lelieveld, K. Korschelt, T. Wang, Y. Wang, T. Reich, U. Pöschl, W. Tremel and H. Tong, *RSC Adv.*, 2019, **9**, 11077–11081.

395 C. Mahapatra, R. K. Singh, J.-H. Lee, J. Jung, J. K. Hyun and H.-W. Kim, *Acta Biomater.*, 2017, **50**, 142–153.

396 F. Corsi, F. Caputo, E. Traversa and L. Ghibelli, *Front. Oncol.*, 2018, **8**, 309.

397 I. Celardo, M. De Nicola, C. Mandoli, J. Z. Pedersen, E. Traversa and L. Ghibelli, *ACS Nano*, 2011, **5**, 4537–4549.

398 F. Caputo, M. De Nicola, A. Sienkiewicz, A. Giovanetti, I. Bejarano, S. Licoccia, E. Traversa and L. Ghibelli, *Nanoscale*, 2015, **7**, 15643–15656.

399 S.-H. Shin, O. Purevdorj, O. Castano, J. A. Planell and H.-W. Kim, *J. Tissue Eng.*, 2012, **3**, 2041731412443530.

400 A. Thill, O. Zeyons, O. Spalla, F. Chauvat, J. Rose, M. Auffan and A. M. Flank, *Environ. Sci. Technol.*, 2006, **40**, 6151–6156.

401 M. Culcasi, L. Benameur, A. Mercier, C. Lucchesi, H. Rahmouni, A. Asteian, G. Casano, A. Botta, H. Kovacic and S. Pietri, *Chem. – Biol. Interact.*, 2012, **199**, 161–176.

402 L. De Marzi, A. Monaco, J. De Lapuente, D. Ramos, M. Borras, M. Di Gioacchino, S. Santucci and A. Poma, *Int. J. Mol. Sci.*, 2013, **14**, 3065–3077.

403 G. Pota, B. Silvestri, G. Vitiello, N. Gallucci, R. Di Girolamo, S. Scialla, M. G. Raucci, L. Ambrosio, M. Di Napoli, A. Zanfardino, M. Varcamonti, A. Pezzella and G. Luciani, *Biomater. Adv.*, 2023, **153**, 213558.

404 K. D. Patel, A. K. Patel, A. G. Kurian, R. K. Singh and H.-W. Kim, in *Nanotheranostics for Treatment and Diagnosis of Infectious Diseases*, ed. K. Jain and J. Ahmad, Academic Press, 2022, pp. 319–352, DOI: [10.1016/B978-0-323-91201-3.00011-6](https://doi.org/10.1016/B978-0-323-91201-3.00011-6).

405 X. Yuan, X. Zhang, L. Sun, Y. Wei and X. Wei, *Part. Fibre Toxicol.*, 2019, **16**, 18.

406 J. Meng, X. Li, C. Wang, H. Guo, J. Liu and H. Xu, *ACS Appl. Mater. Interfaces*, 2015, **7**, 3180–3188.

407 E. J. Comparetti, V. d A. Pedrosa and R. Kaneno, *Bioconjugate Chem.*, 2018, **29**, 709–718.

408 B. D. Holt, P. A. Short, A. D. Rape, Y.-L. Wang, M. F. Islam and K. N. Dahl, *ACS Nano*, 2010, **4**, 4872–4878.

409 B. D. Holt, H. Shams, T. A. Horst, S. Basu, A. D. Rape, Y.-L. Wang, G. K. Rohde, M. R. K. Mofrad, M. F. Islam and K. N. Dahl, *J. Funct. Biomater.*, 2012, **3**, 398–417.

410 B. D. Holt, K. N. Dahl and M. F. Islam, *Small*, 2011, **7**, 2348–2355.

411 M. R. McDevitt, D. Chattopadhyay, B. J. Kappel, J. S. Jaggi, S. R. Schiffman, C. Antczak, J. T. Njardarson, R. Brentjens and D. A. Scheinberg, *J. Nucl. Med.*, 2007, **48**, 1180–1189.

412 B. L. Allen, P. D. Kichambare, P. Gou, I. I. Vlasova, A. A. Kapralov, N. Konduru, V. E. Kagan and A. Star, *Nano Lett.*, 2008, **8**, 3899–3903.

413 V. E. Kagan, N. V. Konduru, W. Feng, B. L. Allen, J. Conroy, Y. Volkov, I. I. Vlasova, N. A. Belikova, N. Yanamala, A. Kapralov, Y. Y. Tyurina, J. Shi, E. R. Kisin, A. R. Murray, J. Franks, D. Stoltz, P. Gou, J. Klein-Seetharaman, B. Fadeel, A. Star and A. A. Shvedova, *Nat. Nanotechnol.*, 2010, **5**, 354–359.

414 F. T. Andón, A. A. Kapralov, N. Yanamala, W. Feng, A. Baygan, B. J. Chambers, K. Hultenby, F. Ye, M. S. Toprak, B. D. Brandner, A. Fornara, J. Klein-Seetharaman, G. P. Kotchey, A. Star, A. A. Shvedova, B. Fadeel and V. E. Kagan, *Small*, 2013, **9**, 2721–2729.

415 K. Bhattacharya, R. El-Sayed, F. T. Andón, S. P. Mukherjee, J. Gregory, H. Li, Y. Zhao, W. Seo, A. Fornara, B. Brandner, M. S. Toprak, K. Leifer, A. Star and B. Fadeel, *Carbon*, 2015, **91**, 506–517.

416 M. Yang and M. Zhang, *Front. Mater.*, 2019, **6**, 225.

417 B. L. Allen, G. P. Kotchey, Y. Chen, N. V. K. Yanamala, J. Klein-Seetharaman, V. E. Kagan and A. Star, *J. Am. Chem. Soc.*, 2009, **131**, 17194–17205.

418 M. Zhang, M. Yang, H. Nakajima, M. Yudasaka, S. Iijima and T. Okazaki, *ACS Appl. Nano Mater.*, 2019, **2**, 4293–4301.

419 J. Ju, S. Regmi, A. Fu, S. Lim and Q. Liu, *J. Biophotonics*, 2019, **12**, e201800367.

420 Z. Jin, N. Dridi, G. Palui, V. Palomo, J. V. Jokerst, P. E. Dawson, Q.-X. A. Sang and H. MattoSSI, *Anal. Chem.*, 2023, **95**, 2713–2722.

421 I. L. Christensen, Y.-P. Sun and P. Juzenas, *J. Biomed. Nanotechnol.*, 2011, **7**, 667–676.

422 V. Ruiz, L. Yate, I. García, G. Cabanero and H.-J. Grande, *Carbon*, 2017, **116**, 366–374.

423 L. Nilewski, K. Mendoza, A. S. Jalilov, V. Berka, G. Wu, W. K. A. Sikkema, A. Metzger, R. Ye, R. Zhang, D. X. Luong, T. Wang, E. McHugh, P. J. Derry, E. L. Samuel, T. A. Kent, A.-L. Tsai and J. M. Tour, *ACS Appl. Mater. Interfaces*, 2019, **11**, 16815–16821.

424 Y. Li, S. Li, Y. Wang, J. Wang, H. Liu, X. Liu, L. Wang, X. Liu, W. Xue and N. Ma, *Phys. Chem. Chem. Phys.*, 2017, **19**, 11631–11638.

425 W. Stahl and H. Sies, *Mol. Aspects Med.*, 2003, **24**, 345–351.

426 K. Okuda, T. Hirota, M. Hirobe, T. Nagano, M. Mochizuki and T. Mashino, *Fullerene Sci. Technol.*, 2000, **8**, 127–142.

427 K. D. Patel, T.-H. Kim, N. Mandakhbayar, R. K. Singh, J.-H. Jang, J.-H. Lee and H.-W. Kim, *Acta Biomater.*, 2020, **108**, 97–110.

428 Y.-M. Li, K. D. Patel, Y.-K. Han, S.-M. Hong, Y.-X. Meng, H.-H. Lee, J. H. Park, J. C. Knowles, J. K. Hyun, J.-H. Lee and H.-W. Kim, *J. Chem. Eng.*, 2023, **466**, 143125.

429 I. Fenoglio, M. Tomatis, D. Lison, J. Muller, A. Fonseca, J. B. Nagy and B. Fubini, *Free Radicals Biol. Med.*, 2006, **40**, 1227–1233.

430 R. M. Luente-Schultz, V. C. Moore, A. D. Leonard, B. K. Price, D. V. Kosynkin, M. Lu, R. Partha, J. L. Conyers and J. M. Tour, *J. Am. Chem. Soc.*, 2009, **131**, 3934–3941.

431 Y. Qiu, Z. Wang, A. C. E. Owens, I. Kulaots, Y. Chen, A. B. Kane and R. H. Hurt, *Nanoscale*, 2014, **6**, 11744–11755.

432 G. de la Torre, G. Bottari and T. Torres, *Adv. Energy Mater.*, 2017, **7**, 1601700.

433 I. L. Christensen, Y. P. Sun and P. Juzenas, *J. Biomed. Nanotechnol.*, 2011, **7**, 667–676.

434 W. Zhang, J. Chavez, Z. Zeng, B. Bloom, A. Sheardy, Z. Ji, Z. Yin, D. H. Waldeck, Z. Jia and J. Wei, *ACS Appl. Nano Mater.*, 2018, **1**, 2699–2708.

435 G. Huang, Y. Lin, L. Zhang, Z. Yan, Y. Wang and Y. Liu, *Sci. Rep.*, 2019, **9**, 19651.

436 Y. Chong, C. Ge, G. Fang, X. Tian, X. Ma, T. Wen, W. G. Wamer, C. Chen, Z. Chai and J. J. Yin, *ACS Nano*, 2016, **10**, 8690–8699.

437 S. S. Maktedar, G. Avashthi and M. Singh, *RSC Adv.*, 2016, **6**, 114264.

438 H.-Y. Chou, H.-M. D. Wang, C.-H. Kuo, P.-H. Lu, L. Wang, W. Kang and C.-L. Sun, *ACS Omega*, 2020, **5**, 6588–6597.

439 G. Choe, S.-W. Kim, J. Park, J. Park, S. Kim, Y. S. Kim, Y. Ahn, D.-W. Jung, D. R. Williams and J. Y. Lee, *Biomaterials*, 2019, **225**, 119513.

440 N. Baali, A. Khecha, A. Bensouici, G. Speranza and N. Hamdouni, *C*, 2019, **5**, 75.

441 C. S. Sharma, S. Sarkar, A. Periyakaruppan, J. Barr, K. Wise, R. Thomas, B. L. Wilson and G. T. Ramesh, *J. Nanosci. Nanotechnol.*, 2007, **7**, 2466–2472.

442 S. K. Manna, S. Sarkar, J. Barr, K. Wise, E. V. Barrera, O. Jejelowo, A. C. Rice-Ficht and G. T. Ramesh, *Nano Lett.*, 2005, **5**, 1676–1684.

443 S. Alarifi and D. Ali, *Int. J. Toxicol.*, 2015, **34**, 258–265.

444 S. Rasras, H. Kalantari, M. Rezaei, M. A. Dehghani, L. Zeidooni, K. Alikarami, F. Dehghani and S. Alboghobeish, *Toxicol. Ind. Health*, 2019, **35**, 497–506.

445 W.-C. Hou, S. BeigzadehMilani, C. T. Jafvert and R. G. Zepp, *Environ. Sci. Technol.*, 2014, **48**, 3875–3882.

446 A. V. Singh, K. K. Mehta, K. Worley, J. S. Dordick, R. S. Kane and L. Q. Wan, *ACS Nano*, 2014, **8**, 2196–2205.

447 J. Zhang, H. Yang, G. Shen, P. Cheng, J. Zhang and S. Guo, *Chem. Commun.*, 2010, **46**, 1112–1114.

448 G. P. Kotchey, B. L. Allen, H. Vedala, N. Yanamala, A. A. Kapralov, Y. Y. Tyurina, J. Klein-Seetharaman, V. E. Kagan and A. Star, *ACS Nano*, 2011, **5**, 2098–2108.

449 Y. Zhu, S. Murali, W. Cai, X. Li, J. W. Suk, J. R. Potts and R. S. Ruoff, *Adv. Mater.*, 2010, **22**, 3906–3924.

450 M. C. Duch, G. R. S. Budinger, Y. T. Liang, S. Soberanes, D. Urich, S. E. Chiarella, L. A. Campochiaro, A. Gonzalez, N. S. Chandel, M. C. Hersam and G. M. Mutlu, *Nano Lett.*, 2011, **11**, 5201–5207.

451 X. Yang, Y. Wang, X. Huang, Y. Ma, Y. Huang, R. Yang, H. Duan and Y. Chen, *J. Mater. Chem.*, 2011, **21**, 3448–3454.

452 M. Kalbacova, A. Broz, J. Kong and M. Kalbac, *Carbon*, 2010, **48**, 4323–4329.

453 T. R. Nayak, H. Andersen, V. S. Makam, C. Khaw, S. Bae, X. Xu, P.-L. R. Ee, J.-H. Ahn, B. H. Hong, G. Pastorin and B. Özylmaz, *ACS Nano*, 2011, **5**, 4670–4678.

454 Z. Liu, J. T. Robinson, X. Sun and H. Dai, *J. Am. Chem. Soc.*, 2008, **130**, 10876–10877.

455 J. T. Robinson, S. M. Tabakman, Y. Liang, H. Wang, H. Sanchez Casalongue, D. Vinh and H. Dai, *J. Am. Chem. Soc.*, 2011, **133**, 6825–6831.

456 T. Parasassi, R. Brunelli, G. Costa, M. De Spirito, E. Krasnowska, T. Lundeberg, E. Pittaluga and F. Ursini, *Sci. World J.*, 2010, **10**, 1192–1202.

457 L. Feng, S. Zhang and Z. Liu, *Nanoscale*, 2011, **3**, 1252–1257.

458 K. Yang, S. Zhang, G. Zhang, X. Sun, S. T. Lee and Z. Liu, *Nano Lett.*, 2010, **10**, 3318–3323.

459 H. Hong, K. Yang, Y. Zhang, J. W. Engle, L. Feng, Y. Yang, T. R. Nayak, S. Goel, J. Bean, C. P. Theuer, T. E. Barnhart, Z. Liu and W. Cai, *ACS Nano*, 2012, **6**, 2361–2370.

460 Y. Wang, J. Lu, L. Tang, H. Chang and J. Li, *Anal. Chem.*, 2009, **81**, 9710–9715.

461 Z. Zhu, J. Qian, X. Zhao, W. Qin, R. Hu, H. Zhang, D. Li, Z. Xu, B. Z. Tang and S. He, *ACS Nano*, 2016, **10**, 588–597.

462 B. Tian, C. Wang, S. Zhang, L. Feng and Z. Liu, *ACS Nano*, 2011, **5**, 7000–7009.

463 H.-S. Hsieh and R. G. Zepp, *Environ. Sci.: Nano*, 2019, **6**, 3734–3744.

464 X. Niu, J. Chen and J. Gao, *Asian J. Pharm. Sci.*, 2019, **14**, 480–496.

465 Y. Liu, G. Li, L. Huan and S. Cao, *Nanoscale*, 2024, **16**, 504–526.

466 T. K. Nguyen, S. Aberoumand and D. V. Dao, *Small*, 2021, **17**, 2101775.

467 X. Li, W. Li, Q. Liu, S. Chen, L. Wang, F. Gao, G. Shao, Y. Tian, Z. Lin and W. Yang, *Adv. Funct. Mater.*, 2021, **31**, 2008901.

468 F. Chen, G. Li, E. R. Zhao, J. Li, G. Hableel, J. E. Lemaster, Y. Bai, G. L. Sen and J. V. Jokerst, *Biomaterials*, 2018, **179**, 60–70.

469 A. Borkowski, M. Szala, P. Kowalczyk, T. Cłapa, D. Narożna and M. Selwet, *Chemosphere*, 2015, **135**, 233–239.

470 J. Pourchez, V. Forest, N. Boumahdi, D. Boudard, M. Tomatis, B. Fubini, N. Herlin-Boime, Y. Leconte, B. Guilhot, M. Cottier and P. Grosseau, *J. Nanopart. Res.*, 2012, **14**, 1143.

471 M. Schieber and N. S. Chandel, *Curr. Biol.*, 2014, **24**, R453–R462.

472 Z. Yi, H. I. Hussain, C. Feng, D. Sun, F. She, J. E. Rookes, D. M. Cahill and L. Kong, *ACS Appl. Mater. Interfaces*, 2015, **7**, 9937–9946.

473 L. Chen, X. Zhou, W. Nie, Q. Zhang, W. Wang, Y. Zhang and C. He, *ACS Appl. Mater. Interfaces*, 2016, **8**, 33829–33841.

474 Q. Zhao, H. Geng, Y. Wang, Y. Gao, J. Huang, Y. Wang, J. Zhang and S. Wang, *ACS Appl. Mater. Interfaces*, 2014, **6**, 20290–20299.

475 R. Cheng, F. Feng, F. Meng, C. Deng, J. Feijen and Z. Zhong, *J. Controlled Release*, 2011, **152**, 2–12.

476 S. Zanganeh, G. Hutter, R. Spitzer, O. Lenkov, M. Mahmoudi, A. Shaw, J. S. Pajarinen, H. Nejadnik, S. Goodman, M. Moseley, L. M. Coussens and H. E. Daldrup-Link, *Nat. Nanotechnol.*, 2016, **11**, 986–994.

477 J.-W. Kim, C. Mahapatra, J.-Y. Hong, M. S. Kim, K. W. Leong, H.-W. Kim and J. K. Hyun, *Adv. Sci.*, 2017, **4**, 1700034.

478 C. Nathan and A. Cunningham-Bussel, *Nat. Rev. Immunol.*, 2013, **13**, 349–361.

479 T.-C. Cheong, E. P. Shin, E.-K. Kwon, J.-H. Choi, K.-K. Wang, P. Sharma, K. H. Choi, J.-M. Lim, H.-G. Kim, K. Oh, J.-H. Jeon, I. So, I.-G. Kim, M.-S. Choi, Y. K. Kim, S.-Y. Seong, Y.-R. Kim and N.-H. Cho, *ACS Chem. Biol.*, 2015, **10**, 757–765.

480 B. Zhu, Y. Li, Z. Lin, M. Zhao, T. Xu, C. Wang and N. Deng, *Nanoscale Res. Lett.*, 2016, **11**, 198.

481 R. Pal, B. Chakraborty, A. Nath, L. M. Singh, M. Ali, D. S. Rahman, S. K. Ghosh, A. Basu, S. Bhattacharya, R. Baral and M. Sengupta, *Int. Immunopharmacol.*, 2016, **38**, 332–341.

482 Y. Lu, Y. Yang, Z. Gu, J. Zhang, H. Song, G. Xiang and C. Yu, *Biomaterials*, 2018, **175**, 82–92.

483 M. Schieber and N. S. Chandel, *Curr. Biol.*, 2014, **24**, R453–R462.

484 C. Gorrini, I. S. Harris and T. W. Mak, *Nat. Rev. Drug Discovery*, 2013, **12**, 931–947.

485 G. Cui, H. Zhang, Q. Guo, S. Shan, S. Chen, C. Li, X. Yang, Z. Li, Y. Mu, H. Shao and Z. Du, *Toxicol. Mech. Methods*, 2020, **30**, 646–655.

486 G. N. Joshi, A. M. Goetjen and D. A. Knecht, *Mol. Biol. Cell*, 2015, **26**, 3150–3164.

487 Y.-J. Lin, C.-C. Yang, I.-T. Lee, W.-B. Wu, C.-C. Lin, L.-D. Hsiao and C.-M. Yang, *Biomedicines*, 2023, **11**, 2628.

488 S. N. Petrache Voicu, D. Dinu, C. Sima, A. Hermenean, A. Ardelean, E. Codrici, M. S. Stan, O. Zărnescu and A. Dinischiotu, *Int. J. Mol. Sci.*, 2015, **16**, 29398–29416.

489 C. Marques, P. Maroni, L. Maurizi, O. Jordan and G. Borchard, *Int. J. Biol. Macromol.*, 2024, **256**, 128339.

490 S. Tenzer, D. Docter, J. Kuharev, A. Musyanovych, V. Fetz, R. Hecht, F. Schlenk, D. Fischer, K. Kiouptsi, C. Reinhardt, K. Landfester, H. Schild, M. Maskos, S. K. Knauer and R. H. Stauber, *Nat. Nanotechnol.*, 2013, **8**, 772–781.

491 Y.-M. Go and D. P. Jones, *J. Biol. Chem.*, 2013, **288**, 26512–26520.

492 R. Kumar, G. R. Pulikanti, K. R. Shankar, D. Rambabu, V. Mangili, L. R. Kumbam, P. S. Sagara, N. Nakka and M. Yogesh, in *Metal Oxides for Biomedical and Biosensor Applications*, ed. K. Mondal, Elsevier, 2022, pp. 205–231, DOI: [10.1016/B978-0-12-823033-6.00007-7](https://doi.org/10.1016/B978-0-12-823033-6.00007-7).

493 R. K. Singh, K. D. Patel, K. W. Leong and H.-W. Kim, *ACS Appl. Mater. Interfaces*, 2017, **9**, 10309–10337.

494 A. Luchini and G. Vitiello, *Front. Chem.*, 2019, **7**, 343.

495 S. F. Lim and R. H. Austin, in *Applications of Nanoscience in Photomedicine*, ed. M. R. Hamblin and P. Avci, Chandos Publishing, Oxford, 2015, pp. 377–391, DOI: [10.1533/9781908818782.377](https://doi.org/10.1533/9781908818782.377).

496 S. Wen, J. Zhou, K. Zheng, A. Bednarkiewicz, X. Liu and D. Jin, *Nat. Commun.*, 2018, **9**, 2415.

497 A. Priyam, N. M. Idris and Y. Zhang, *J. Mater. Chem.*, 2012, **22**, 960–965.

498 Y. He, S. Guo, L. Wu, P. Chen, L. Wang, Y. Liu and H. Ju, *Biomaterials*, 2019, **225**, 119501.

499 W.-H. Chen, G.-F. Luo, W.-X. Qiu, Q. Lei, S. Hong, S.-B. Wang, D.-W. Zheng, C.-H. Zhu, X. Zeng, J. Feng, S.-X. Cheng and X.-Z. Zhang, *Small*, 2016, **12**, 733–744.

500 L. Diebold and N. S. Chandel, *Free Radicals Biol. Med.*, 2016, **100**, 86–93.

501 S. Kumari, A. K. Badana, M. M. G, S. G and R. Malla, *Biomarker Insights*, 2018, **13**, 1177271918755391.

502 A. D. Pandya, E. Jager, S. Bagheri Fam, A. Hocherl, A. Jager, V. Sincari, B. Nystrom, P. Stepanek, T. Skotland, K. Sandvig, M. Hruby and G. M. Maelandsmo, *Int. J. Nanomed.*, 2019, **14**, 6269–6285.

503 P. Sonkusre and S. S. Cameotra, *J. Nanobiotechnol.*, 2017, **15**, 43.

504 A. Khurana, S. Tekula, M. A. Saifi, P. Venkatesh and C. Godugu, *Biomed. Pharmacother.*, 2019, **111**, 802–812.

505 A. P. Bidkar, P. Sanpui and S. S. Ghosh, *Nanomedicine*, 2017, **12**, 2641–2651.

506 C.-W. Chen, Y.-C. Chan, M. Hsiao and R.-S. Liu, *ACS Appl. Mater. Interfaces*, 2016, **8**, 32108–32119.

507 H. Luo, F. Wang, Y. Bai, T. Chen and W. Zheng, *Colloids Surf., B*, 2012, **94**, 304–308.

508 L. Kong, Q. Yuan, H. Zhu, Y. Li, Q. Guo, Q. Wang, X. Bi and X. Gao, *Biomaterials*, 2011, **32**, 6515–6522.

509 Y. Zhuang, L. Li, L. Feng, S. Wang, H. Su, H. Liu, H. Liu and Y. Wu, *Nanoscale*, 2020, **12**, 1389–1396.

510 L. Chan, L. He, B. Zhou, S. Guan, M. Bo, Y. Yang, Y. Liu, X. Liu, Y. Zhang, Q. Xie and T. Chen, *Chem. – Asian J.*, 2017, **12**, 3053–3060.

511 F. L. Heppner, R. M. Ransohoff and B. Becher, *Nat. Rev. Neurosci.*, 2015, **16**, 358–372.

512 F. Fanizza, M. Campanile, G. Forloni, C. Giordano and D. Albani, *J. Tissue Eng.*, 2022, **13**, 1–20, DOI: [10.1177/20417314221095339](https://doi.org/10.1177/20417314221095339).

513 O. Devinsky, A. Vezzani, S. Najjar, N. C. De Lanerolle and M. A. Rogawski, *Trends Neurosci.*, 2013, **36**, 174–184.

514 D. Kempuraj, R. Thangavel, P. A. Natteru, G. P. Selvakumar, D. Saeed, H. Zahoor, S. Zaheer, S. S. Iyer and A. Zaheer, *J. Neurol. Neurosurg. Spine*, 2016, **1**, 1003.

515 M. T. Lin and M. F. Beal, *Nature*, 2006, **443**, 787–795.

516 S. Gandhi and A. Y. Abramov, *Oxid. Med. Cell. Longevity*, 2012, **2012**, 428010.

517 E. Radi, P. Formichi, C. Battisti and A. Federico, *J. Alzheimer's Dis.*, 2014, **42**(Suppl 3), S125–S152.

518 A. Federico, E. Cardaioli, P. Da Pozzo, P. Formichi, G. N. Gallus and E. Radi, *J. Neurol. Sci.*, 2012, **322**, 254–262.

519 P. J. Landrigan, B. Sonawane, R. N. Butler, L. Trasande, R. Callan and D. Droller, *Environ. Health Perspect.*, 2005, **113**, 1230–1233.

520 L. M. Billings, S. Oddo, K. N. Green, J. L. McGaugh and F. M. LaFerla, *Neuron*, 2005, **45**, 675–688.

521 E. D. Roberson, K. Scearce-Levie, J. J. Palop, F. Yan, I. H. Cheng, T. Wu, H. Gerstein, G.-Q. Yu and L. Mucke, *Science*, 2007, **316**, 750–754.

522 T. Yin, L. Yang, Y. Liu, X. Zhou, J. Sun and J. Liu, *Acta Biomater.*, 2015, **25**, 172–183.

523 L. Yang, Q. Chen, Y. Liu, J. Zhang, D. Sun, Y. Zhou and J. Liu, *J. Mater. Chem. B*, 2014, **2**, 1977–1987.

524 N. Huang, X. Chen, X. Zhu, M. Xu and J. Liu, *Biomaterials*, 2017, **141**, 296–313.

525 S. Mukherjee, V. S. Madamsetty, D. Bhattacharya, S. Roy Chowdhury, M. K. Paul and A. Mukherjee, *Adv. Funct. Mater.*, 2020, **30**, 2003054.

526 G. H. Kim, J. E. Kim, S. J. Rhie and S. Yoon, *Exp. Neurobiol.*, 2015, **24**, 325–340.

527 H. E. Moon and S. H. Paek, *Exp. Neurobiol.*, 2015, **24**, 103–116.

528 J. Blesa, I. Trigo-Damas, A. Quiroga-Varela and V. R. Jackson-Lewis, *Front. Neuroanat.*, 2015, **9**, 91.

529 W. J. Szlachcic, P. M. Switonski, W. J. Krzyzosiak, M. Figlerowicz and M. Figiel, *Dis. Models Mech.*, 2015, **8**, 1047–1057.

530 G. Cenini, A. Lloret and R. Cascella, *Oxid. Med. Cell. Longevity*, 2019, **2019**, 2105607.

531 S. Kausar, F. Wang and H. Cui, *Cells*, 2018, **7**(12), 274.

532 A. Grzelak, M. Wojewodzka, S. Meczynska-Wielgosz, M. Zuberek, D. Wojciechowska and M. Kruszewski, *Redox Biol.*, 2018, **15**, 435–440.

533 A. Gupta, S. Das and S. Seal, *Nanomedicine*, 2014, **9**, 2725–2728.

534 S. Naz, J. Beach, B. Heckert, T. Tummala, O. Pashchenko, T. Banerjee and S. Santra, *Nanomedicine*, 2017, **12**, 545–553.

535 H. Zhou, Y. Gong, Y. Liu, A. Huang, X. Zhu, J. Liu, G. Yuan, L. Zhang, J.-A. Wei and J. Liu, *Biomaterials*, 2020, **237**, 119822.

536 H. J. Kwon, D. Kim, K. Seo, Y. G. Kim, S. I. Han, T. Kang, M. Soh and T. Hyeon, *Angew. Chem., Int. Ed.*, 2018, **57**, 9408–9412.

537 L. Zhang, P.-F. Wei, Y.-H. Song, L. Dong, Y.-D. Wu, Z.-Y. Hao, S. Fan, S. Tai, J.-L. Meng, Y. Lu, J. Xue, C.-Z. Liang and L.-P. Wen, *Biomaterials*, 2019, **216**, 119248.

538 X. Li, J. Tsibouklis, T. Weng, B. Zhang, G. Yin, G. Feng, Y. Cui, I. N. Savina, L. I. Mikhalovska, S. R. Sandeman, C. A. Howel and S. V. Mikhalovsky, *J. Drug Targeting*, 2017, **25**, 17–28.

539 D. K. Sarko and C. E. McKinney, *Front. Neurosci.*, 2017, **11**, 82.

540 S. M. ElMorsy, D. A. Gutierrez, S. Valdez, J. Kumar, R. J. Aguilera, M. Noufal, H. Sarma, S. Chinnam and M. Narayan, *J. Colloid Interface Sci.*, 2024, **670**, 357–363.

541 R.-R. Lin, L.-L. Jin, Y.-Y. Xue, Z.-S. Zhang, H.-F. Huang, D.-F. Chen, Q. Liu, Z.-W. Mao, Z.-Y. Wu and Q.-Q. Tao, *Adv. Sci.*, 2024, **11**, 2306675.

542 H. Tan, Y. Huang, S. Dong, Z. Bai, C. Chen, X. Wu, M. Chao, H. Yan, S. Wang, D. Geng and F. Gao, *Small*, 2023, **19**, 2303530.

543 X. Song, Q. Ding, W. Wei, J. Zhang, R. Sun, L. Yin, S. Liu and Y. Pu, *Small*, 2023, **19**, 2206959.

544 R. Ruotolo, G. De Giorgio, I. Minato, M. G. Bianchi, O. Bussolati and N. Marmiroli, *Nanomaterials*, 2020, **10**(2), 235.

545 W. DeCoteau, K. L. Heckman, A. Y. Estevez, K. J. Reed, W. Costanzo, D. Sandford, P. Studlack, J. Clauss, E. Nichols, J. Lippis, M. Parker, B. Hays-Erlichman, J. C. Leiter and J. S. Erlichman, *Nanomedicine*, 2016, **12**, 2311–2320.

546 W. Cong, R. Bai, Y.-F. Li, L. Wang and C. Chen, *ACS Appl. Mater. Interfaces*, 2019, **11**, 34725–34735.

547 A. M. Khan, B. Korzeniowska, V. Gorshkov, M. Tahir, H. Schrøder, L. Skytte, K. L. Rasmussen, S. Khandige, J. Møller-Jensen and F. Kjeldsen, *Nanotoxicology*, 2019, **13**, 221–239.

548 H. J. Kwon, M.-Y. Cha, D. Kim, D. K. Kim, M. Soh, K. Shin, T. Hyeon and I. Mook-Jung, *ACS Nano*, 2016, **10**, 2860–2870.

549 Z. Gao, Y. Nakanishi, S. Noda, H. Omachi, H. Shinohara, H. Kimura and Y. Nagasaki, *J. Biomater. Sci., Polym. Ed.*, 2017, **28**, 1036–1050.

550 Y. Shen, B. Cao, N. R. Snyder, K. M. Woepel, J. R. Eles and X. T. Cui, *J. Nanobiotechnol.*, 2018, **16**, 13.

551 P. Boonruamkaew, P. Chonpathompikunlert, L. B. Vong, S. Sakaue, Y. Tomidokoro, K. Ishii, A. Tamaoka and Y. Nagasaki, *Sci. Rep.*, 2017, **7**, 3785.

552 L. Ling, Y. Jiang, Y. Liu, H. Li, A. Bari, R. Ullah and J. Xue, *J. Photochem. Photobiol. B*, 2019, **201**, 111657.

553 A. V. Ivanov, B. Bartosch and M. G. Isagulians, *Oxid. Med. Cell. Longevity*, 2017, **2017**, 3496043.

554 U. Z. Paracha, K. Fatima, M. Alqahtani, A. Chaudhary, A. Abuzenadah, G. Damanhouri and I. Qadri, *Virol. J.*, 2013, **10**, 251.

555 S. Li, H. Li, X. Xu, P. E. Saw and L. Zhang, *Theranostics*, 2020, **10**, 1262–1280.

556 N. Thakur, P. Manna and J. Das, *J. Nanobiotechnol.*, 2019, **17**, 84.

557 Y. Huang, M. Zhang, M. Jin, T. Ma, J. Guo, X. Zhai and Y. Du, *Adv. Healthcare Mater.*, 2023, **12**, 2300748.

558 M. G. Schappi, V. Jaquet, D. C. Belli and K. H. Krause, *Semin. Immunopathol.*, 2008, **30**, 255–271.

559 Q. Ren, S. Sun and X.-D. Zhang, *Nano Res.*, 2021, **14**, 2535–2557.

560 T. Kuijpers and R. Lutter, *Cell. Mol. Life Sci.*, 2012, **69**, 7–15.

561 K. S. Kim, D. Lee, C. G. Song and P. M. Kang, *Nanomedicine*, 2015, **10**, 2709–2723.

562 T. Hemnnani and M. S. Parihar, *Indian J. Physiol. Pharmacol.*, 1998, **42**, 440–452.

563 A. Chompoosor, K. Saha, P. S. Ghosh, D. J. Macarthy, O. R. Miranda, Z. J. Zhu, K. F. Arcaro and V. M. Rotello, *Small*, 2010, **6**, 2246–2249.

564 U. S. Srinivas, B. W. Q. Tan, B. A. Vellayappan and A. D. Jeyasekharan, *Redox Biol.*, 2019, **25**, 101084.

565 A. Grzelak, M. Wojewódzka, S. Meczynska-Wielgosz, M. Zuberek, D. Wojciechowska and M. Kruszewski, *Redox Biol.*, 2018, **15**, 435–440.

566 P. Patel, K. Kansara, R. Singh, R. K. Shukla, S. Singh, A. Dhawan and A. Kumar, *Int. J. Nanomed.*, 2018, **13**, 39–41.

567 K. Mortezaee, M. Najafi, H. Samadian, H. Barabadi, A. Azarnezhad and A. Ahmadi, *Chem.-Biol. Interact.*, 2019, **312**, 108814.

568 Y. Li, S. Yu, Q. Wu, M. Tang, Y. Pu and D. Wang, *J. Hazard. Mater.*, 2012, **219–220**, 221–230.

569 K. R. Smith, L. R. Klei and A. Barchowsky, *Am. J. Physiol.: Lung Cell. Mol. Physiol.*, 2001, **280**, L442–L449.

570 S. J. Soenen, P. Rivera-Gil, J.-M. Montenegro, W. J. Parak, S. C. De Smedt and K. Braeckmans, *Nano Today*, 2011, **6**, 446–465.

571 K. Bedard, H. Attar, J. Bonnefont, V. Jaquet, C. Borel, O. Plastre, M. J. Stasia, S. E. Antonarakis and K. H. Krause, *Hum. Mutat.*, 2009, **30**, 1123–1133.

572 J. A. Nogueira-Machado and M. M. Chaves, *Expert Opin. Ther. Targets*, 2008, **12**, 871–882.

573 Y. Zhang, T. Peng, H. Zhu, X. Zheng, X. Zhang, N. Jiang, X. Cheng, X. Lai, A. Shunnar, M. Singh, N. Riordan, V. Bogin, N. Tong and W. P. Min, *J. Transl. Med.*, 2010, **8**, 133.

574 R. F. Loeser, *Trans. Am. Clin. Climatol. Assoc.*, 2017, **128**, 44–54.

575 Y. Henrotin, G. Deby-Dupont, C. Deby, M. De Bruyn, M. Lamy and P. Franchimont, *Br. J. Rheumatol.*, 1993, **32**, 562–567.

576 M. L. Tiku, J. B. Liesch and F. M. Robertson, *J. Immunol.*, 1990, **145**, 690–696.

577 Y. E. Henrotin, P. Bruckner and J. P. L. Pujol, *Osteoarthritis Cartilage*, 2003, **11**, 747–755.

578 M. A. Altay, C. Erturk, A. Bilge, M. Yapti, A. Levent and N. Aksoy, *Rheumatol. Int.*, 2015, **35**, 1725–1731.

579 C. Erturk, M. A. Altay, S. Selek and A. Koçyigit, *Scand. J. Clin. Lab. Invest.*, 2012, **72**, 433–439.

580 C. M. Davies, F. Guilak, J. B. Weinberg and B. Fermor, *Osteoarthritis Cartilage*, 2008, **16**, 624–630.

581 V. N.-S. Lucas José Sá da Fonseca, M. Oliveira Fonseca Goulart and L. Antas Rabelo, *Oxid. Med. Cell. Longevity*, 2019, **2019**, 16.

582 R. Bordy, P. Totoson, C. Prati, C. Marie, D. Wendling and C. Demougeot, *Nat. Rev. Rheumatol.*, 2018, **14**, 404–420.

583 D. Chen, J. Shen, W. Zhao, T. Wang, L. Han, J. L. Hamilton and H.-J. Im, *Bone Res.*, 2017, **5**, 16044.

584 J. S. Lee, M. L. Cho, J. Y. Jhun, S. Y. Min, J. H. Ju, C. H. Yoon, J. K. Min, S. H. Park, H. Y. Kim and Y. G. Cho, *J. Clin. Immunol.*, 2006, **26**, 204–212.

585 D. Jawaheer, M. F. Seldin, C. I. Amos, W. V. Chen, R. Shigeta, C. Etzel, A. Damle, X. Xiao, D. Chen, R. F. Lum, J. Monteiro, M. Kern, L. A. Criswell, S. Albani, J. L. Nelson, D. O. Clegg, R. Pope, H. W. Schroeder, Jr., S. L. Bridges, Jr., D. S. Pisetsky, R. Ward, D. L. Kastner,

R. L. Wilder, T. Pincus, L. F. Callahan, D. Flemming, M. H. Wener and P. K. Gregersen, *Arthritis Rheum.*, 2003, **48**, 906–916.

586 A. Mirshafiey and M. Mohsenzadegan, *Iran. J. Allergy, Asthma Immunol.*, 2008, **7**, 195–202.

587 M. Hultqvist, P. Olofsson, J. Holmberg, B. T. Bäckström, J. Tordsson and R. Holmdahl, *Proc. Natl. Acad. Sci. U. S. A.*, 2004, **101**, 12646–12651.

588 S. Mangialaio, H. Ji, A. S. Korganow, V. Kouskoff, C. Benoist and D. Mathis, *Arthritis Rheum.*, 1999, **42**, 2517–2523.

589 A. Corthay, A. S. Hansson and R. Holmdahl, *Arthritis Rheum.*, 2000, **43**, 844–851.

590 K. Kannan, R. A. Ortmann and D. Kimpel, *Pathophysiology*, 2005, **12**, 167–181.

591 K. A. Gelderman, M. Hultqvist, L. M. Olsson, K. Bauer, A. Pizzolla, P. Olofsson and R. Holmdahl, *Antioxid. Redox Signaling*, 2007, **9**, 1541–1567.

592 S. Saxena, H. Vekaria, P. G. Sullivan and A. W. Seifert, *Nat. Commun.*, 2019, **10**, 4400.

593 C. Dunnill, T. Patton, J. Brennan, J. Barrett, M. Dryden, J. Cooke, D. Leaper and N. T. Georgopoulos, *Int. Wound J.*, 2017, **14**, 89–96.

594 H. Dou, S. Wang, J. Hu, J. Song, C. Zhang, J. Wang and L. Xiao, *J. Tissue Eng.*, 2023, **14**, 1–23, DOI: [10.1177/20417314231172584](https://doi.org/10.1177/20417314231172584).

595 S. Zhou, M. Xie, J. Su, B. Cai, J. Li and K. Zhang, *J. Tissue Eng.*, 2023, **14**, 1–28, DOI: [10.1177/20417314231185848](https://doi.org/10.1177/20417314231185848).

596 Y. Yao, H. Zhang, Z. Wang, J. Ding, S. Wang, B. Huang, S. Ke and C. Gao, *J. Mater. Chem. B*, 2019, **7**, 5019–5037.

597 T. Wang, Y. Zheng, Y. Shen, Y. Shi, F. Li, C. Su and L. Zhao, *Artif. Cells, Nanomed., Biotechnol.*, 2018, **46**, 138–149.

598 T. Tang, H. Jiang, Y. Yu, F. He, S. Z. Ji, Y. Y. Liu, Z. S. Wang, S. C. Xiao, C. Tang, G. Y. Wang and Z. F. Xia, *Int. J. Nanomed.*, 2015, **10**, 6571–6585.

599 M. Nakayama, R. Sasaki, C. Ogino, T. Tanaka, K. Morita, M. Umetsu, S. Ohara, Z. Tan, Y. Nishimura, H. Akasaka, K. Sato, C. Numako, S. Takami and A. Kondo, *Radiat. Oncol.*, 2016, **11**, 91.

600 T. Thenmozhi, *3 Biotech.*, 2020, **10**, 82.

601 H. M. Fahmy, N. M. Ebrahim and M. H. Gaber, *J. Trace Elem. Med. Biol.*, 2020, **60**, 126481.

602 K.-I. Lee, J.-W. Lin, C.-C. Su, K.-M. Fang, C.-Y. Yang, C.-Y. Kuo, C.-C. Wu, C.-T. Wu and Y.-W. Chen, *Toxicol. In Vitro*, 2020, **63**, 104739.

603 S. R. Choudhury, J. Ordaz, C. L. Lo, N. P. Damayanti, F. Zhou and J. Irudayaraj, *Toxicol. Sci.*, 2017, **156**, 261–274.

604 S. May, C. Hirsch, A. Rippl, N. Bohmer, J.-P. Kaiser, L. Diener, A. Wichser, A. Bürkle and P. Wick, *Nanoscale*, 2018, **10**, 15723–15735.

605 E. Abbasi-Oshaghi, F. Mirzaei and M. Pourjafar, *Int. J. Nanomed.*, 2019, **14**, 1919–1936.

606 O. M. Abd El-Moneim, A. H. Abd El-Rahim and N. A. Hafiz, *Toxicol. Rep.*, 2018, **5**, 771–776.

607 L. M. Rossbach, D. H. Oughton, E. Maremonti, C. Coutris and D. A. Brede, *Sci. Total Environ.*, 2020, **721**, 137665.

608 M. Ahamed, M. J. Akhtar, M. A. M. Khan, S. A. Alrokayan and H. A. Alhadlaq, *Chemosphere*, 2019, **216**, 823–831.

609 X. Shi, Y. Tian, S. Zhai, Y. Liu, S. Chu and Z. Xiong, *Front. Chem.*, 2023, **11**, 1115440.

610 J. Bouayed and T. Bohn, *Oxid. Med. Cell. Longevity*, 2010, **3**(4), 228–237.

611 A. Adhikari, S. Mondal, S. Darbar and S. Kumar Pal, *Biomol. Concepts*, 2019, **10**(1), 160–174.

612 S. Hua, M. B. C. de Matos, J. M. Metselaar and G. Storm, *Front. Pharmacol.*, 2018, **9**, 790.

613 P. C. Naha, K. C. Lau, J. C. Hsu, M. Hajfathalian, S. Mian, P. Chhour, L. Uppuluri, E. S. McDonald, A. D. A. Maidment and D. P. Cormode, *Nanoscale*, 2016, **8**(28), 13740–13754.

614 D. P. Cormode, L. Gao and H. Koo, *Trends Biotechnol.*, 2018, **36**(1), 15–29.

615 A. Nel, T. Xia, H. Meng, X. Wang, S. Lin, Z. Ji and H. Zhang, *Acc. Chem. Res.*, 2013, **46**(3), 607–621.

616 B. C. Nelson, C. W. Wright, Y. Ibuki, M. Moreno-Villanueva, H. L. Karlsson, G. Hendriks, C. M. Sims, N. Singh and S. H. Doak, *Mutagenesis*, 2017, **32**(1), 215–232.